Master's thesis

NTNU
Norwegian University of Science and Technology
Faculty of Engineering
Department of Energy and Process Engineering

Henrik Alvestad

Characterization of thermal energy needs of swimming pools using building performance simulation

Master's thesis in Energy and Environmental Engineering
Supervisor: Laurent Georges
June 2019

NTNU
Kunnskap for en bedre verden

Henrik Alvestad

Characterization of thermal energy needs of swimming pools using building performance simulation

Master's thesis in Energy and Environmental Engineering
Supervisor: Laurent Georges
June 2019

Norwegian University of Science and Technology
Faculty of Engineering
Department of Energy and Process Engineering

NTNU
Norwegian University of
Science and Technology

Preface

This master thesis of 30 ECTS credits is submitted to the Department of Energy and Process Engineering at the Norwegian University of Science and Technology (NTNU). This is the final report of this master work, and I hope you enjoy reading. Great thanks to my supervisor Laurent Georges and my co-supervisor Ole Øiene Smedegård for guidance.

I would also like to thank Kjetil Øvretveit in Pirbadet for cooperating regarding measurements in the swimming facility and in the belonging air handling unit.

Henrik Alvestad, MSc. student

Trondheim, 06.06.19

Abstract

Swimming facilities are energy consuming buildings with highly advanced air conditioning systems compared to e.g. residential and office buildings. Especially the huge need of dehumidification is defining for swimming facilities. Due to high indoor air temperature and pool water temperature, also the heating need is huge in such facilities. In order to improve the buildings, their technical installations and procedure, a good understand of the energy needs for the different posts is essential. This master thesis aims to simulate the dynamic thermal behaviour of an existing swimming pool using the building performance simulation (BPS) tool IDA ICE. The goal is to determine how accurate these simulations can predict thermal needs and how this BPS tool can be used to build more energy efficient swimming pools.

This report also contains an extensive literature review about use, design of the building envelope and air conditioning system.

A part of Pirbadet, a swimming facility in Trondheim, was used for modelling and measurements. The two hot water pools and their belonging air handling unit (AHU) was modelled in IDA ICE. The purpose was not to model a copy of the AHU in Pirbadet, but to make a model that ensured the same indoor climate and recycled thermal energy from the return air. To be able to validate the model to the real system, there were performed measurements in the AHU in Pirbadet. There were installed temperature and relative humidity (RH) sensors, as well as the integrated volume flow sensors, to be able to do energy calculations for the AHU.

The results from the measurements in Pirbadet and the simulations were compared to decide whether the pool and building model was correct in terms of thermal energy need or not. Afterwards the thermal energy need of the AHU was investigated.

The IDA ICE pool model works as intended regarding evaporation rate compared to Pirbadet. Compared to theoretical calculations, there is a big leap in the results, but it corresponded quite good to the method of Basin & and Krumm.

The heating need from the ventilation system was a lot higher for the real hall in Pirbadet than for the IDA ICE model. This indicates that the model has less heat loss than the reality and consequently has less AHU heating need as well.

Due to a different control strategy, the dehumidifying power for the two cases are very different. The fact that the IDA ICE model was made without a heat pump also makes an impact on the use of the dehumidifier which is the evaporator of the heat pump. To be able to evaluate IDA ICE further, a more correct model in terms of heating need must be tested.

Sammendrag

Svømmeanlegg er svært energikrevende bygg med svært avansert luftbehandlingsanlegg sammenlignet med for eksempel bolighus eller kontorbygg. Spesielt det store behovet for avfukting er karakteristisk for svømmeanlegg. På grunn av høy innendørs lufttemperatur og bassengvannstemperatur er også varmebehovet ved slike anlegg stort. I den hensikt å forbedre slike bygg, de tilhørende tekniske installasjonene og styring er det viktig å skaffe innsikt i energibruken til de forskjellige delene i et slikt anlegg. Denne masteroppgaven tar for seg simulering av dynamisk termisk opptreden av en eksisterende svømmehall ved bruk av simuleringsverktøyet IDA ICE. Målet er å bestemme hvor nøyaktig slike simuleringer kan anslå termisk energibehov og dermed kunne være til nytte ved energieffektivisering av svømmeanlegg.

Denne rapporten inneholder også et omfattende teorikapittel om bruk av svømmehaller, design av bygningskropp og luftbehandlingsanlegg.

En del av Pirbadet, et svømmeanlegg i Trondheim, ble brukt for modellering og til å utføre målinger i. Pirbadets to helsebad og det tilhørende luftbehandlingsaggregatet ble modellert i IDA ICE. Målet var ikke å modellere en eksakt kopi av aggregatet i Pirbadet, men å lage en modell som sørger for det samme inneklimaet og som gjenvinner den termiske energien fra returlufta fra hallen. For å kunne validere modellen med virkeligheten ble det gjort målinger i luftbehandlingsaggregatet i Pirbadet. Det ble installert temperatursensorer og sensorer for relativ fuktighet for å kunne gjøre energiberegninger. I tillegg var det allerede to integrerte sensorer for volumstrøm som ble benyttet.

Resultatene fra målingene i Pirbadet og simuleringene ble sammenlignet mot hverandre for å avgjøre om IDA ICE modellen var riktig med hensyn til termisk energibehov. Etterpå ble det termiske energibehovet til luftbehandlingsaggregatet undersøkt.

IDA ICE bassengmodellen virker som ønsket når det gjelder fordamping sammenlignet med fordamping i Pirbadet. Sammenligner man derimot med teoretisk kalkulerte verdier er det stort sprik i resultatene. Fordampingen stemmer ganske godt overens med kalkulerte verdier fra metoden til Basin & Krumm som også i andre studier er fremhevet som passende.

Varmebehovet fra ventilasjonssystemet viste seg å være mye høyere i virkeligheten enn i IDA ICE modellen. Dette kan være en indikasjon på at modellen har mindre varmetap enn virkeligheten og som en konsekvens også trenger mindre varmetilførsel i luftbehandlingsaggregatet.

På grunn av forskjellig regulering er behovet for effekt i avfukteren ganske forskjellig i modellen og det som ble målt i Pirbadet. Det faktum at IDA ICE modellen ble modellert uten varmepumpe vil også ha innvirkning på bruken av avfukteren, da den er fordamperen til varmepumpa. For å kunne evaluere IDA ICE bedre vil man ha behov for å teste en modell som er bedre, i form av mer korrekt varmebehov, enn den utviklet i dette prosjektet.

Content

List of figures

List of tables

List of symbols and abbreviations

$\dot{Q}$	[W]	heat rate
$\dot{V}$	[m^3/s]	volume flow rate
$\dot{m}$	[kg/s]	mass flow rate
h	[J/kg]	enthalpy
A	[m^2]	area
p	[Pa]	saturation pressure
F_a	[-]	activity factor
Y	[J/kg]	latent heat of vaporization at water surface
x	[$kg_{water}/kg_{dry,air}$]	water content in air
ρ	[kg/m^3]	density
n_{50}	[ach]	number of times the volume of air is changed in one hour at 50 Pa underpressure
ψ"	[$W/(m^2K)$]	normalized thermal bridge
v	[m^3/kg]	specific volume
c_p	[kJ/(kgK)]	specific heat capacity
T	[°C]	temperature
RH	[%RH]	relative humidity

a	air
ach	air changes per hour
ae	air extract
as	air supply
awe	extracted water content in air
aws	supplied water content in air
CLO	clothing
comp	compressor
conv	convection
DP	dew point
EA	exhaust air

envLossHall	envelope loss for hall
envLossPool	envelope loss for pool
evap	evaporation
FA	fresh air
gen	generated
HR	heat recovery unit
internal	people, technical equipment, lights, showers
MET	metabolism
moist	moisture
n	net
OA	outdoor air
ps	pool surface
RA	return air
rad	radiation
SA	supply air
trans	transmission
UA	usable area
we	water extract
ws	water supply

1. Introduction

1.1 Background and motivation

According to the Norwegian law of climate[1], Norway´s target within 2030 is to reduce greenhouse gas emissions with at least 40 % compared to the reference year 1990 [1]. Since the Norwegian buildings is accounting for around 40 % of the total energy use in Norway, to reduce the energy demand for Norwegian buildings can contribute to a large extent in reaching this target [2]. Among all Norwegian buildings, swimming halls are huge consumers of energy. In 2012 Wolfgang Kampel et al. published an article about energy-use in Norwegian swimming halls. They stated that there were registered about 850 swimming facilities in Norway and found the potential reduction of the final annual energy consumption of these to be around 28 % [3]. This explains the need of research within this topic.

Over the past decades, the new building standards have ensured more leakage proof and better insulated buildings. This changes the properties of the building envelope and new research is needed to optimize the use of it. Also, the building performance simulation programs have been developed, so the possibility for research is better than ever.

There has been some research on for example solar gain for both outdoor and indoor swimming pools and CFD analysis of indoor pools regarding temperature and humidity by use of OpenFOAM software [4]. There is also been done some experiments on water evaporation compared to calculation methods. However, there is not yet much experience or research on using simulation tools in design of swimming halls and their belonging technical systems.

1.2 Problem description

Swimming pools are buildings with an intensive energy use with complex indoor environment parameters. They have continuous heating needs during the entire year. Existing projects show a large variation of technical solutions also characterized with large variations of investments and energy costs of operation. A good understand of the energy needs for the different posts (or services) is essential in order to improve the current buildings and their technical installations, as well as to improve their procedure. Understanding of the energy needs is also a necessary background to start on optimization process for such buildings.

[1] Norwegian: Klimaloven

To contribute to this goal, the master thesis aims to simulate the dynamic thermal behaviour of an existing swimming pool using building performance simulation. This will be done using IDA ICE combined with a dedicated plugin for swimming pools. The objective is to determine how accurate these simulations can predict thermal needs and how this BPS tool can be used to build more energy efficient swimming pools. During the master thesis, the focus will firstly be on the air handling unit and the pool heating. Then, the heating plant of the swimming pool will be investigated. In order to validate simulations, technical specifications and measurement data from an existing swimming pool should be obtained. A critical physical phenomenon is the amount of water evaporation from the swimming pool. This should be investigated, for instance using measurements, and used in the simulation model. Finally, based on a validated model of a swimming pool, a comprehensive sensitivity analysis should be performed in order to optimize and understand its energy performance.

1.2.1 Adjustments

The purpose was not to model a true copy of the AHU in Pirbadet, but to make a model that ensured the same indoor climate and recycled thermal energy from the return air. Further on this simple model should be compared to measurements to determine if such a model can be used as a tool for swimming pool design.

Due to lack of possibility to measure and log the pool heating, this part is not in focus in this thesis. The heat pump was not modelled due to the complexity of modelling a heat pump in IDA ICE. A cooler was used for the evaporator and a heating coil for the condenser. So, only the output of the heating plant is considered. As a result of a not perfect building model, a sensitivity analysis in order to optimize and understand the energy performance of the swimming facility was not of interest. This must be done for a correct model to be valuable.

1.3 Structure of the report

Chapter 2 is a theory part giving an overview over use of swimming pools, challenges appearing in these buildings, requirements and technical equipment used in swimming pools. Further on, chapter 3 is about methodology and gives some information about the swimming facility used, the measuring process and further use of the measurements. Further on, the software used and how the pool is modelled and simulated is presented. Chapter 4 presents the results from the measurements and simulations including some analysis. In chapter 5, the results are discussed while chapter 6 contains a conclusion of the work. There is also a chapter 7 for further work.

2. Theory about swimming pools

2.1 Use of swimming pools

Swimming facilities is built to create good and safe conditions for indoor swimming and other indoor water activities. One wants to be able to do the activity in a comfortable indoor environment. When designing and building a swimming facility, the most important goal is to facilitate for the use of the building.

There are different types of activities with need of different pools and different impact on the indoor climate. There are for example small swimming pools used by schools for swimming lessons, larger swimming pools for different kind of sports and there are these huge facilities with different types of pools and water attractions like slides. Due to diverse use of the different facilities, they are designed their own way to ensure a best possible indoor climate for the users.

The different use of swimming pools leads to different evaporation rates from the water surface due to different water surface area. This effect has its own factor, which is called the activity factor (F_a). This factor is used to calculate the evaporation energy from the pool as in Equation (2-3).

Table 2-1: Typical activity factor for different type of pools [5, 6]

Type of pool	Typical activity factor (F_a).
Covered	0.1
Baseline (unoccupied)	0.5
Residential	0.5
Condominium	0.65
Therapy	0.65
Hotel	0.8
Public, schools	1
Whirlpools, spas	1
Wavepools, water slides	1.5

2.2 Design of swimming pools

2.2.1 The building structure

Swimming pools are seldomly built as separate buildings, but rather often inside buildings containing several facilities. This might for example be larger sport arenas housing many different sports or schools with internal swimming pool. This means there are often one or more walls connected to another heated part of the building which is beneficial regarding condensation and energy loss.

In 2012, the average age of the Norwegian swimming pools were 37 years [3]. Over these years there has been an almost continuous change of the building requirements, the materials and technical equipment used. When Pirbadet in Trondheim was built, the "Byggteknisk forskrift" (TEK97) was giving building requirements. Today, the current restrictions are given in TEK17 for all buildings and in the Norwegian standard NS3701 for non-residential passive house buildings. There are not specific restrictions for indoor swimming facilities in these standards, but they are subordinate of buildings for sport. The maximum allowable energy demand for sports buildings is 145 kWh/m^2 heated area each year according to TEK17 [7]. The average energy demand of 27 Norwegian swimming facilities over one year was found to be 401 kWh/m$^2_{UA}$ in a study from 2004 [8]. So, swimming facilities have much higher energy demand than the typical Norwegian sports buildings.

Table 2-2: Requirements for U-values [9] [7] [10]

	TEK97[2] [W/(m^{2}K)]	TEK17 [W/(m^{2}K)]	NS3701 [W/(m^{2}K)]
External walls	≤ 0.22	≤ 0.22	≤ 0.22
External roofs	≤ 0.15	≤ 0.18	≤ 0.18
Floor to ground	≤ 0.15	≤ 0.18	≤ 0.18
Windows and doors	≤ 2	≤ 1,2	≤ 0.8

Table 2-3: Other requirements regarding building structure [7] [10]

	TEK17	NS3701
Leakage n_{50} [ach]	≤ 1.5	≤ 0.6
Normalized thermal bridge ψ" [W/(m^{2}K)]	≤ 0.05	≤ 0.03

[2] Valid for non-residential houses with indoor temperature ≥ 20 °C

2.2.2 Pool specifications

There exist several types of swimming pools made for different purposes with different properties. When it comes to size, it ranges from small pools for swimming lessons at schools to large pools for sport or recreation. The water temperature is set to be comfortable for the activity in the specific pool. A pool for sport has colder water than a pool for therapy for example.

Table 2-4: Requirements for water temperature in different type of pools [11]

Type of pool	Required water temperature [°C]
Training pool	28-34
Baby swimming pool	33
Swimming pool	26-29
Competition pool	26-27
Diving pool	26-32
Whirlpool	37-40
Waterpark pool	28-34

Testing of different water temperatures in IDA ICE by Ole Ø. Smedegård at Jøa indicates that a lower water temperature results in less evaporation from the pool, which is preferable [6]. Regarding the evaporation from the pool surface to the hall air, Byggforsk has some numbers on this based on experience tabulated in Table 2-5.

Table 2-5: Evaporation from pool surface based on experience [8]

Category	Water temperatures [°C]	Evaporation [kg/(m^2h)]
Private pool	27-28	0.10
Hotel	27	0.18
Night-time		0.10
Public pool	28	0.25
Heated pools	32-36	0.35-0.50
Whirlpools	36-38	0.9-1.0

There has been done some experiments on evaporation rates by use of small pool models. Ilona Rzeźnik has done such an experiment and compared the results against several methods for calculating evaporation rate. There was done experiments both with and without occupancy,

and the models Shah and Baisin & Krumm gave results most equal to the results from the laboratory. The models are shown in Attachment 3.

Showers/Wardrobes

According to Byggforsk, the recommended air temperature in the wardrobe is 21-23 °C, while the recommended air temperature in the showers is 25-27 °C [12]. Due to the amount of water in the showers compared to the more or less dry wardrobes and the difference in recommended air temperature, the wardrobe and showers can be separated in two ventilation zones. The todays normal practice is to ventilate the showers with the same AHU as used for the swimming hall, and another AHU for the dry wardrobes.

2.2.3 The energy system (balance)

When studying the energy balance of a system it is very important to understand the boundary lines of the system. Figure 2-1 is a simple sketch of the system used in this project and some relevant energy balance equations is shown in the sections below. For simplicity, the hall and wardrobes are assumed to be one zone only.

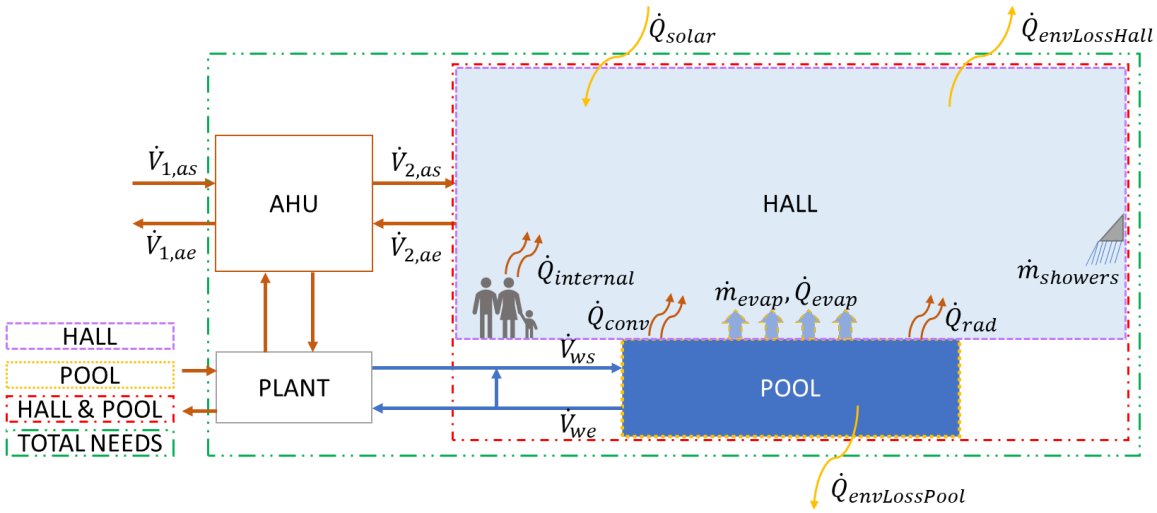

Figure 2-1: Energy system with boundary lines

In an article from the Faculty of Mechanical Engineering in the University of Nis (Serbia) there is done simulations using TRNSYS software to get to understand the thermal performance of an indoor swimming pool. Their simulation showed that pool water heating accounted for about 22 % while the ventilation and heating of the pool hall for about 60 % of the total pool hall heat demand. They also found the evaporation losses to be around 46-54 % of the total pool losses. In other words, there is a huge interaction between pool, hall and ventilation system. [13]

2.2.3.1 Energy balance for the hall air space

In this section, the energy balance for the swimming hall within the purple system boundary line is presented.

Equation (2-1) is the balance equation for the heat energy in the hall.

$$\dot{Q}_{n,as} + \dot{Q}_{internal} + \left(\dot{Q}_{evap} + \dot{Q}_{rad} + \dot{Q}_{conv}\right)_{ps} + \dot{Q}_{solar} = \dot{Q}_{envLossHall} \quad (2\text{-}1)$$

Where Equation (2-2) is the net thermal energy supplied to the hall by the AHU

$$\dot{Q}_{n,as} = (\dot{m}_{as} * \mathrm{h_{as}}) - (\dot{m}_{ae} * \mathrm{h_{ae}}) \quad (2\text{-}2)$$

and Equation (2-3) is the energy released from the pool due to evaporation [5].

$$\dot{Q}_{evap} = 4 * 10^{-5} * A\left(p_{ps} - p_a\right)F_a * Y \quad (2\text{-}3)$$

It is important to know that the airflow used in Equation (2-2) is the supplied air to the hall (marked 2), not the fresh air supplied to the AHU (marked 1).

2.2.3.2 Energy balance for the swimming hall with pool

In this section, the energy balance for the swimming hall within the red system boundary line is presented.

Equation (2-4) is the balance equation for the heat energy in the hall with the pool.

$$\dot{Q}_{n,as} + \dot{Q}_{internal} + \dot{Q}_{solar} + \dot{Q}_{n,ws} = \dot{Q}_{envLossHall} + \dot{Q}_{envLossPool} \quad (2\text{-}4)$$

Where Equation (2-5) is the net thermal energy in the water supplied to the pool

$$\dot{Q}_{n,ws} = \dot{Q}_{ws} - \dot{Q}_{we} \quad (2\text{-}5)$$

2.2.3.3 Water vapor mass balance for the hall air space

In this section, the water vapor mass balance for the swimming hall within the purple system boundary line is presented.

Equation (2-6) is the balance equation for the water vapor mass in the hall.

$$\dot{m}_{evap} + \dot{m}_{showers} = \dot{m}_{awe} - \dot{m}_{aws}{}^{3} \quad (2\text{-}6)$$

Where Equation (2-7) is the evaporated mass from the pool[4] [5]

$$\dot{m}_{evap} = 4 * 10^{-5} * A\left(p_{ps} - p_a\right)F_a \quad (2\text{-}7)$$

[3] Assuming no infiltration or exfiltration

[4] Equation used in IDA ICE calculations

and Equation (2-8) is the water mass extracted from the hall to the AHU

$$\dot{m}_{awe} = x_{ae} * \dot{V}_{2,ae} * \rho_{air,dry} \quad (2\text{-}8)$$

and Equation (2-9) is the water mass supplied to the hall from the AHU.

$$\dot{m}_{aws} = x_{as} * \dot{V}_{2,as} * \rho_{air,dry} \quad (2\text{-}9)$$

2.2.4 System diagram

Figure 2-2 illustrates the total system for a typical "easy" swimming pool. In this case the pool at Jøa is used.

1. The swimming pool
2. Water inlet
3. Stop valve for draining the pool
4. Buffer vessel
5. Wastewater
6. Hydronic heating circuit
7. Closed heating circuit
8. Air handling unit
9. Integrated heat pump in the AHU
10. Water supply
11. Air supply
12. Water heater
13. Exhaust air

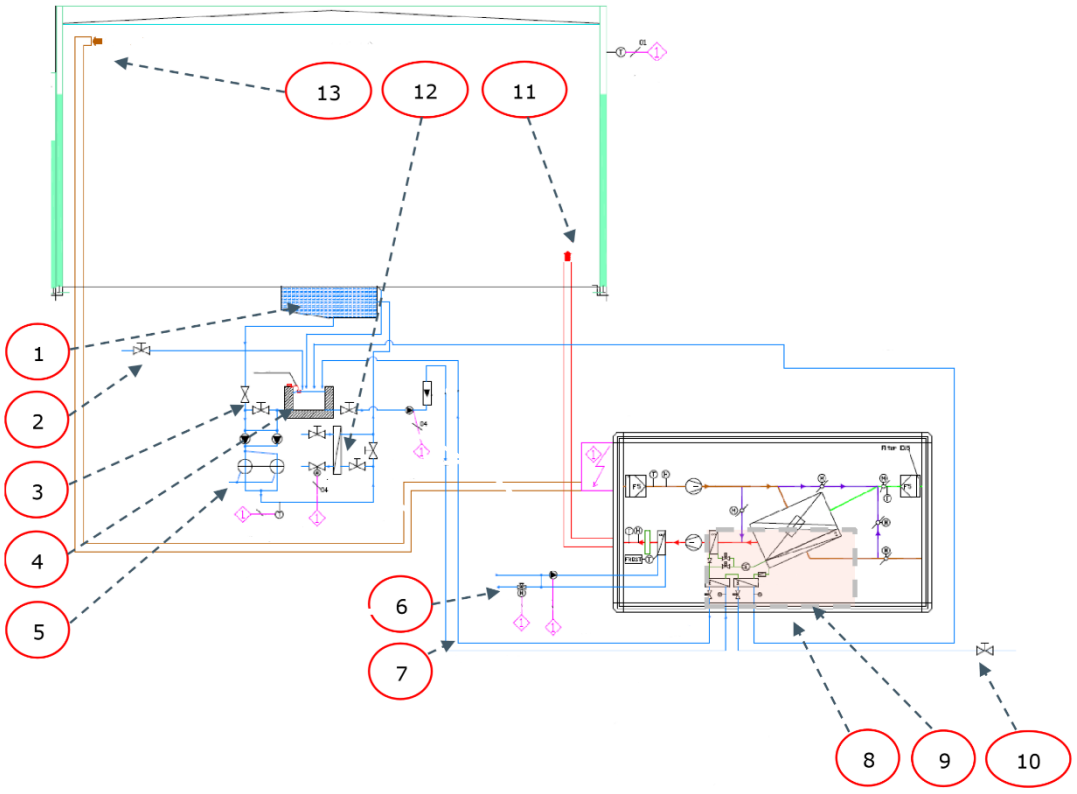

Figure 2-2: The Jøa swimming pool facility system diagram [6]

2.3 Water treatment

In the manual dealing with water treatment in public pools from Norsk Bassengbad Teknisk Forening (NBTF) there are several important guidelines. There are mainly three important actions in the water treatment. These are circulation, filtering and supply of fresh water. The water treatment system should ensure hygienic conditions for the users of the pool.

The amount of circulating water and fresh water is given by the number of users of the pool. For pools larger than 4 m^3 and water temperature below 34 °C the amount of circulating water should be minimum 2 m^3/hour per visitor and the amount of fresh water should be minimum 30 liters/day per visitor (60 liters/day per visitor if water temperature is above 34 °C) [14].

To ensure this hygienic water conditions, the circulated water is filtered and disinfected. Chlorine is a well-known chemical agent for disinfection, but has to be used within some recommended amounts to avoid harm to the visitors. This topic is mentioned more specific in section 2.4. A solution for reducing the use of chlorine is to use ultra violet (UV) light. The UV light starts a chemical process that lame the cell division of microorganisms as well as it reduce the amount of bound chlorine [14]. Direct eye contact with the UV light is dangerous.

2.4 Ventilation

In many of today's swimming pools, chlorine is used to clean the water for bacteria that can be hazardous to humans. But this action doesn't come without consequences. Chemicals such as dichloramine and trichloramine are formed when chlorine binds to water contaminants [8]. These chloramines are off-gassed to the pool space air and can result in irritated skin and eyes, respiratory health hazard and corrosion on building materials [15]. One way to reduce this effect is to use other water treatment methods, like UV system, to clean the water and then reduce the amount of chlorine. Another way, which is to be considered in this project, is to ventilate the air to remove the chloramines.

Besides ensuring fresh air, ventilation is important for heating, dehumidification and to provide a satisfying indoor climate in the entire swimming hall. There will be heat loss through the building envelope and in the ventilation that needs to be covered. Due to constant evaporation from the pool, a dehumidification method must be used to limit the moisture level in the air as described more in detail in section 2.4.3.

2.4.1 Air rates

Since there are different purposes of the ventilation, all the purposes should be investigated to decide the correct air rates. We also divide in need of fresh air and total air rates.

The amount of fresh air (outdoor air) needed depends on dehumidification method as described in section 2.5.1. Anyway, the minimum requirements for fresh air supply is the amount needed to ensure a good air quality.

To decide the fresh air rates after the method used in TEK17, the amount of fresh air is evaluated based on:

a emissions from people

b emissions from materials and inventory

c emissions from activities and processes

The largest value of (a + b) and (c) is the value used for deciding fresh air rates for ventilation. The different numbers for (a) and (b) are given in Table 2-6, while the numbers for (c) is in this case given by The American Society of Heating, Refrigerating and Air-Conditioning Engineers (ASHRAE) and Byggforsk described below.

Table 2-6: Air rates for fresh air based on person and material load [7]

	a [m^3/h per person]	b [m^3/h per m^2]
In use	26	2.5
Not in use		0.7

According to ASHRAE, the minimum ventilation rate (outdoor air) required to be delivered to the breathing zone is 2.4 L/s per m^2 for swimming pool and deck area [15]. (The breathing zone ranges from 79 mm to 1.8 m above the floor [15].) This corresponds quite good to the values in Table 2-7 given by Byggforsk. There are given two values, one per area of water surface and floor, and one only per area of water surface. The highest value is to be used as the value (c) as described above.

Table 2-7: Minimum ventilation rate of fresh air (outdoor air) according to Byggforsk [8].

Ventilation rate of fresh air per area of water surface and floor	1.4 L/s per m^2
Ventilation rate of fresh air per area of water surface	2.8 L/s per m^2

The total air flow rate should though be larger than the fresh air supply and is set to ensure enough heating and dehumidification of the air. Byggforsk suggests to use between 4 and 7 air changes per hour (ach) for normal swimming pools and between 8 and 10 ach for therapy baths [8]. According to ASHRAE, the number of ach should be 4-6 for normal recreational pools and 6-8 for competition pools with spectators [15]. Therefore, ASHRAE recommend starting with 6 ach and just lower it if possible.
The air volume flow in showers are high due to the large evaporation rate. According to TEK17, the (c) is 54 m^3/h per shower [7].
According to the authors of an ASHRAE journal from 2017, the exhaust air rate should be 2 % to 10 % higher than the supply air to ensure a favourable underpressure in the hall [15]. Here, they recommend using 10 % to be conservative [15]. The underpressure is preventing the humid indoor air to damage the building envelope. Another result of the underpressure is that the outdoor air of same amount as the excess exhaust air will enter the building through infiltration. If the outdoor air is colder and contains less water than the indoor air, this effect dehumidifies and cools the indoor air.

The air must enter the hall with some air velocity to be able to mix the air sufficiently. A study done by Smith, C. C., et al, where they measured evaporated water by measuring the water level, states that a higher air velocity results in higher evaporation rate [16]. This effect also works on wet bodies, where a too high air velocity will speed up the evaporation on the bodies and have a cooling effect. So, both to minimize pool water evaporation and to ensure comfort for the users, the air velocity should be limited. ASHRAE states that the air velocity should be below 0.5 m/s while The Norwegian Labour Inspection Authority recommend a maximum air velocity of 0.15 m/s in occupied zone [17] [18].

2.4.2 Temperature

The temperature should be comfortable to the users of the swimming hall as well as it should minimize the evaporation from the swimming pool. A low air temperature will speed up the evaporation rate from the body and can be similar to the feeling of draft while a high air temperature will make the water feel cold. So, both a too high and too low air temperature can result in thermal discomfort for the users.

Regarding evaporation, a higher air temperature is favourable. This is seen of Equation (2-7) since a higher temperature implies a higher saturation pressure at room air dew point which again means a lower evaporation rate.

As stated by Byggforsk, a normal rule is that the air temperature should be 2 °C higher than the water temperature [11].

2.4.3 Humidity

The humidity should have upper restrictions to reduce possibility of damages on the building structure. An overview over sources for process-caused building damages shows that up to 76 % of all damages is caused by humidity [19]. This study though, is based on damages in the period 1993-2002, a period where the requirements for U-values was less strict than today's new buildings. Condensation is a huge risk to building damage and occurs when the inner surfaces reach the dew point temperature. Simple hand-calculations give us some indication of window inside surface temperature. Figure 2-3 shows the resulting surface temperature given an inside air temperature of 30 °C.

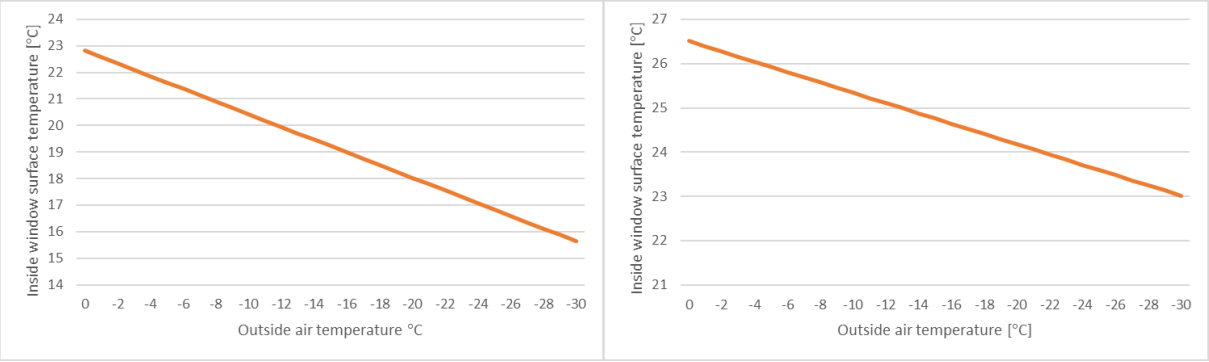

Figure 2-3: Graphs of window inside surface temperature as a function of outside air temperature (total U-value of windows: 2 W/m^{2}K (left graph) 0.8 W/m^{2}K (right graph))

For normal outdoor temperatures, the inside surface temperature will be over about 18 °C for a window with a U-value of 2 W/m^{2}K and about 24 °C for a window with a U-value of 0.8 W/m^{2}K. During winter, with an indoor air temperature at 30 °C and a dew point temperature of 18 °C, a RH of approximately 50 % will be enough for condensation to occur as shown in Figure 2-4. For the window with a dew point temperature of 24 °C, a RH of approximately 70 % will be enough for condensation to occur. This illustrates the difference between new and old windows. Anyway, Byggforsk recommend a RH below 55 % during winter and below 65 % rest of the year to reduce risk of building damage [8].

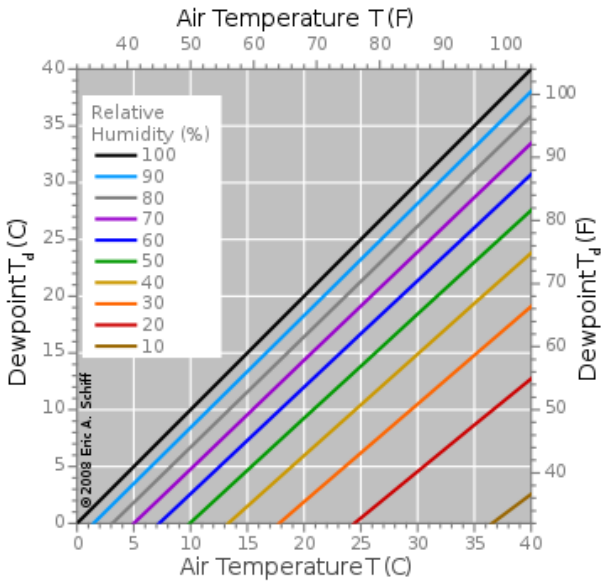

Figure 2-4: Graph of dewpoint as a function of air temperature at varying RH [20]

The lower limit for RH is set to ensure a comfortable indoor climate for the users of the pool. A RH below 50 % will give the users the same feeling as draft, due to increased evaporation from the body [8].

Table 2-8: Recommended RH depending on season [8]

Recommended RH setpoints during winter	50-55 %
Recommended RH setpoints rest of the year	50-65 %

2.4.4 Ventilation methods

The usual way to ventilate a pool facility is to supply dry hot air to the window façade with intention to avoid condensation. The air is supplied from bottom of the window façade, rises along the façade and mixes in the room afterwards. A combination of high and low return air should ensure a good mixing and effective removal of chloramines as well as it prevents stratification [21]. For the calculated example in section 2.4.3, where there in theory would occur condensation at the window on the coldest days, this ventilation method would be a possible solution.

For new swimming facilities that are built as passive house buildings, or even better, does not necessarily need the air supplied along the window façades. This is the case for a swimming facility at Jøa in the northern part of Trøndelag. This facility has a type of displacement ventilation with supply in the ceiling and return air at deck level while the supply under the windows is just for security [6]. The air is mixed due to convective forces from the evaporation and natural convection along the window façade [6].

2.5 Air handling unit

Table 2-9: Requirements regarding components in the AHU [7] [10]

	TEK17	NS3701
Heat recovery efficiency [%]	≥ 70	≥ 80
Specific fan power (SFP) factor [kW/(m^3/s)]	≤ 2.0	≤ 1.5

2.5.1 Dehumidifying

Johansson et al. describes the three most used dehumidification techniques for swimming facilities, which are the conventional system, the mechanical heat pump system and the open absorption system [22]. They all dehumidify the air as well as heat is recovered to some extent.

2.5.1.1 The conventional system

At least in Norway, the outdoor air contains quite little water compared to the indoor air in a swimming pool. This is utilized in the conventional system where outdoor air is heated up and supplied to the building. This method is very energy demanding, so the outdoor air is mixed with a circulation flow from the swimming pool facility to reduce need of heating to some extent. This is anyway not an energy efficient way to do dehumidification. [22]

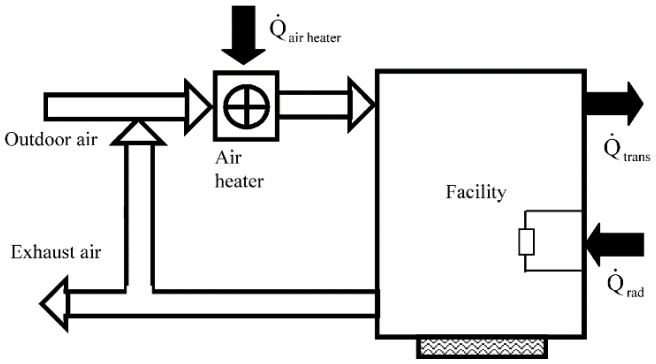

Figure 2-5: Conventional dehumidifying system [22]

2.5.1.2 The mechanical heat pump system

Many of today's swimming pool facilities use a mechanical heat pump in the AHU to dehumidify the air. This is done by cooling a part of the air from the swimming facility through the heat pump evaporator, and water vapor is condensed. This dehumidified air is then first mixed with rest of the exhaust air, and secondly part of the exhaust air is mixed with outdoor air before heated through the heat pump condenser. A heating coil is placed after the heat pump condenser to ensure a correct supply air temperature. When the swimming pool is closed, the air only circulates, and no outdoor air is supplied. [22]

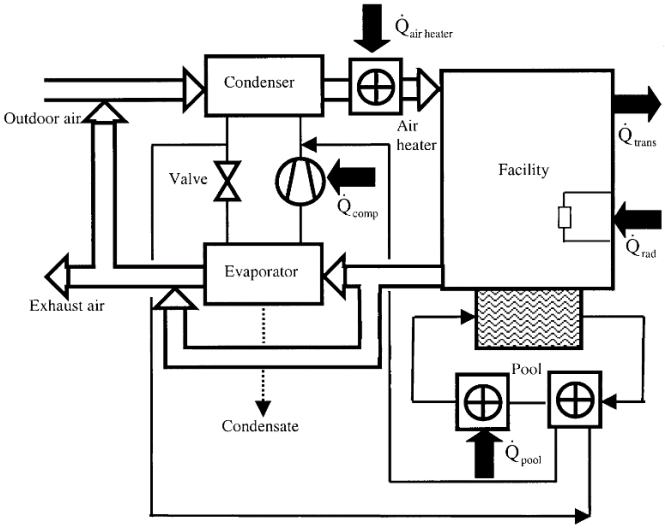

Figure 2-6: Mechanical heat pump dehumidifying system [22]

2.5.1.3 The open absorption system

In this system, an absorber is used to remove water vapor from the circulated air before mixing with the outdoor air and then heated in a heating coil. As well as the air is dehumidified, the air temperature is increased somewhat through the absorber. The absorption solution in the absorber transports the water to a boiler. Since the boiling-point of the absorption solution is higher than for the water, the water is evaporated. The absorption solution is brought back to the absorber while the water vapor is brought to a condenser where heat is released to e.g. pool water. Similar to the system with mechanical heat pump, the air only circulates outside the opening hours for the swimming pool since the absorption solution absorbs the evaporated water. [22]

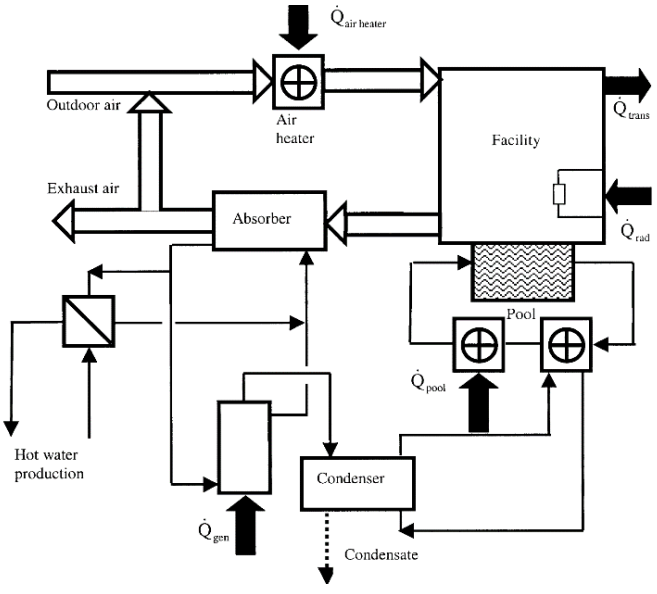

Figure 2-7: The open absorption dehumidifying system [22]

2.5.2 Mollier diagram (HX)

The Mollier diagram is known as a basic design tool for engineers and is an illustration of the relationship between air enthalpy, moisture content and temperature. The diagram was created in 1904 by Richard Mollier, a professor of mechanical engineering [23]. The different processes in an AHU is described and illustrated in the Mollier diagram in Figure 2-8.

HEATING in terms of sensible heat is illustrated with a vertical arrow directing upwards as the red one in Figure 2-8. This means an increase in temperature and enthalpy. The air maintains the same absolute humidity, but a decreased relative humidity.

COOLING in terms of sensible cooling is illustrated with a vertical arrow directing downwards as the dark blue one in Figure 2-8, just opposite of heating. The temperature and enthalpy decrease, the absolute humidity stays the same while the relative humidity increases. Sensible cooling occurs when air is cooled by a surface with a temperature above the dewpoint temperature of the air. In Figure 2-8, the dewpoint (DP) for "Air 1" is marked at the saturation curve. The dewpoint temperature is the corresponding temperature of this point, about 20.5 °C for "Air 1".

DEHUMIDIFICATION in terms of latent cooling is illustrated with an arrow directing downwards to left as the light blue one in Figure 2-8. In this case, the air is cooled by a surface with a temperature below the dewpoint temperature of the air. The resulting air is along the line from the original air condition to the saturation point of the cold surface. In Figure 2-8, "Air 1" is cooled by a surface with surface temperature 18 °C. The resulting air ends up on a line between "Air 1" and the saturation point at 18 °C. The more the air is cooled by the surface, the further down this line the air ends up.

MIXING of two airflows is illustrated with purple arrows in Figure 2-8. Here "Air 1" and "Air 2" is mixed and the resulting mix ends up on a straight line between these air properties in the Mollier diagram. In the example in Figure 2-8, the portion of "Air 1" is slightly larger than the portion of "Air 2". Therefore, the resulting air mix ends up closer to "Air 1" than "Air 2".

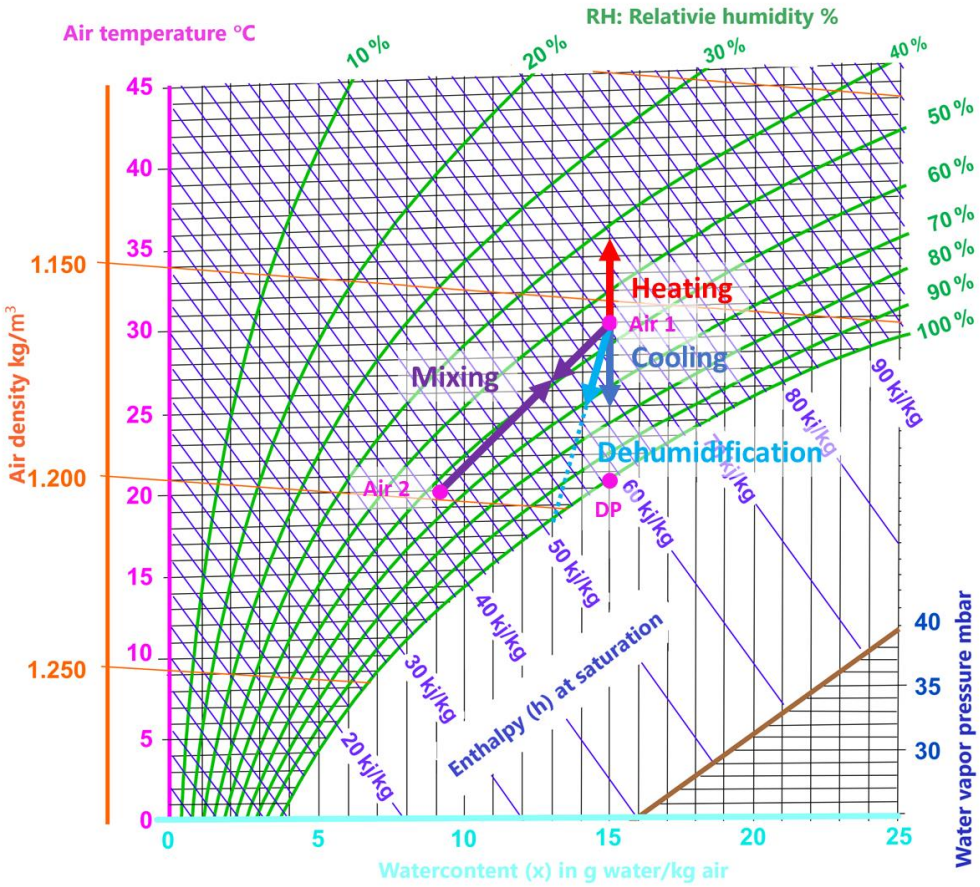

Figure 2-8: Mollier diagram illustrating the AHU processes

2.6 Power calculations

Equation (2-10) shows the calculation of power given to (if positive) or extracted from (if negative) an airflow as in Figure 2-9.

$$Q = \dot{m} * c_p * \Delta T = \dot{m} * C_p * (T_2 - T_1) \quad (2\text{-}10)$$

Where Q is the power [kW], $\dot{m}$ is the massflow [kg/s], C_p is the specific heat capacity [kJ/(kg*K)] and T is temperature [°C]. The specific heat capacity of air is varying with temperature as tabulated in Table 2-10.

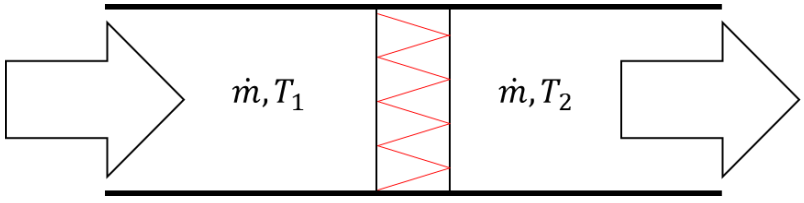

Figure 2-9: Illustration of an airflow with mass $\dot{m}$ in a pipe being heated from T_1 to T_2

Table 2-10: Specific heat capacity of air [24]

Temperature [K]	C_p [kJ/(kg*K)]
240	1.003
260	1.003
280	1.004
300	1.005
320	1.006

2.7 Existing energy evaluation methods

To be able to evaluate the energy use of a building, the value for energy use must be comparable to e.g. restrictions and to other buildings. Therefore, researchers should use the same building energy index in their research. As well as it is important that the energy index is comparable, it should really characterize the energy use.

2.7.1 Energy efficiency index (EEI)

The EEI is known to be the most commonly used index for comparing performance of energy use in buildings [25]. Just the fact that it is widely spread makes it beneficial to use. EEI is presented in Equation (2-11) as the ratio of energy input to a factor related to the energy using component [25].

$$\text{EEI} = \frac{\text{Energy input}}{\text{Factor related to the energy using component}} \tag{2-11}$$

The energy input is mostly defined as energy consumption (kWh) during a year or another appropriate timespan. Regarding the "factor related to energy using component", area (m^2) is a often used factor for most building types. In TEK17, the requirements for maximum net energy consumption use the factor area (m^2).

For swimming pools, the most commonly used factors related to the energy using component is usable area (UA) and water surface area (WS). These corresponds to the EEI kWh/m^2_{UA} and kWh/m^2_{WS}. According a study by Wolfgang Kampel, the delivered energy can have low values when water surface is used and high values when usable area is used and vice versa [26]. In the same study, an analysis showed that the correlation between delivered energy and water usage is highest, followed by the correlation between delivered energy and visitors [26]. Based on the same study, Bjørn Aas claims that one should use kWh/m^2 when comparing swimming pools with other types of buildings and kWh/visitor when comparing different swimming pools [27].

3. Methodology

To characterize the thermal energy needs of a swimming pool, the building performance simulation software IDA ICE is used together with a dedicated extension for swimming pools and ice rinks. This tool is used to build a model of a pool facility in Trondheim and is validated by comparing the results to measurements from the same pool. In this section, IDA ICE, the modelling of the facility and the measurements are described.

3.1 IDA ICE

IDA ICE is a simulation tool for indoor climate and energy by EQUA Simulation AB, a Swedish company founded in 1995 [21]. The tool allows the user to model a building with its technical systems and do simulations to ensure a low energy consumption and best possible indoor climate. The tool uses Neutral Model Format (NMF) and is transparent, so the user can easily look into the NMF to figure out how components work. The possibility to log any variable is also an advantage of this simulation tool. In IDA ICE, the air in a zone is assumed fully mixed. Therefore, simulation in IDA ICE does not give results for local differences in a zone.

For the IDA ICE version 4.7.1, the old version, sensitivity analysis is done by a method called "simulation tree". In this method, a mother version is made first and then one can make one or more child versions with changing parameters to perform sensitivity analysis. Then, by changing anything in the mother version, all child versions are changed as well. The downside of this method is that the sensitivity analysis is restricted to the number of child versions made. So, it is not a continuous sensitivity analysis between some borders. Another downside is that one must extract the results manually from each of the child versions, which is quite time-consuming for good analyses.

In the new version of IDA ICE, version 4.8, there is a method for sensitivity analysis called parametric run. This allows the user to choose an input parameter to be changed and one or more output parameters for use in the sensitivity analysis. The user can then decide the number of simulations for the input parameter between a minimum and a maximum value. This means that the parametric run does not provide a continuous sensitivity analysis, but by increasing the number of simulations, the resulting sensitivity analysis is getting closer to continuous. IDA ICE can also plot the input parameter against the output in a diagram defined by the user. The parametric run is much easier and faster to use than the simulation tree, so IDA ICE version 4.8 and parametric run is used in this master thesis.

3.1.1 Pool extension

To be able to simulate a pool in IDA ICE, the ice rinks and pools extension is needed. This extension provides the opportunity to simulate an open water surface in a zone and the needed heating of the water as illustrated in Figure 3-1. Mass transfer, as well as heat transfer is simulated between the water surface and the zone.

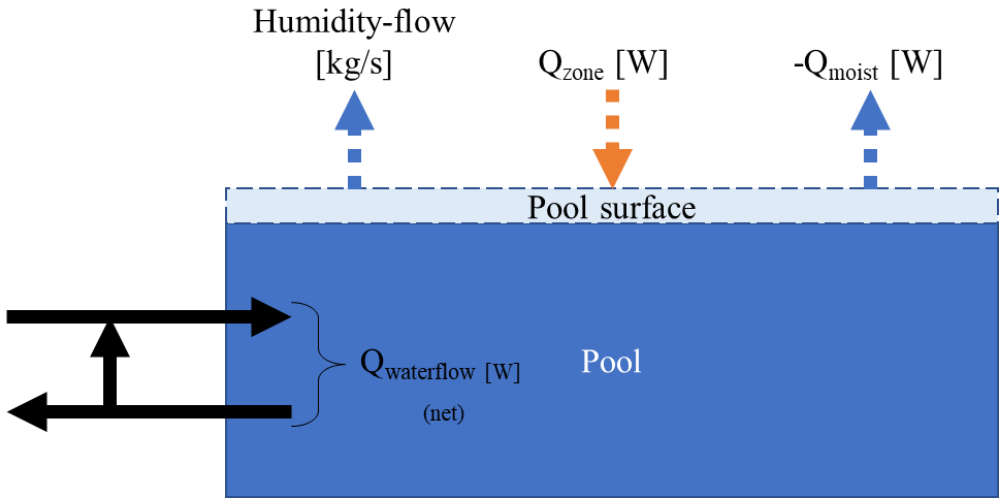

Figure 3-1: Illustration of pool-system in IDA ICE (Q_{moist} is negative due to opposite direction in IDA ICE)

3.1.2 IDA ICE components in the AHU

3.1.2.1 Heat recovery unit

The heat recovery unit in IDA ICE is a latent heat recovery unit with temperature control. An effectiveness parameter eta is set by the user. The supply temperature of the heat recovery unit is if possible adjusted to the given setpoint. The capacity control is attained by adjusting the eta from 0 to the value set by the user.

The dewpoint is set as the entering temperature of the opposite medium. So, the dewpoint for the exhaust air is set as the entering supply air. Leaving air state lies on a straight line between entering air state and the apparatus dewpoint as shown in the Mollier diagram in Figure 3-3.

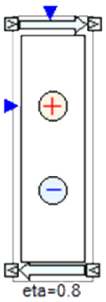

Figure 3-2: IDA ICE heat recovery unit

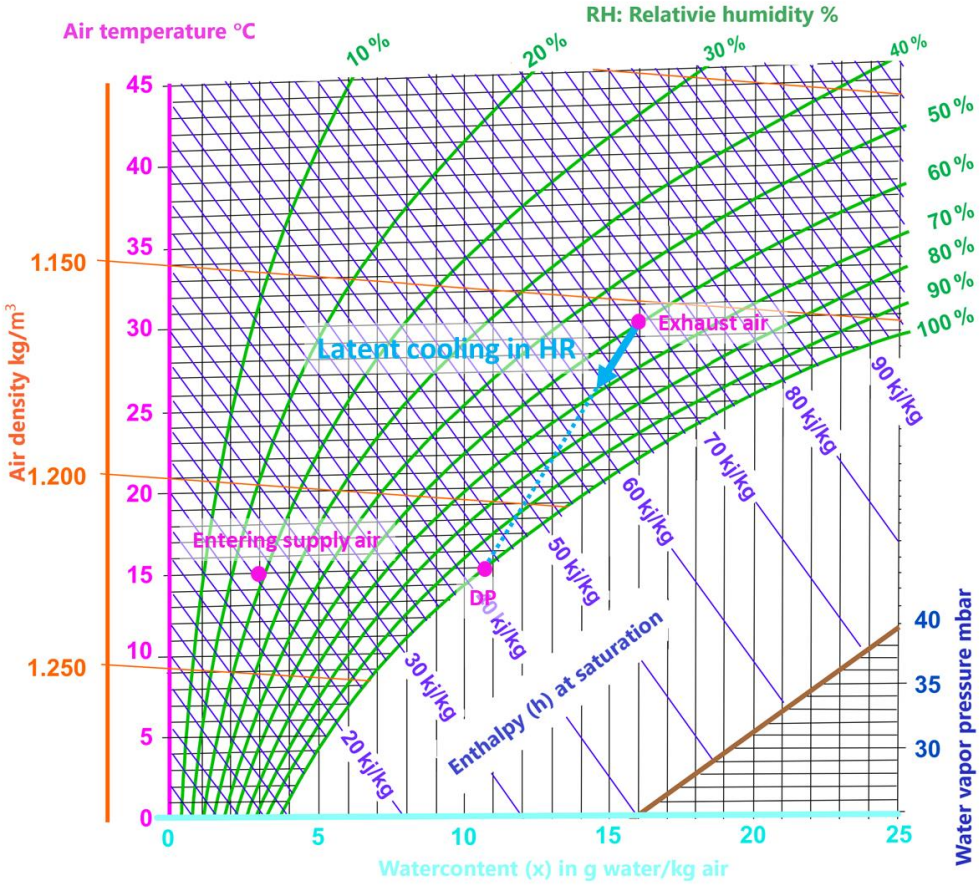

Figure 3-3: Mollier diagram illustrating the working of the IDA ICE heat recovery unit

3.1.2.2 Mixing box

The mixing box in IDA ICE can be controlled in two ways. Either by governing the fresh air mass flow or by governing the fraction fresh air over supply air. The model takes account of possible condensation in the mixing process. The process is illustrated in Figure 2-8 and further described in section 2.5.2.

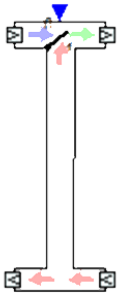

Figure 3-4: IDA ICE mixing box

3.1.2.3 Fan

The fan in IDA ICE is on/off controlled and ensures a given pressure rise as well as a temperature rise. The temperature rise is either given or calculated based on the motor effect. The efficiency of the fan is set as a given eta.

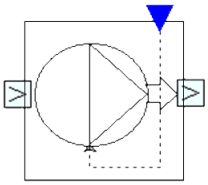

Figure 3-5: IDA ICE fan

3.1.2.4 Sensor

The sensor component in IDA ICE can measure different parameters and one can log the parameters to an output-file or connect the output of the sensor to another component. The parameters possible to measure is the following:

Pressure difference [Pa]
Mass flow [kg/s]
Temperature of air flow [°C]
Pollutant ratio of air flow [µg/kg dry air]
Relative humidity of air flow [%]
Airflow [L/s]
CO_2 ratio [PPM (vol)]
Enthalpy [J/kg]
Humidity ratio [kg/kg]
Wet bulb [°C]
Dew point [°C]

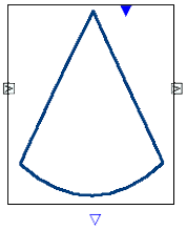

Figure 3-6: IDA ICE sensor

3.1.2.5 Heating coil (electric)

The electric heating coil in IDA ICE is a temperature-controlled heater with a given electrical effect. The process is showed in the Mollier diagram in Figure 3-8.

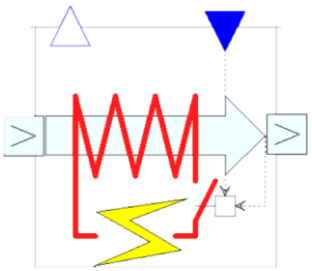

Figure 3-7: IDA ICE electrical heater

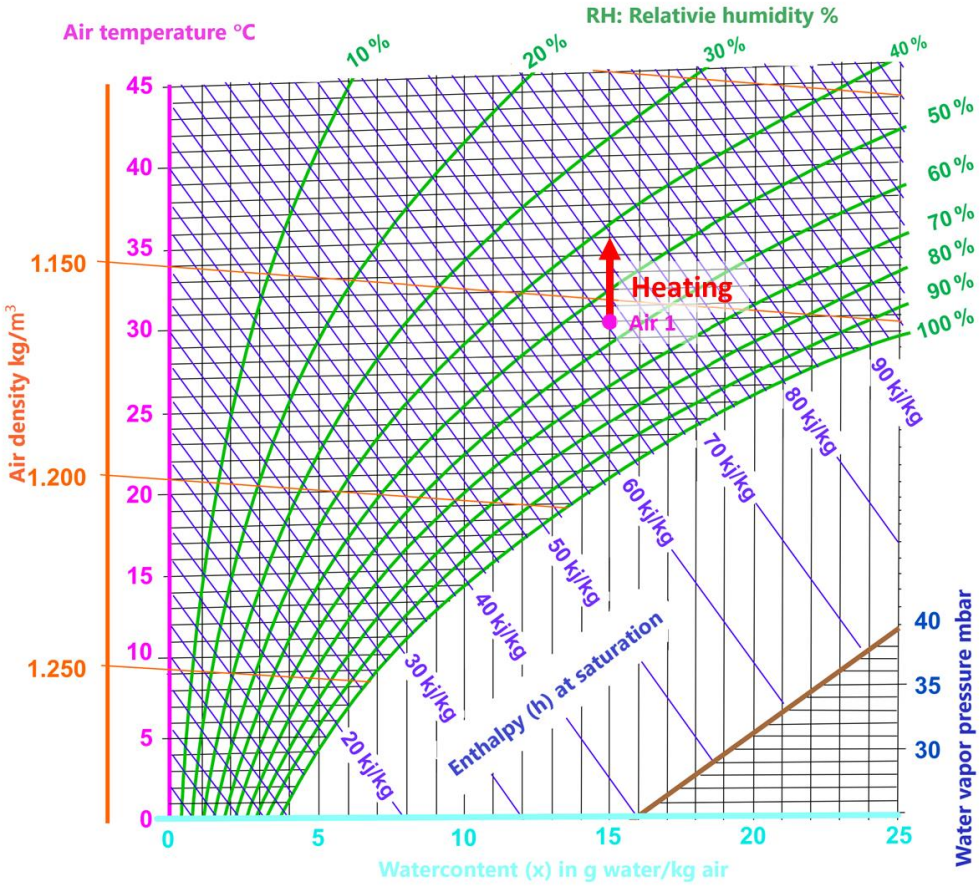

Figure 3-8: Mollier diagram illustrating the working of the IDA ICE heater

3.1.2.6 Cooling coil

The cooling coil in IDA ICE is a temperature controlled liquid cooler. The liquid side temperature drop is given while the effect is adjusted by liquid flowrate. The process is showed in the Mollier diagram in Figure 3-10.

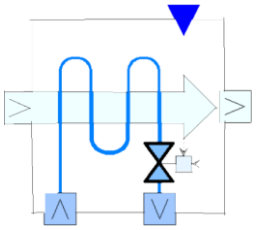

Figure 3-9: IDA ICE cooling coil

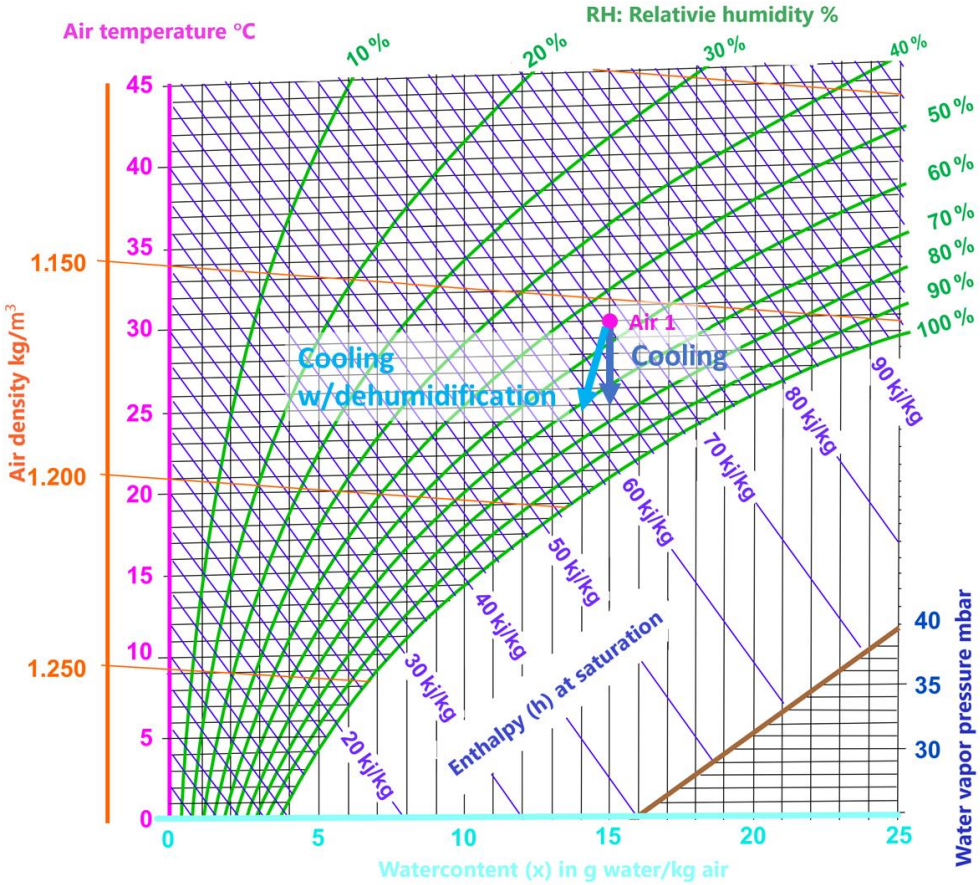

Figure 3-10: Mollier diagram illustrating the working of the IDA ICE cooler

3.2 Swimming pool for validation

3.2.1 Requirements

Before choosing a swimming facility for validation of the IDA ICE model, there were made some requirements to increase the quality of the validation. First of all, the swimming facility should be possible to model. Most likely, the facility should be easy to model to reduce the possibility of errors. A rectangular hall with a rectangular pool is sort of the “best case”.

In order to make a good model of the indoor swimming pool climate, the airflows in and out of the hall, for example through doors and patches, should be known. But this is often not known, so the absolute best case would be a hall without any open doors or other openings.

An important requirement is that the AHU must only serve the modelled swimming hall. Else, the energy use of the AHU does not correspond to the need of the modelled swimming hall.

To be able to use a swimming facility in this validation, availability for both installation and if necessary, changing the setup of the sensors in the AHU was essential.

3.2.2 Location & climate

The used swimming facility in this project was Pirbadet in Trondheim, at 63°26'27"N 10°24'05"E. The swimming facility is built just beside the sea water in the harbour of Trondheim. Trondheim has a climate close to a maritime climate. Between 1946 and 2018, the coldest month average temperature was -3.2 °C (January), while the warmest month average temperature was 13.9 °C (July) [28].

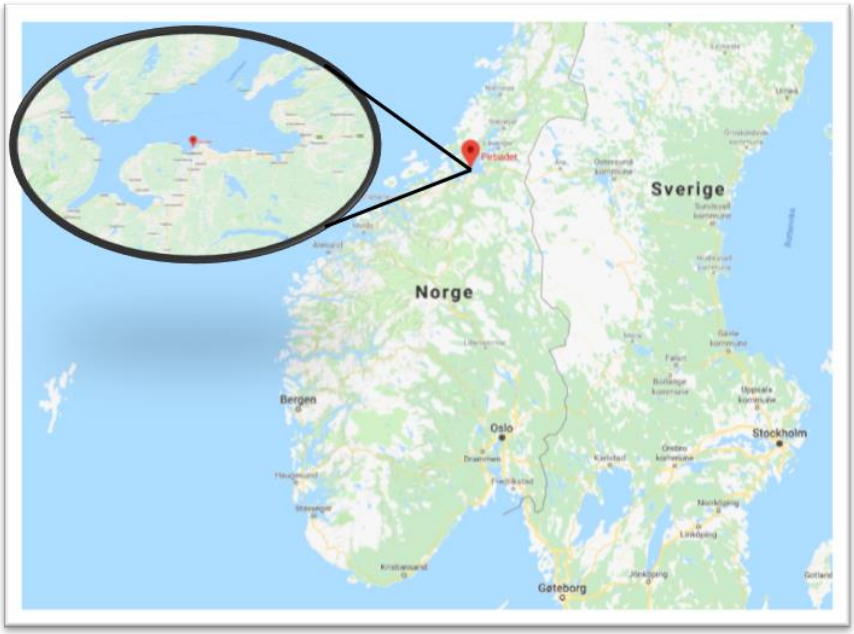

Figure 3-11: Location of Pirbadet in Trondheim (Norway) [29]

3.2.3 The building

Pirbadet in Trondheim is a large swimming facility with several pools of different kinds that opened in June 2001 [30]. There are for example pools dedicated to swim training for children, whirlpools, water slides, hot water pools and swimming pools for adults. In this project, two hot water pools that are connected to the same AHU is studied. These pools (pool 1 & pool 2) are in separated halls (respectively H1 & H2) just beside each other as shown in Figure 3-12. The same AHU is also serving a small steam sauna marked yellow in Figure 3-12.

The only external wall for these halls is the one marked with green colour in Figure 3-12. This is mostly covered by windows. Rest of the walls are internal walls facing against rest of the building. The internal walls marked with yellow colour are facing a fitness studio, while the walls marked with red are facing rest of the swimming facility and the sauna area.

The building is rotated such that the external façade is facing north-east.

Both pools have a water temperature of 34 °C and a hall air temperature of 30.8 °C. Both pools have an average depth of about 1.5 meters. Pool 1 is 149 m^2, while Pool 2 is 192 m^2 in size.

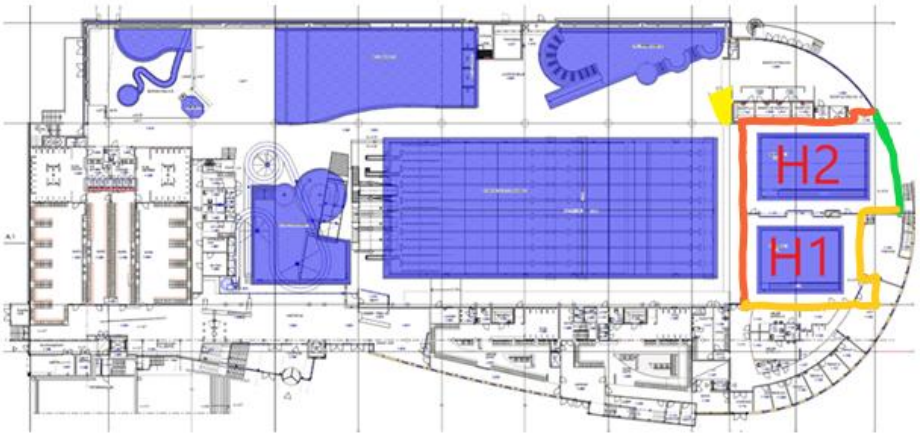

Figure 3-12: Blueprint of ground floor in Pirbadet in Trondheim

3.2.4 Use of the pools

The two hot water pools are normally used for group sessions by the local fitness studio (H2) and physiotherapy activity by the local physiotherapists (H1) during weekdays. H2 is on the other hand normally open for all users in the weekends (Saturdays and Sundays) while H1 is locked.

After doing some research (asking the employees in Pirbadet), a reasonable average use would be about 20 persons in each group session in H2 and 12 in H1. The group sessions in H2 are scheduled from 9am until 2pm and from 4pm until 8pm, each with a duration of one hour. The group sessions in H1 are scheduled from 15pm until 18pm, also these with a duration of one hour.

3.2.5 Ventilation system

The ventilation system serves both H1 and H2 as well as a steam sauna. The AHU for this system is a MENERGA ThermoCond product from 2016 with maximum delivering capacity of 25 000 m^3/h. The AHU is set to hold the air temperature in the halls at 30.8 °C and the RH at 55 % as well as to ensure fresh air and a small underpressure in the halls.

The defrosting damper is used to avoid frost in the supply side of the heat recovery unit. By opening the defrosting damper and at the same time closing the fresh air damper, the warm return air will heat up the supply side of the heat recovery unit and remove frost.
The dehumidification damper is opened when the dehumidifier is used for dehumidifying. Dehumidified air is then mixed together with the fresh air before supplied again.
The recirculation damper opens when there are less or no need of dehumidification or fresh air. The return air is then sent to supply air for recirculation (and heated if necessary).

The heat pump in the AHU in Pirbadet is placed as illustrated in Figure 3-13. The heat pump consists of an evaporator (the dehumidifier) and three condensers. The only condenser considered in this thesis is the one heating the ventilation air in the AHU, placed just after the heat pump. Else, there is a condenser for the pool water heating and a subcooler.

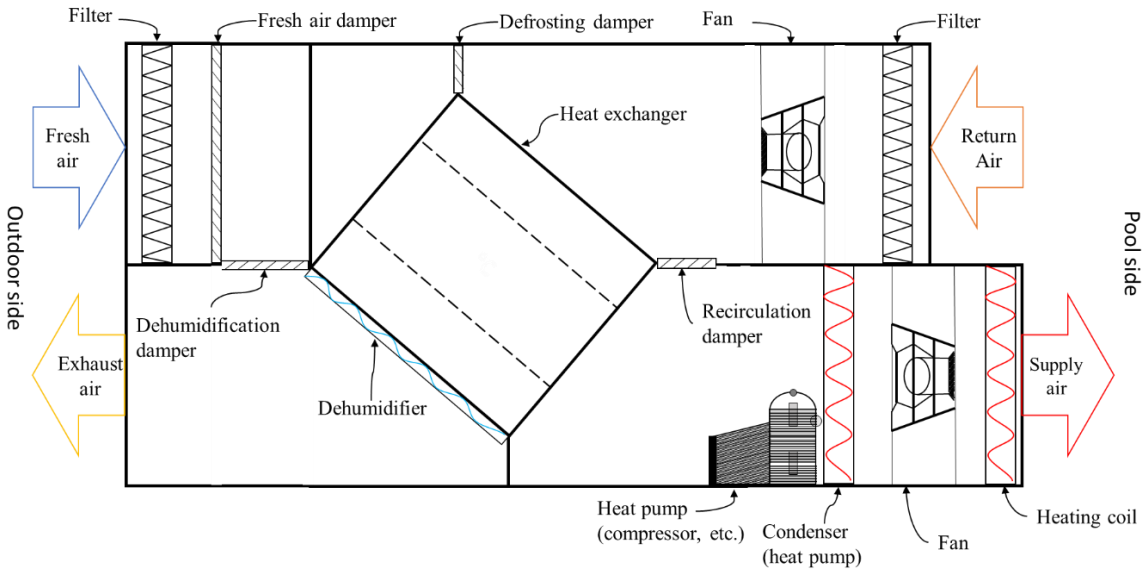

Figure 3-13: Sketch of the MENERGA AHU in Pirbadet in Trondheim

3.2.5.1 Air handling unit mode

Since the activity of the swimming pool is varying a lot, the return air to the AHU is not constant and the AHU has to react likewise. Different activity factors, as described in section 2.1, introduce different levels of evaporation from the pool. Thereby, the AHU must be able to handle different air loads and be able to control itself.

There are mainly four different modes for a swimming pool AHU described and sketched below.

STANDBY MODE is used when there is no need of fresh air, heating or dehumidification. The AHU only works for circulation of the air. Its function is sketched in Figure 3-14.

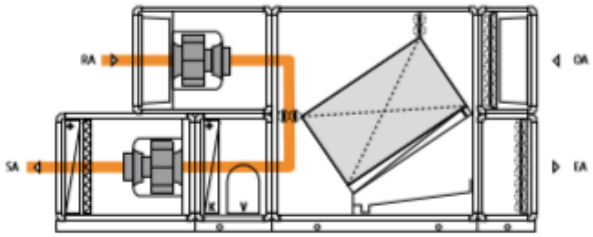

Figure 3-14: AHU in standby mode

RECIRCULATION WITH HEATING MODE is used when there is no need of fresh air or dehumidification, but a need of heating. The AHU recirculates the air and the heat battery heats the supply air before entering the facility. Its function is sketched in Figure 3-15.

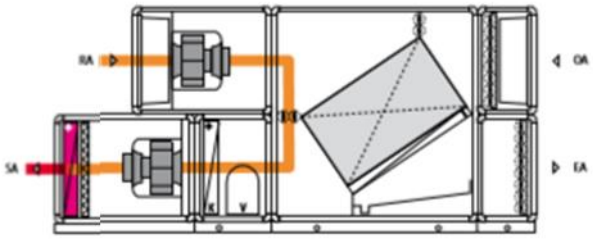

Figure 3-15: AHU in recirculation with heating mode

NORMAL MODE is used when there is need of fresh air, heating and dehumidification. In this mode, a part of the return air goes through the heat recovery unit, which heats the incoming outside air. In an AHU with a mechanical heat pump dehumidifying system, the return air is further cooled in the heat pump evaporator while the supply air is heated in the heat pump condenser.

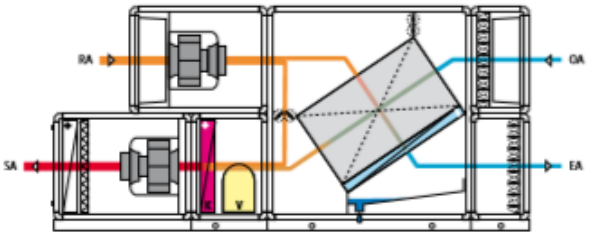

Figure 3-16: AHU in normal mode

OUTSIDE AIR MODE is used when the outside air humidity is sufficient, so that recirculation is unnecessary. In this mode, all the return air is lead through the heat recovery unit. In an AHU with a mechanical heat pump dehumidifying system, the return air is further cooled in the heat pump evaporator before the exhaust. The outside air is first heated through the heat recovery unit and further heated in the heat pump condenser before supplied to the hall.

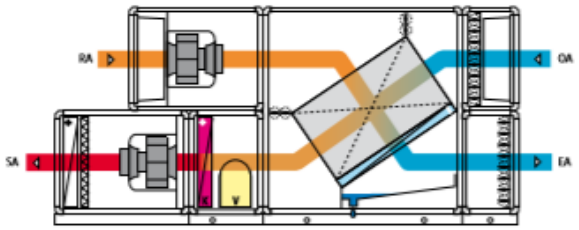

Figure 3-17: AHU in outside air mode

3.2.6 Measurements

3.2.6.1 Purpose

The purpose of doing measurements in the AHU is to be able to compare the in/out airflows to the simulated airflows as well as to be able to compare heating and cooling needs to the simulated model. The measured supply and return air can be used to calculate the evaporation rate from the pool. This can be compared to both standards and simulated model. All these comparisons are done for validation of the IDA ICE model.

3.2.6.2 Equipment

The built-in sensors for volume flow rate were used. They are delivered by SE-ELECTRONIC GMBH and is named M 05 10 61_C-VS3_GB. There were two of these, one placed in the supply air and one in the return air. The sensors measure the pressure difference and temperature difference over the fans and calculate the volume flow rates. The accuracy of the volume flow sensors are ±2 %.

An advantageous scenario would be to measure the volume flow rate in all four in/out airflows. Since there only was these two sensors available, the other airflows had to be calculated.

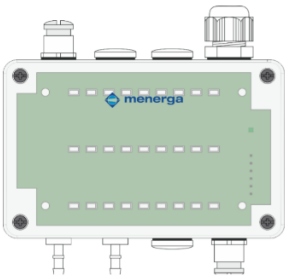

Figure 3-18: Volume flow sensor of type M 05 10 61_C-VS3_GB

For measuring RH and temperature, 6 EasyLog EL-USB-2+ sensors from LASCAR electronics were installed in the AHU. This datalogger measures and stores relative humidity and temperature in the range from 0 to 100 % RH and -35 to 80 °C. The datalogger is protected to IP67 standard when the plastic cap and seal are fitted. The logger can store up to 16 382 readings of RH and the same for temperature and there are 7 optional logging rates (10s, 1m, 5m, 30m, 1hr, 6hr, 12hr). A logging rate of 1 minute was chosen. The accuracy of the RH measurement is ±2.0 %RH and the accuracy of the temperature measurement is ±0.3 °C.
Following loggers were used (sensor name, serial number): (5, 010011449), (3, 010011462), (4, 10203180), (6, 10204439), (7, 010012319), (8, 010011665)

Figure 3-19: RH and temperature data logger of type EL-USB-2+

For measuring the rest of the temperatures, where RH data was not needed, thermocouple probes connected to a 12-channel temperature recorder Lutron Electronic was used. The temperature recorder was of model BTM-4208SD.
The temperature recorder measures and stores temperature in the range of -100 to 1300 °C by using type K thermocouple probes. The data is stored at a 1 GB SD memory card. The accuracy of the temperature measurements in the range from -50 to 999.9 °C is ± (0.4 % + 0.5 °C). The recorder used has serial number 465212.

Figure 3-20: 12 channel temperature recorder (left) and type K thermocouple probe (right)

3.2.6.3 Placing of the sensors

As, stated in section 3.2.6.1, the properties of the airflows in/out of the AHU and the heating and cooling power is of interest. In order to determine these, the sensors showed in Figure 3-21 and Table 3-1 was installed together with the already installed volume flow sensors. The further calculations to determine the airflow rate on the outdoor side of the AHU is shown in section 3.2.6.5.

Airflow 1, 2, 4, 5, 10 and 11 is supposed to be fully mixed since they are just after the fans or in a distance from another components. Airflow 3, 6, 7, 8 and 9 appears just after a damper, the heat recovery unit or the condenser, and is therefore assumed not fully mixed.

Table 3-1: Overview of the sensors

Sensor	*Type*	*Measuring*	*Placement*
1	Integrated	Volume flow	Over the return fan
2	Integrated	Volume flow	Over the supply fan
3	EasyLog	Temperature, RH	Return air, before filter
4	EasyLog	Temperature, RH	Exhaust air, end of AHU
5	EasyLog	Temperature, RH	Fresh air, before filter
6	EasyLog	Temperature, RH	Supply air, attached to end of HR, on upper half
7	EasyLog	Temperature, RH	Supply air, attached to end of HR, on lower half
8	EasyLog	Temperature, RH	Supply air, after heating coil
9	Thermocouple	Temperature	Return air, after fan
10	Thermocouple	Temperature	Supply air before condenser, upper half

11	Thermocouple	Temperature	Supply air before condenser, lower half
12	Thermocouple	Temperature	Supply air, between condenser and fan, upper half
13	Thermocouple	Temperature	Supply air, between condenser and fan, lower half
14	Thermocouple	Temperature	Supply air, between fan and heating coil

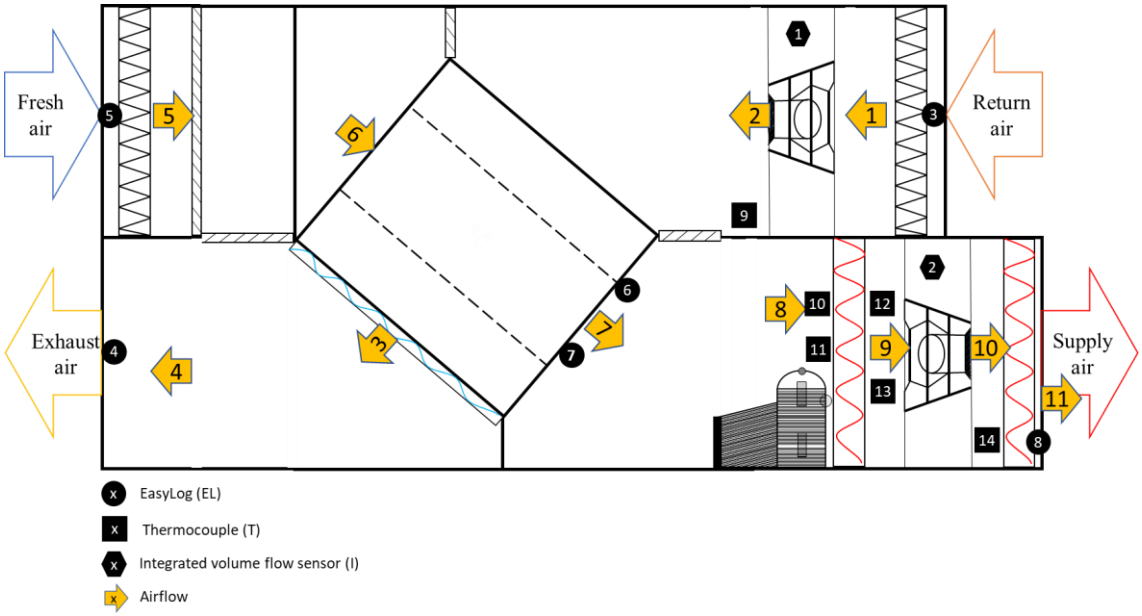

Figure 3-21: Illustration of the placement of the sensors

3.2.6.4 Extraction of measuring data

The temperature data from the 12-channel temperature recorder was imported to a computer as an Excel file (.csv) with a memory card. The data from the EasyLog units were imported to a computer as Excel files (.csv) through its USB-output. The data from the integrated volume flow sensors is stored in the AHU control system. This data was therefore exported from the system to an Excel-file (.csv).

The clock at the AHU user monitor was 22 minutes behind real time, so the data obtained from the integrated AHU sensors was shifted 22 minutes ahead in time to match the other sensors.

The sensors were logging over an extended period of time, but the data used for analysis is from Wednesday April 10th, 2019. Therefore, only this day is considered in rest of this thesis.

3.2.6.5 Determining airflow properties

All the gathered data was put into an Excel sheet for processing. The setup of needed airflow properties below was made, and the dataset was updated with the calculated airflow properties. In order to calculate some of the unknown airflow properties, an Excel extension called hxLib was used[5]. This is an application for calculation of refrigeration technology systems. The functions used was the following:

Specific volume	HX_Vtoerr_trh
Absolute humidity	HX_X_trh

When all the needed airflow properties was set up in the Excel sheet, it was possible to calculate the heating and cooling power as well as the evaporation rate as described in section 3.2.6.6 and 3.2.6.7 below. For all calculations, the atmospheric pressure was used.

Airflow 1

Temperature [°C]	$T_1 = EL3$
Relative humidity [%]	$RH_1 = EL3$
Humidity [$kg_{wet\_air}/kg_{dry\_air}$]	$x_1 = HX\_X\_trh(p, T_1, RH_1)$
Specific volume [m^3/kg_{dry_air}]	$v_1 = HX\_Vtoerr\_trh(p, T_1, RH_1)$
Massflow [kg/s]	$\dot{m}_1 = \frac{\dot{V}_1}{v_1 * 3600}$ *(3-1)*
Volumeflow [m^3/h]	$\dot{V}_1 = I1$

[5] Information about the program can be found here (Norwegian): https://nkf-norge.no/litteratur-dataprogrammer/dataprogrammer/

Airflow 2

Temperature [°C]	$T_2 = T9$	
Humidity [$kg_{wet\_air}/kg_{dry\_air}$]	$x_2 = x_1$	
Specific volume [m^3/kg_{dry_air}]	$v_2 = HX\_Vtoerr\_trh(p, T_2, RH_2)$	
Massflow [kg/s]	$\dot{m}_2 = \frac{\dot{V}_2}{v_2 * 3600}$	*(3-2)*
Volumeflow [m^3/h]	$\dot{V}_2 = \dot{V}_1$	

Airflow 3

Temperature [°C]	$T_3 = T_4$	
Humidity [$kg_{wet\_air}/kg_{dry\_air}$]	$x_3 = x_4$	
Massflow [kg/s]	$\dot{m}_3 = \dot{m}_2 - (\dot{m}_8 - \dot{m}_7)$	*(3-3)*

Airflow 4

Temperature [°C]	$T_4 = EL4$	
Relative humidity [%]	$RH_4 = EL4$	
Humidity [$kg_{wet\_air}/kg_{dry\_air}$]	$x_4 = HX\_X\_trh(p, T_4, RH_4)$	
Specific volume [m^3/kg_{dry_air}]	$v_4 = HX\_Vtoerr\_trh(p, T_4, RH_4)$	
Massflow [kg/s]	$\dot{m}_4 * x_4 = \dot{m}_3 * x_3 - (\dot{m}_6 - \dot{m}_5) * x_3$	*(3-4)*
	$\Rightarrow \dot{m}_4 = \frac{\dot{m}_3 * x_3 - (\dot{m}_6 - \dot{m}_5) * x_3}{x_4}$	*(3-5)*
Volumeflow [m^3/h]	$\dot{V}_4 = \dot{m}_4 * v_4 * 3600$	*(3-6)*

Airflow 5

Temperature [°C]	$T_5 = EL5$	
Relative humidity [%]	$RH_5 = EL5$	
Humidity [$kg_{wet\_air}/kg_{dry\_air}$]	$x_5 = HX\_X\_trh(p, T_5, RH_5)$	
Specific volume [m^3/kg_{dry_air}]	$v_5 = HX\_Vtoerr\_trh(p, T_5, RH_5)$	
Massflow [kg/s]	$\dot{m}_5 * x_5 = \dot{m}_6 * x_6 - (\dot{m}_6 - \dot{m}_5) * x_3$	*(3-7)*
	$\Rightarrow \dot{m}_5 = \frac{\dot{m}_6 * (x_6 - x_3)}{x_5 - x_3}$	*(3-8)*
Volumeflow [m^3/h]	$\dot{V}_5 = \dot{m}_5 * v_5 * 3600$	*(3-9)*

Airflow 6

Temperature [°C]	$T_6 * \dot{m}_6 = T_5 * \dot{m}_5 + T_4 * (\dot{m}_3 - \dot{m}_4)$	*(3-10)*
	$\Rightarrow T_6 = \frac{T_5 * \dot{m}_5 + T_4 * (\dot{m}_3 - \dot{m}_4)}{\dot{m}_6}$	*(3-11)*
Humidity [$kg_{wet\_air}/kg_{dry\_air}$]	$x_6 = x_7$	
Massflow [kg/s]	$\dot{m}_6 = \dot{m}_7$	

Airflow 7

Temperature [°C]	$T_7 = average(EL6, EL7)$	
Relative humidity [%]	$RH_7 = average(EL6, EL7)$	
Humidity [$kg_{wet\_air}/kg_{dry\_air}$]	$x_7 = HX\_X\_trh(p, T_7, RH_7)$	
Massflow [kg/s]	$\dot{m}_8 * x_8 = \dot{m}_7 * x_7 + (\dot{m}_8 - \dot{m}_7) * x_1$	*(3-12)*
	$\Rightarrow \dot{m}_7 = \frac{\dot{m}_8 * (x_8 - x_1)}{x_7 - x_1}$	*(3-13)*

Airflow 8

Temperature [°C]	$T_8 = average(T10, T11)$	

Airflow 9

Temperature [°C]	$T_9 = average(T12, T13)$	

Airflow 10

Temperature [°C]	$T_{10} = T14$

Airflow 11

Temperature [°C]	$T_{11} = EL8$
Relative humidity [%]	$RH_{11} = EL8$
Humidity [$kg_{wet\_air}/kg_{dry\_air}$]	$x_{11} = HX\_X\_trh(p, T_{11}, RH_{11})$
Specific volume [m^3/kg_{dry_air}]	$v_{11} = HX\_Vtoerr\_trh(p, T_{11}, RH_{11})$
Massflow [kg/s]	$\dot{m}_{11} = \frac{\dot{V}_{11}}{v_{11} * 3600}$ *(3-14)*
Volumeflow [m^3/h]	$\dot{V}_{11} = I2$

3.2.6.6 Calculating heating and cooling power

The heating/cooling power in this section is calculated by using Equation (2-10). The specific heat capacity is taken from Table 2-10. Based on an assumed temperature range from 0 °C (273 K) to 40 °C (313 K) in the AHU, the specific heat capacity is assumed constant at 1.005 [kJ/(kgK)] in all further calculations.

Heating power from condenser is calculated based on the properties of airflow 8 and 9:

$$\mathrm{Q_{condenser}} = \dot{m}_8 * 1.005 * (\mathrm{T_9} - \mathrm{T_8}) \quad (3\text{-}15)$$

Heating power from the heating coil is calculated based on the properties of airflow 10 and 11:

$$\mathrm{Q}_{heating\ coil} = \dot{m}_{10} * 1.005 * (\mathrm{T_{11}} - \mathrm{T_{10}}) \quad (3\text{-}16)$$

Cooling power from the dehumidifier is a bit trickier to calculate since the temperature between the heat recovery unit and the dehumidifier (T_b) is unknown. This temperature is also hard/impossible to measure as the dehumidifier and heat recovery unit are too close to each other. One way to calculate T_b is to use Equation (2-10) and set the heat recovery unit heating power (Q_h) equal to the heat recovery unit cooling power (Q_c) as in Equation (3-17) below.

$$\dot{m}_6 * 1.005 * (\mathrm{T_7} - \mathrm{T_6}) = \dot{m}_3 * 1.005 * (\mathrm{T_2} - \mathrm{T}_b) \quad (3\text{-}17)$$

And then isolating T_b on the left side.

$$T_b = \frac{\dot{m}_3 * T_2 - \dot{m}_6 * (T_7 - T_6)}{\dot{m}_3} \quad (3\text{-}18)$$

The resulting cooling power from the dehumidifier is defined in Equation (3-19).

$$Q_{DH} = \dot{m}_3 * 1.005 * (T_b - T_3) \quad (3\text{-}19)$$

Delivered heating power to the swimming hall through ventilation is calculated with the mass flow in the supply and the difference between supply air and return air temperature.

$$Q_{hall} = \dot{m}_{11} * 1.005 * (T_{11} - T_1) \quad (3\text{-}20)$$

Dumped heating power to the outdoor is calculated the same way as the delivered heating power to the swimming hall through ventilation. It depends on the exhaust mass flow and the difference between exhaust airflow and fresh airflow (outdoor) temperature.

$$Q_{dumped} = \dot{m}_4 * 1.005 * (T_4 - T_5) \quad (3\text{-}21)$$

3.2.6.7 Calculating evaporation rate of the swimming pools

As long as the indoor humidity is kept constant, the difference between water content in return air and supply air to the swimming halls equals the evaporation rate from the pools. This is not completely true since some dry air from outside and the fitness studio is infiltrated and dries the air as well as some air leaks from the halls to the surrounding halls. These airflows are however neglected in order to limit the workload of this thesis. Also, the activity in the steam sauna is neglected. The indoor humidity might not always be constant, but the average indoor humidity should be more or less constant due to the control of the AHU.

The water content in the return and supply airflow is the product of massflow [kg/s] and humidity [kg_{water}/kg]. Therefore, the evaporation rate from the pools is the following.

$$\dot{m}_{evap} = \dot{m}_1 * x_1 - \dot{m}_{11} * x_{11} \quad (3\text{-}22)$$

By multiplying $\dot{m}_{evap}$ with 3600, the evaporation rate in kg per hour is achieved.

3.2.6.8 Temperature after heat recovery unit in supply air

As illustrated in Figure 3-21, there are placed two sensors after the heat recovery unit in the supply air (EL6 and EL7). The logged temperatures from these sensors are presented in a graph to check if there are any difference of matter between them. A hypothesis is that the dehumidifier connected to the bottom side of the heat recovery unit cools the air in the lower part where EL 7 is placed.

3.2.6.9 Fault analysis

When doing measurements, measuring fault is something that will occur. The error is possible to reduce by using more accurate measuring equipment, but it cannot be eliminated. Often the uncertainty of a measured result is dependent on several individual factors, and the outcome is not available before several parameters have been measured. There was done a fault analysis based on the accuracy of the sensors used. The fault is presented as a shaded error band around the lines in the graphs in the chapter with results.

The fault analysis method used is the Gauss' law of error propagation.

$$\mathrm{N} = \mathrm{f}(\mathrm{u}_1, \dots, u_n) \tag{3-23}$$

Where N is the result of the function and u_1 to u_n is the individual factors that are directly measured. Each measured factor has its own uncertainty Δu_1 to Δu_n.

The goal is to find the uncertainty (ΔN) of the function N.

$$\mathrm{N} \pm \Delta\mathrm{N} = \mathrm{f}(\mathrm{u}_1 \pm \Delta\mathrm{u}_1, \dots, u_n \pm \Delta\mathrm{u}_n) \tag{3-24}$$

Isolating $\pm\Delta$N on one side:

$$(\mathrm{N} \pm \Delta\mathrm{N}) - N = \pm\Delta\mathrm{N} \tag{3-25}$$

By using a Taylor's series development where elements of higher order are removed, the following can be found:

$$\mathrm{f}(\mathrm{u}_1 \pm \Delta\mathrm{u}_1, \dots, u_n \pm \Delta\mathrm{u}_n) - \mathrm{f}(\mathrm{u}_1, \dots, u_n) = \frac{\delta f}{\delta u_1}\Delta u_1 + \cdots + \frac{\delta f}{\delta u_n}\Delta u_n \tag{3-26}$$

The resulting error can then be predicted as:

$$\Delta\mathrm{N} = \pm\sqrt{\left(\frac{\delta f}{\delta u_1}\Delta u_1\right)^2 + \cdots + \left(\frac{\delta f}{\delta u_n}\Delta u_n\right)^2} \tag{3-27}$$

The calculations for the error propagation are presented in Attachment 2.

3.3 The pool and AHU model

3.3.1 Location and climate

In IDA ICE there are some predefined weather files that can be downloaded from a database. In this master thesis, the weather file for Værnes in Stjørdal, at 63°28'01"N 10°55'59"E, is used. Værnes is just 25 km east of Pirbadet (Trondheim), is at the same altitude and has the same climate. The different locations are showed in Figure 3-22.

Figure 3-22: Map with placing of Pirbadet (black arrow) and Værnes (orange arrow)

3.3.2 Designing the building model

3.3.2.1 Sizing

The model made in IDA ICE is representing the two swimming halls and the steam sauna connected to the same AHU. The swimming halls H1 and H2 are in reality divided by a wall, but since the ventilation rate for the two halls is unknown, they are modelled as one zone together with the steam sauna. For simplicity, the steam sauna is only represented as extra area in the bottom right corner in Figure 3-23.

The model is rotated with the external facade facing east.

The model is sized after the blueprint in Attachment 1. Since the lengths of all elements are not on the blueprint, an estimation based on ratios on the blueprint is done. The resulting lengths are shown in Figure 3-23. The height used in the IDA ICE model is the height of the two halls which is measured to 3.5 meters. At the external wall, there is a window covering the whole width. The window starts at floor height and is 2.3 meters high.

The pools are both modelled with a depth of 1.5 meters. Pool 1 is 13.8 x 10.8 meters and Pool 2 is 17.8 x 10.8 meters. The placing of the pools in the zone is not of importance for the

simulation since IDA ICE operates with the zone as a point. However, the pools are placed more or less as in reality.

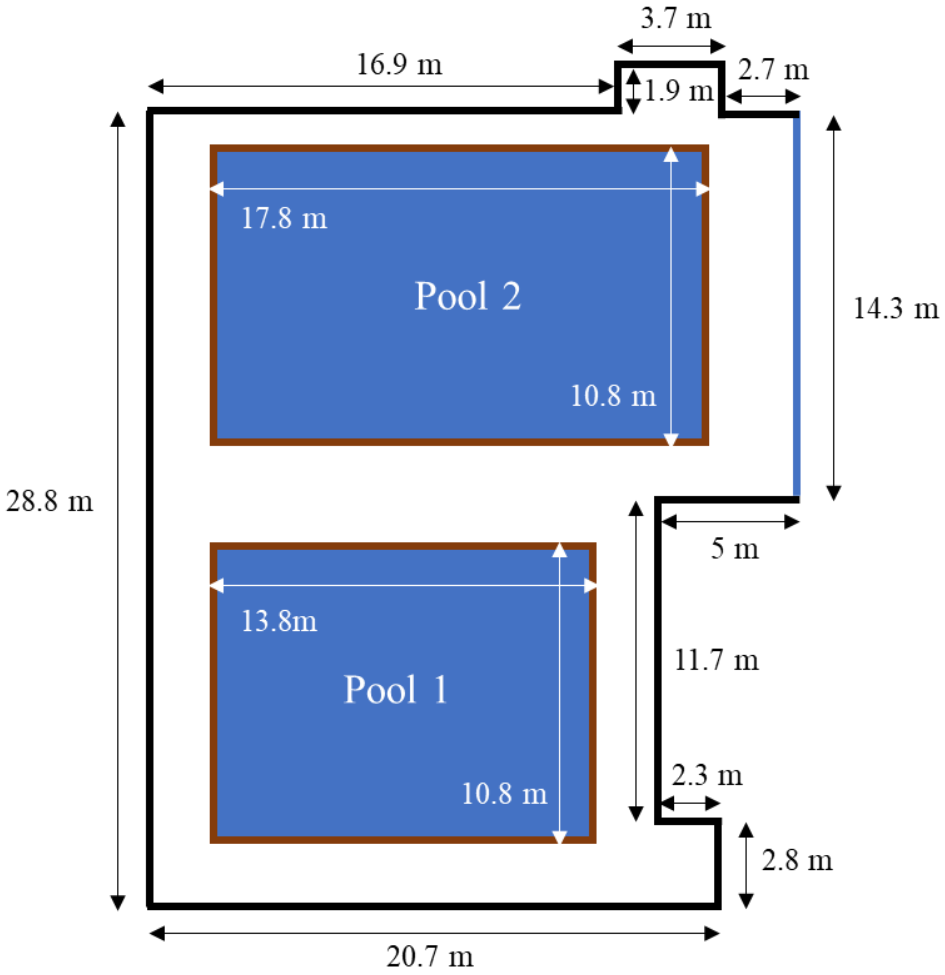

Figure 3-23: Sketch of the building model with lengths

3.3.2.2 U-values

The window in the model is a 2-pane glazing with a total U-value of 2 W/(m^{2}K). The external wall U-value is 0.22 W/(m^{2}K). Both these U-values are assumed values based on the Norwegian technical building regulations of 1999.

The normalized thermal bridge value is set as 0.1 W/(m^{2}K), assumed to be twice as large as the TEK17 requirement.

The inner walls have an assumed U-value of 2.9 W/(m^{2}K) while the floor and ceiling have an assumed U-value of 2 W/(m^{2}K).

3.3.2.3 Pool properties

The water setpoint temperature in both pools is 34 °C, while the design supply water temperature is 36 °C for both pools. The fresh water supply is assumed to be 60 liters/day per visitor as described in section 2.3. This amount of water is supplied between 3am and 4am.

This results in a fresh water supply of $\frac{60\frac{\frac{l}{day}}{visitor} * 188\frac{visitors}{day}}{3600\ s} = 3.14\frac{l}{s}$ during the one hour at night for pool 2 and $\frac{60\frac{\frac{l}{day}}{visitor} * 36\frac{visitors}{day}}{3600\ s} = 0.6\frac{l}{s}$ for pool 1.

The two hot water pools are mostly used by a fitness studio and for physiotherapy, so the activity factor is assumed to be as pools for therapy. Following Table 2-1, the activity factor during occupancy therefore is set as 0.65, while when unoccupied, it is set as 0.5.

3.3.2.4 Use of the pools

First of all, the use of the steam sauna is completely neglected. The use of the two pools are divided in each occupancy component in IDA ICE. Both groups have an assumed activity level of 3 MET and clothing level of 0.2 CLO.

The occupancy component for pool 2 is following the schedule in Figure 3-24, where 100 % means there are 20 people in the group. This corresponds to 20 people per hour during group sessions and 4 people per hour during the break.

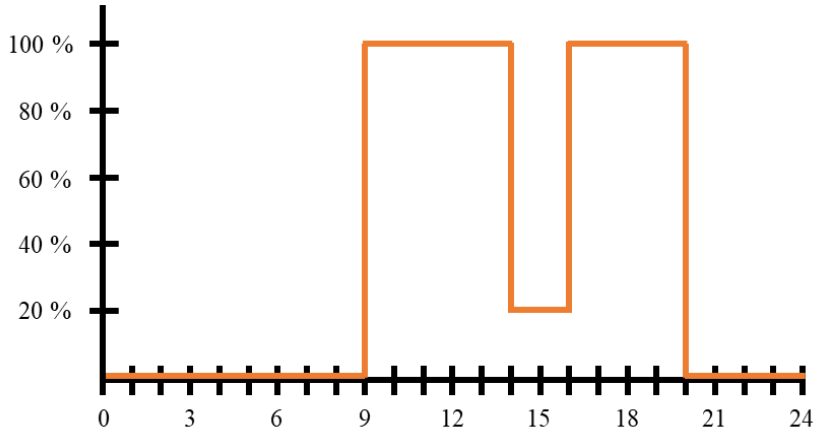

Figure 3-24: Schedule of occupancy in pool 2

The occupancy component for pool 1 is following the schedule in Figure 3-25, where 100 % means there are 12 people in the group.

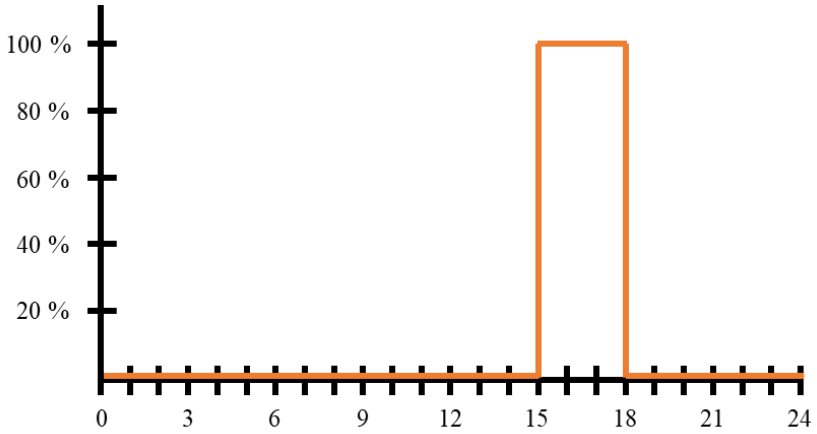

Figure 3-25: Schedule of occupancy in pool 1

3.3.3 Designing the AHU model

3.3.3.1 Key values

In order to figure out these key values, the AHU control system was used to collect some data as well as an engineer at Menerga was helpful with some essential details about this specific AHU.

After an inspection of the logged data in the AHU control system, the daytime for the AHU is set between 8am and 10:30pm.

The volume flow rates in supply and return was found in the AHU control system. The volume flow rates were different in daytime and night-time and the return air was at average 2.4 % higher than supply air. The average supply volume flow rate at night-time was just below 14 000 m^3/h, and just below 19 000 m^3/h at daytime. A constant value throughout the whole day had to be used in IDA ICE, so the average value, 17 000 m^3/h, was therefore used for supply air. For return air, 17 400 m^3/h was used.

The fresh air volume flow rate to the pools are decided based on information from Menerga. The minimum fresh air during daytime is 5 % of supply air, while there is no fresh air supplied at night. In reality, there is an option for supplying fresh air also at night if there is an extensive need of cooling or dehumidification, but this is neglected in this case.

Beyond the minimum fresh air volume flow rate, it increases with 50 m^3/h per evaporated kg of water to ensure a comfortable indoor air quality. As the supply air volume flow rate is 17 000 m^3/h, the fresh air volume flow rate is controlled as in Figure 3-26 during daytime. The amount

of evaporated water in kg/s is calculated from Equation (3-28). This value is multiplied with 3600 s/h before inserted in the control in Figure 3-26.

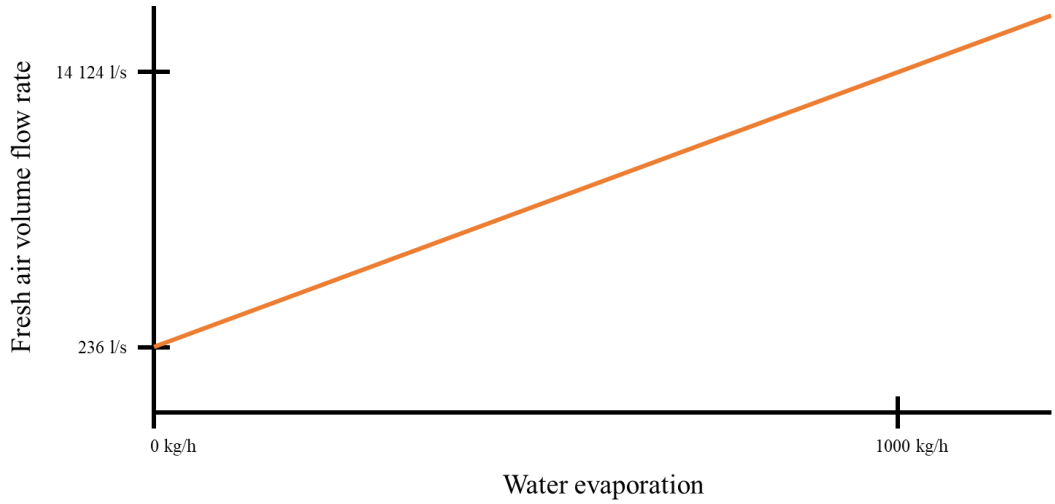

Figure 3-26: Control of fresh air volume flow rate at daytime

The setpoint temperature for heating found in the AHU control system and further used in the IDA ICE model was 30.8 ℃.

The supply air temperature is set to operate between the return air temperature and 53 ℃, also based on the log in the AHU control system.

The heat recovery unit in Pirbadet is a cross plate heat recovery unit with 78 % temperature efficiency in wet operation [31]. This efficiency was used in the air to air heat recovery unit in the IDA ICE model.

The setpoint for RH found in the AHU control system was 55 %. And by watching the RH logging curve from the AHU control system, it is mostly varying between 50 % and 60 %. Therefore, 55 % is used as the lower setpoint for RH and 60 % is used as upper setpoint for RH to make it as similar as possible.

3.3.3.2 AHU setup

The AHU in IDA ICE is illustrated in Figure 3-27. On the right side, the airflows are connected to the zone and on the left side they are connected to the outdoor. In between there is a heat recovery unit, a cooling coil, heating coil, two bypass units and two fans. The defrosting damper is neglected in this model since it is the normal operation modes that are to be considered for energy efficiency.

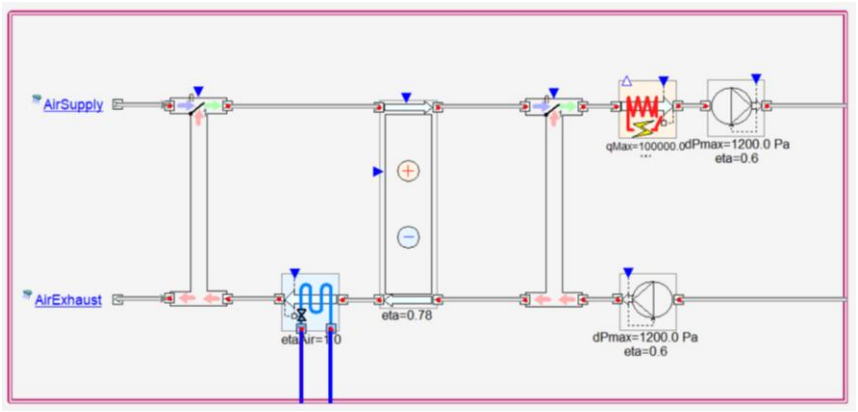

Figure 3-27: IDA ICE AHU without control components

The fans are both given a SFP of 2 kW/(m^3/s) as in TEK17 and a efficiency (electrical to air) of 0.6 which is the standard value in IDA ICE. The fans are always on.

The heating coil, which is supposed to represent both the heat from the heat pump condenser and the heating coil is seen as ideal. Therefore, the maximum power is set as 100 000 W.

The cooling coil, which is supposed to represent the dehumidifier, is also seen as ideal with its cooling capacity of 99 999 kW. The air side effectiveness is set as 1 and the liquid side temperature rise is set as 5 ℃ as standard in IDA ICE.

3.3.3.3 AHU control strategy

Control of bypasses

The outer bypass (closest to outside) is controlled to ensure the correct amount of fresh air to the AHU. During daytime, the bypass input signal is the fresh air volume flow rate ($\dot{V}_{FA}$) divided by the volume flow rate between the two bypasses ($\dot{V}_B$). $\dot{V}_{FA}$ is as illustrated in Figure 3-26, while $\dot{V}_B$ is logged by a sensor in the AHU. (Since the bypasses actually are controlled by mass flow ratios, the resulting fresh air volume flow is some wrong.) During night-time, the bypass input signal is 0.001. This is supposed to be 0, but IDA ICE would not simulate without a small amount of fresh air. Therefore, the negligible value 0.001 was used. A switch component controlled by an on/off schedule switches between daytime mode and night-time mode.

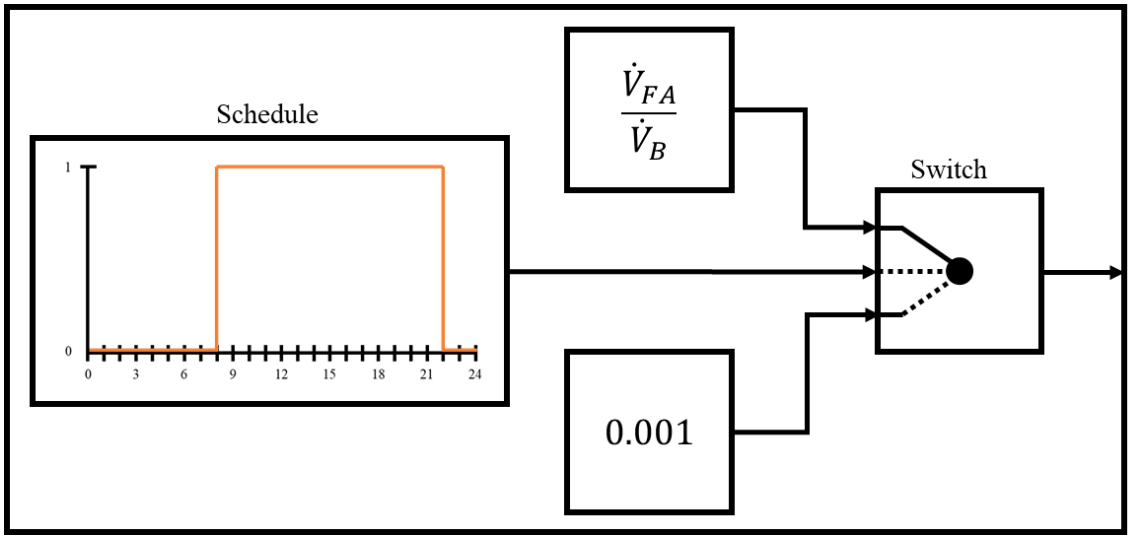

Figure 3-28: Outer bypass control

The inner bypass is controlled after the humidity level in the return air. If the humidity of the return air is higher than the setpoint (55 %) the bypass closes. If opposite, the bypass opens to avoid further dehumidification of the air. This is controlled by a proportional-integral-controller (PI) by comparing the measured RH and the setpoint. However, this bypass is controlled to always let through the minimum needed fresh air. This is illustrated in Figure 3-29.

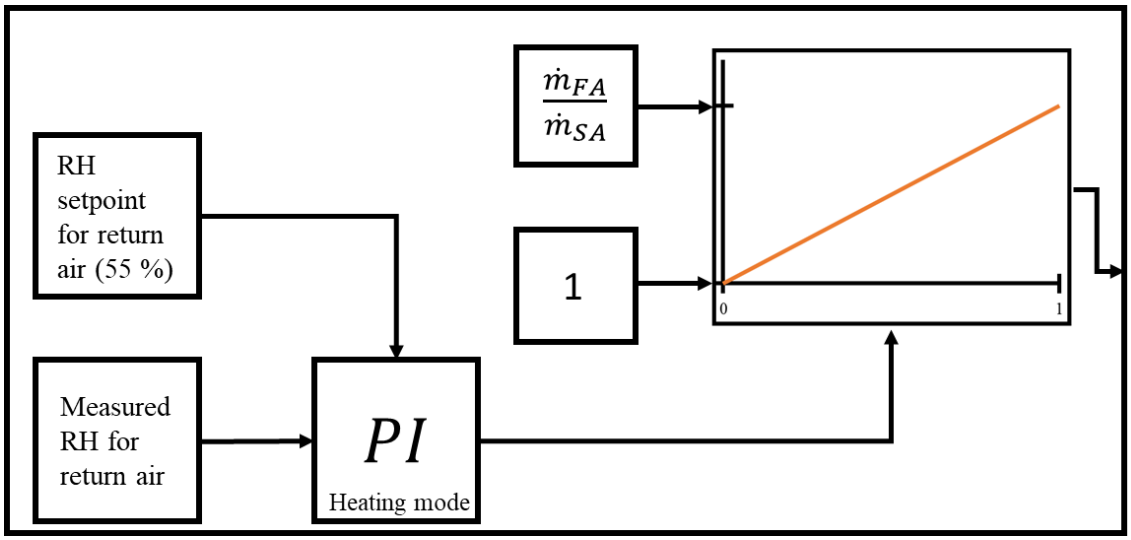

Figure 3-29: Inner bypass control

Control of dehumidifier

The air needs dehumidification if the RH in the return air is over a certain value. This upper value is set in order to avoid condensation on the building envelope and is set to 60 % as described in section 3.3.3.1.

A PI controller regulates the amount of dehumidification needed by comparing the measured RH in return air and the upper value for RH. The output from the PI-controller is between 0 (no dehumidification) and 1 (max dehumidification). Since the dehumidifier/cooling coil is controlled by inserting the temperature after the cooler, a linear transformation is performed, where 10 °C is max dehumidification and the temperature before the cooler is set as the value for no dehumidification as in Figure 3-30.

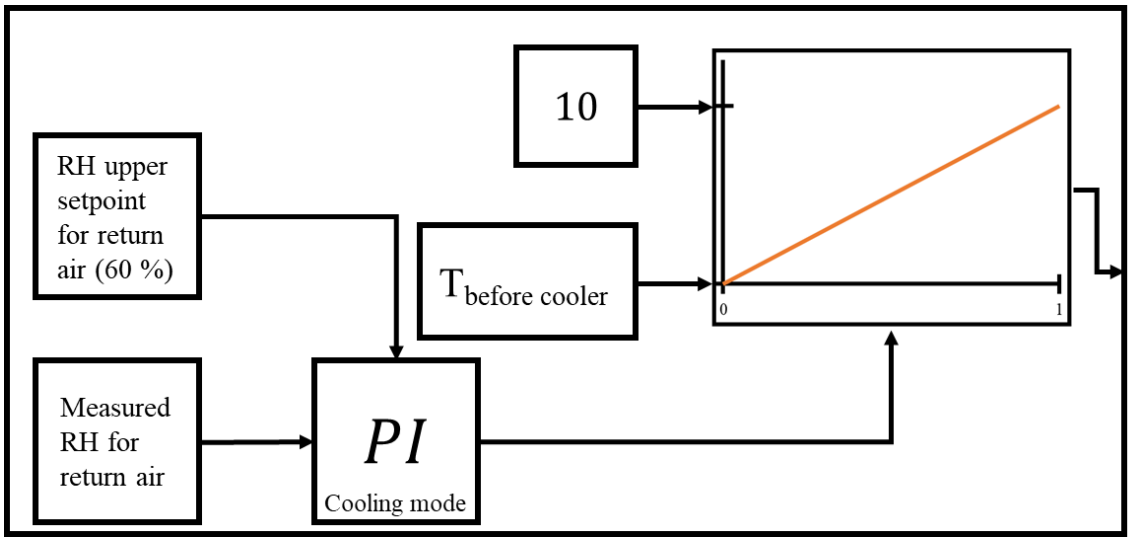

Figure 3-30: Dehumidifier control

Heating control

Like the heat recovery unit in Pirbadet, the heat recovery unit in the IDA ICE model is always on. This is controlled by setting the setpoint temperature very high (55 ℃ in this case).
The heating coil in the IDA ICE model is controlled as illustrated in Figure 3-31.

A PI-controller regulates the heating needed by comparing the measured temperature in return air and the setpoint temperature for return air. The output from the PI-controller is between 0 (no heating) and 1 (max heating). Since the heating coil is controlled by inserting the temperature after the cooler, a linear transformation is performed, where 53 °C is max heating and the temperature measured in the return air is set for min heating.

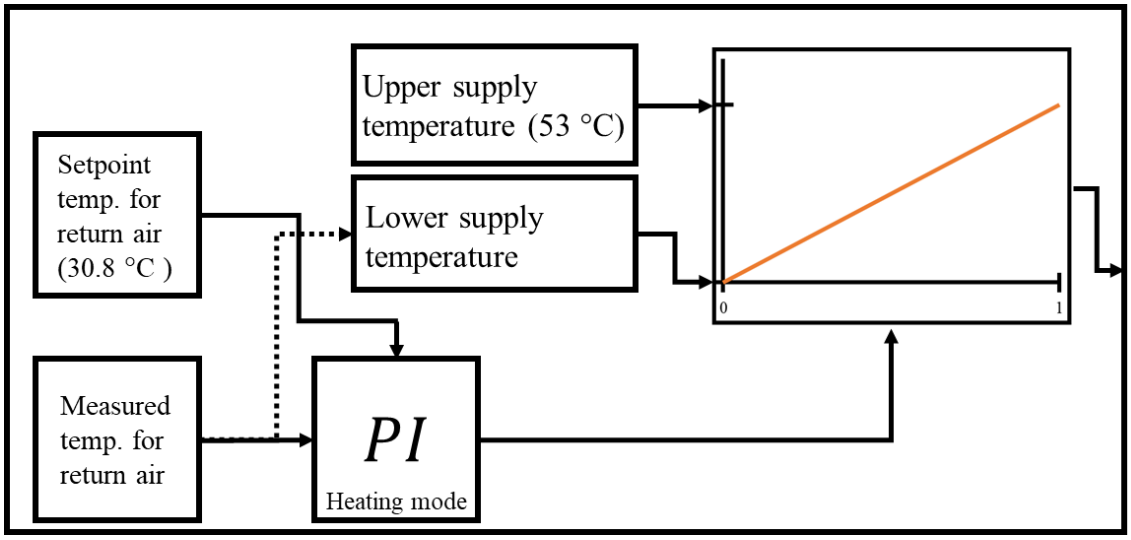

Figure 3-31: Heating control

General information about the PI-controllers

The PI-controllers used in the IDA ICE model get a setpoint signal and a measured signal to calculate the error. This error is then used to calculate a control variable between for example 0 and 1. 0 means e.g. the bypass is off, while 1 means on. Linear transformations are then used to convert the control variable to a physical entity just before the process. E.g. the condenser that is controlled with outlet temperature of the condenser. A block diagram of the controllers is presented in Figure 3-32.

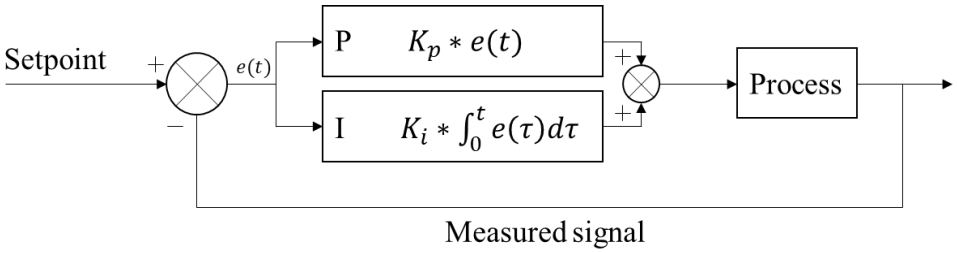

Figure 3-32: Block diagram of the PI-controllers (general)

The control parameters used is the standard ones in IDA ICE tabulated in Table 3-2.

Table 3-2: Control parameters used in IDA ICE

Parameter	Value	Description
K [-]	0.3	Gain parameter
T_i [s]	300	Integration time in seconds
T_t [s]	30	Tracking time in seconds
Mode	0	0 = heating, 1 = cooling
Hi_{limit}	1	High limit for out-signal
Lo_{limit}	0	Low limit for out-signal
Tau	0	Time constant on in-signal
Conv_unit	1	Unit conversion factor for sensed signal

3.3.4 Validating the model

To ensure that the model of the two hot water pools in Pirbadet works as intended, a sensitivity analysis is done on some essential parameters. This is mainly done by using the parametric run tool in IDA ICE version 4.8. The analysed parameters are listed in Table 3-3. They are analysed against the resulting heating need from the ventilation system and the heating need in the pool. Some are also analysed against the average water evaporation rate.

There is done a manual sensitivity analysis on the pool activity factor since there is no possibility for using the parametric run tool on this parameter. This is since the pool activity factor is given as a schedule. The activity factor is analysed against the resulting average evaporation rate over a day.

Table 3-3: Parameters for sensitivity analysis

Parameter	Initial	Unit	Analysis range	Resolution[6]
Zone height	3.5	m	2.5 → 5	10
Window frame U-value	2	W/m^2K	0.001 → 5	10
External wall insulation thickness	0.15	m	0.001 → 2	10
Internal floor/roof thickness	0.5	m	0.25 → 2	10
Length of pool 2	17.8	m	1 → 20	10
Pool 2 water temperature	34	°C	20 → 40	10
Air setpoint temperature	30.8	°C	20 → 50	10
Pool activity factor for both pools when used[7]	0.65	-	0.5 → 1.5	10

An increased zone height and window frame U-value and a decreased external wall insulation thickness and internal floor/roof thickness will all increase the heat loss of the zone. A valid model would therefore need more heating, mostly by the ventilation system and thereafter by the pool.

A longer pool 2, a higher water temperature in pool 2 and a lower air temperature will for a valid model result in higher evaporation rate and heat loss from the pool to the zone. Therefore, the pool heating is supposed to increase while the ventilation heating is supposed to decrease.

An increased pool activity factor will for a valid model result in a higher evaporation rate. As the increase in activity factor is linear, the resulting increase in evaporation rate should be linear as well.

[6] This is the planned resolution. Some parameters might have a lower number of results due to simulation error.
[7] Only the activity factor defining use of the pools is changed. The activity factor for unused pools is always 0.5.

3.3.5 Comparing evaporation rate in pool model and calculated evaporation rate based on water content in return and supply airflow

The evaporation rate from the pools is an important parameter of such experiment as this. Therefore, this is investigated in the beginning. In the IDA ICE pool model, there is a possibility to log the evaporated mass from the pool to the air in kg/s. This value was therefore logged for both pools, summarized and multiplied by 3600 s/h in order to get a common result in kg/h.

Since there are no direct measurement of this evaporation rate in Pirbadet, the evaporation rate in the IDA ICE model is also calculated as the difference in water content in the return and supply airflow.

$$\dot{m}_{\text{evap}} = \dot{m}_{RA} * x_{RA} - \dot{m}_{SA} * x_{SA} \quad (3\text{-}28)$$

3.3.6 Some calculations

3.3.6.1 Delivered heating power to the swimming hall through ventilation

Delivered heating power to the swimming hall through ventilation is calculated with the mass flow in the supply and the difference between supply air and return air temperature.

$$\mathrm{Q_{hall}} = \dot{m}_{SA} * 1.005 * (\mathrm{T}_{SA} - \mathrm{T_{RA}}) \quad (3\text{-}29)$$

3.3.6.2 Dumped heating power to the outdoor

Dumped heating power to the outdoor is calculated the same way as the delivered heating power to the swimming hall through ventilation. It depends on the exhaust mass flow and the difference between exhaust airflow and fresh airflow (outdoor) temperature.

$$\mathrm{Q}_{dumped} = \dot{m}_{EA} * 1.005 * (\mathrm{T}_{EA} - \mathrm{T}_{FA}) \quad (3\text{-}30)$$

3.3.7 Extraction of IDA ICE results

In order to extract results from IDA ICE, OUTPUT-FILES are used. These are objects that can receive logging data and present the data in tables, graphs and that has the possibility to export logging data to Excel. All interesting results are therefore logged to such OUTPUT-FILES and further exported to Excel. They are all exported as minute values. For use of hourly values, the arithmetic average is calculated in Excel.

3.4 Comparison of measured data and simulation results

3.4.1 Thermal properties of return and supply air

The temperature and RH for the return and supply air is illustrated in graphs, both for the measured data and simulation results.

3.4.2 Delivered heating power to the swimming hall through ventilation

The amount of heat delivered to the swimming halls is compared and is a way to understand if the model needs the same amount of energy as the measured swimming pools in Pirbadet. The heating power is calculated in Excel using Equation (3-20) for the measured data and Equation (3-29) for the simulated data.

3.4.3 Dumped heating power to the outdoor

The dumped heating power to the outdoor can say something about the heat recovery of the AHU. A good model of Pirbadet should give the correct result of dumped heat power to the outdoor, therefore the simulated results and the measured data are compared. The dumped heating power to the outdoor is calculated in Excel using Equation (3-21) for the measured data and Equation (3-30) for the simulated data.

3.4.4 Volume flow rates

The volume flow rates are presented in a diagram to show the difference of the simulated model and the measured supply and return volume flow rates. Also, the resulting fresh air and exhaust air volume flow rates are compared and should be equal in a good model.

3.4.5 Evaporation rate

The evaporation rate calculated based on water content in the return and supply airflow for the IDA ICE model and in Pirbadet are both presented in a diagram for comparison.

Also, the theoretical assumed evaporation rate based on the experienced numbers in Table 2-5 and the Basin & Krumm method, showed in Attachment 3, are compared to the evaporation rates.

For calculating the evaporation rate using the method of Basin & Krumm, the number of users (N), pool area (F), water vapor partial pressure at water temperature in boundary layer at

saturation state (p''_w) and water vapor partial pressure at the air temperature (p_w) was used as inputs.

N is set to 20 people and F is 341 m^2.

p''_w is found to be 53.26 hPa for a water temperature of 34 °C from The Engineering Toolbox [32].

Calculation of p_w:

$$RH = \frac{p_w}{p_{ws}} * 100\ \% \tag{3-31}$$

where p_{ws} is the water saturation vapor partial pressure at the air temperature. Rearranging Equation (3-31) we get

$$p_w = \frac{RH * p_{ws}}{100\ \%} \tag{3-32}$$

p_{ws} is found to be 44.47 hPa for an air temperature of 30.8 °C from The Engineering Toolbox [32]. Using Equation (3-32) with a RH of 55 %, p_w is found to be 24.46 hPa.

3.4.6 AHU heating need

The heating need in the modelled AHU and the measured AHU in Pirbadet is compared in a diagram. In order to be able to use IDA ICE for designing swimming pools and their belonging AHU, a correct sizing of the heating need is essential and should be like the real heating need.

3.4.7 AHU dehumidification

Just like the AHU heating need, the AHU dehumidification need is essential to be like the real dehumidification need to be a good supportive tool for design of swimming pools and their belonging AHU. Therefore, also the needed AHU dehumidification in the model and in Pirbadet is compared in a diagram.

4. Results & analysis

In this chapter the results from both the simulation and the measurements are presented. First, the results from the sensitivity analysis of the IDA ICE model are presented to be able to determine whether the model is valid or not. Thereafter, a validation of the calculation method for evaporation rate is presented. The valid IDA ICE model is then compared to the measured data from Pirbadet. In the end, also a result of the measured temperature after the heat recovery unit is presented.

4.1 Simulation results

4.1.1 Model validation

Zone height (volume)

A higher room or a zone with a larger volume has higher heating need, both for ventilation and pool heating. A larger volume implies larger envelope surface and therefore larger heat loss which must be covered. Figure 4-1 shows that the increased heating need mostly is covered by the ventilation system, but also somewhat by heat loss from the pool.

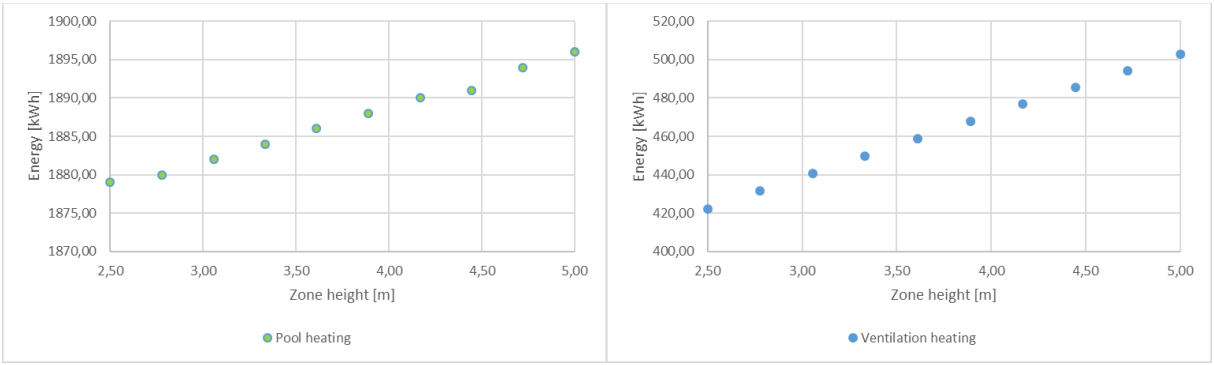

Figure 4-1: Sensitivity analysis of zone height

Window frame U-value

A larger U-value of the window frame results in a larger heat loss and therefore an increased heating need. From Figure 4-2, one can see that the heating need is increased by about 7-8 kWh that day. The ventilation system manages to cover most of the extra heat loss, while the pool heating increases by 1 kWh.

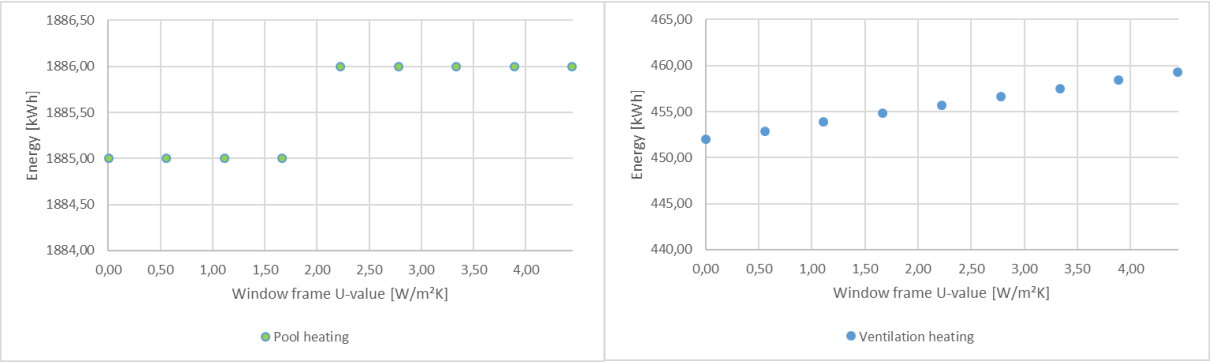

Figure 4-2: Sensitivity analysis of window frame U-value

External wall insulation thickness

As the thickness of insulation in the outer wall is increased, the pool and ventilation heating decrease as showed in Figure 4-3 due to less heat loss to the outdoor. The change of thickness from 0 to 0,3 meters makes an impact on the heating need, while further increase makes less impact.

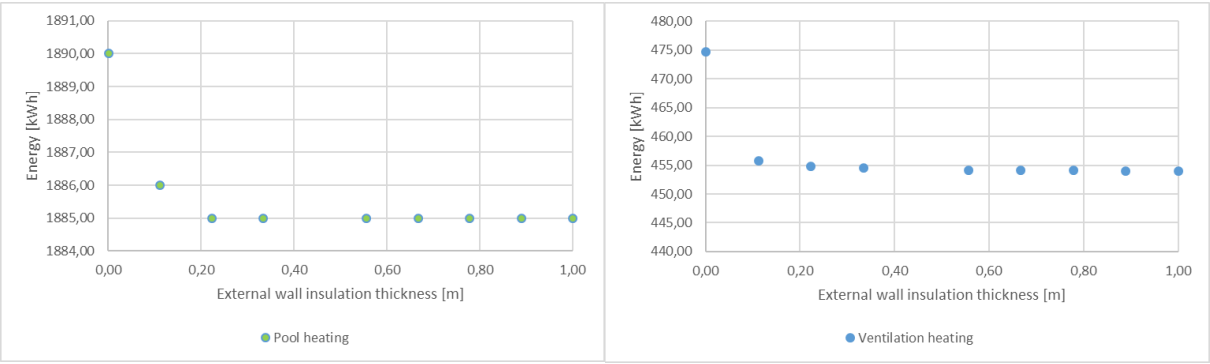

Figure 4-3: Sensitivity analysis of external wall insulation thickness

Inner floor/roof thickness

A thicker inner floor/roof results in less heating need for both the pool and from the ventilation system due to less heat loss through the floor and roof as showed in Figure 4-4. The change of energy need is much larger then for the other parameters due to the large area of the floor and roof.

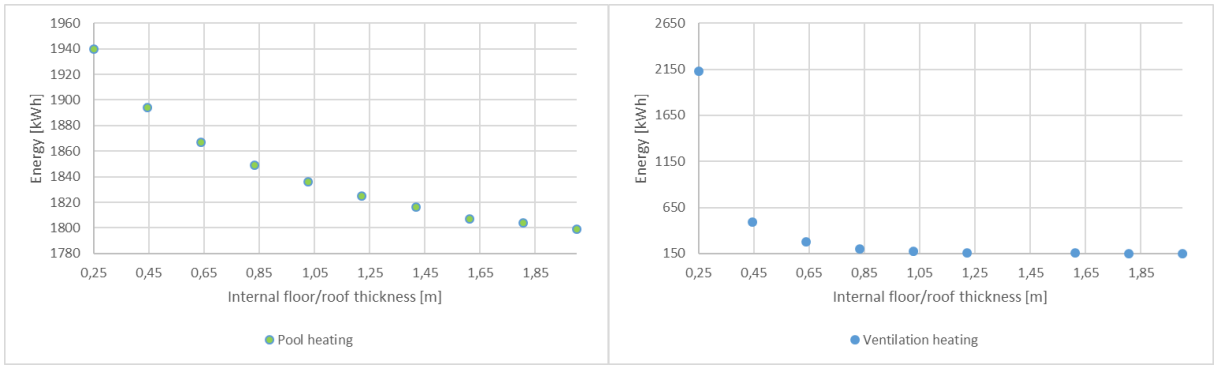

Figure 4-4: Sensitivity analysis of inner floor/roof thickness

Length of pool 2

When the pool length is increased, the pool area is increased. This means a larger pool surface area for heat loss and evaporation to the zone. Therefore, the pool heating and water evaporation increases while the ventilation system can deliver less heat as showed in Figure 4-5. Here, the pool heating off course varies more than ventilation heating with an increasing pool length. The pool heating needs almost doubles from 1 m pool length to 20 m. At the same time also the evaporation rate doubles which makes sense since the evaporation stands for about 50 % of the pool losses as mentioned in section 2.2.3.

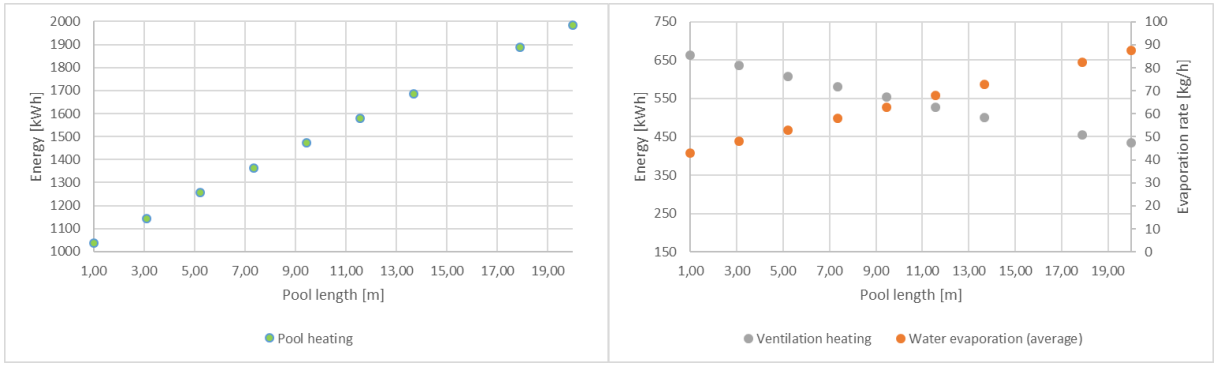

Figure 4-5: Sensitivity analysis of pool length

Water temperature of pool 2

An increasing pool temperature results in increased heat loss and evaporation to the zone as seen from Equation (2-3) and Equation (2-7). Therefore, the pool heating need and water evaporation increases while the ventilation heating decreases as illustrated in Figure 4-6. There occurred simulation error for temperatures above 34 °C, which explains the lack of data between 34 and 40 °C.

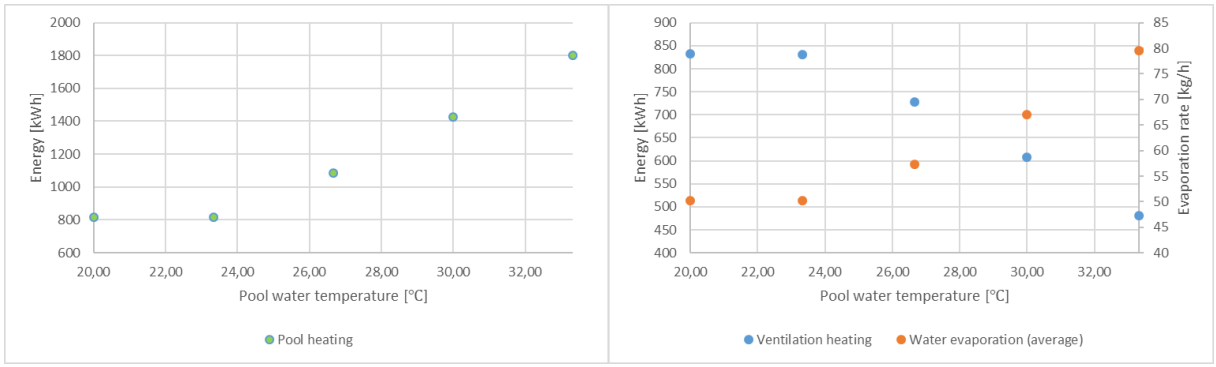

Figure 4-6: Sensitivity analysis of pool water temperature

Zone air temperature

A higher air temperature works just the opposite of a higher pool temperature as seen in Figure 4-7. The heat loss and evaporation from the pool to the zone decreases as the air temperature increases. The ventilation heating increases to cover the increasing envelope heat loss.

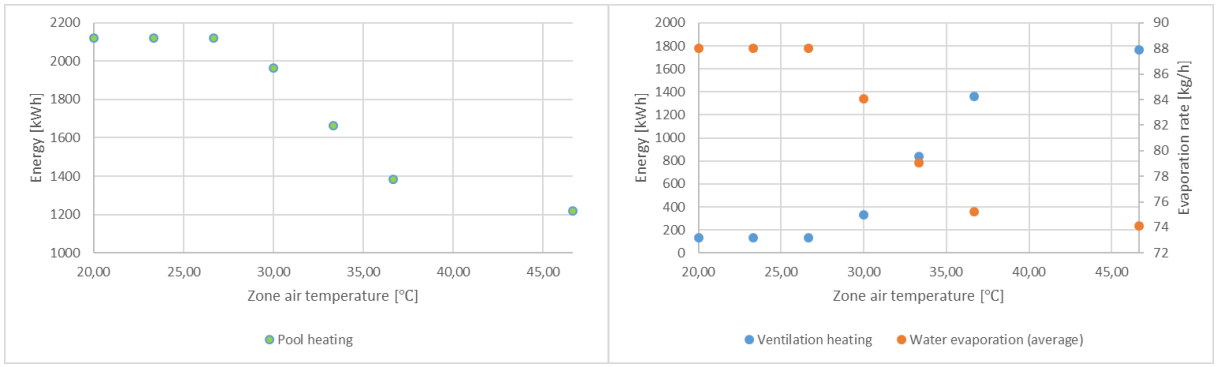

Figure 4-7: Sensitivity analysis of zone air temperature

Pool activity factor

An increasing pool activity factor results in a higher evaporation rate from the pool as illustrated in Figure 4-8. The increase in evaporation rate per increasing activity factor is linear, starting at about 72 kg/h for an activity factor of 0.5 and increasing to about 113 kg/h for an activity factor of 1.5.

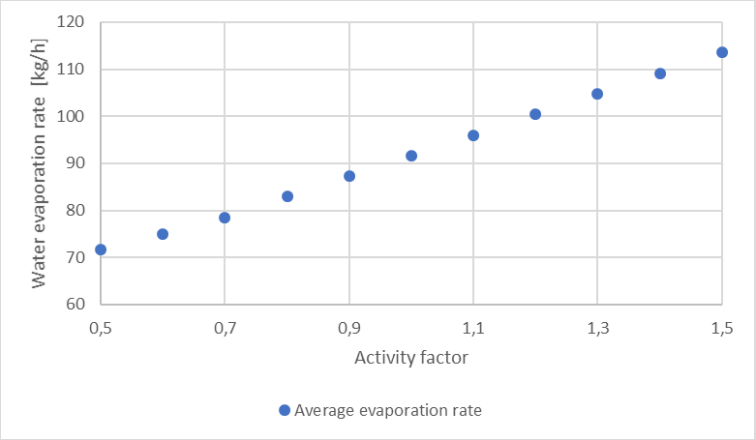

Figure 4-8: Sensitivity of activity factor and resulting average evaporation rate over a day

The results from the sensitivity analysis is as expected for a valid model explained in section 3.3.4. Therefore, the model can be used in further analysis. This does not mean the model gives the correct results, but it reacts as expected to change in the tested parameters.

4.1.2 Evaporation rate calculating method

Figure 4-9 shows the water evaporation rate for the integrated variable for evaporation rate in IDA ICE and the calculated evaporation rate based on water content in the return and supply airflow. All over, the calculated evaporation rate is higher than the integrated variable. It was reasonable to think that this is due to infiltration and occupancy. Therefore, the same model, but without occupancy, with minimal infiltration and balanced ventilation ($\dot{V}_{SA} = \dot{V}_{RA}$) was simulated and compared with the integrated pool variable in Figure 4-10. Here there are minimal difference between those two rates of water evaporation.

During night-time, the calculated evaporation rate is only a couple kilograms per hour higher than the integrated variable in the standard model. During daytime on the other hand, the difference is up to 18 kg/h. This is since there is always infiltration while the occupancy only occurs at daytime.

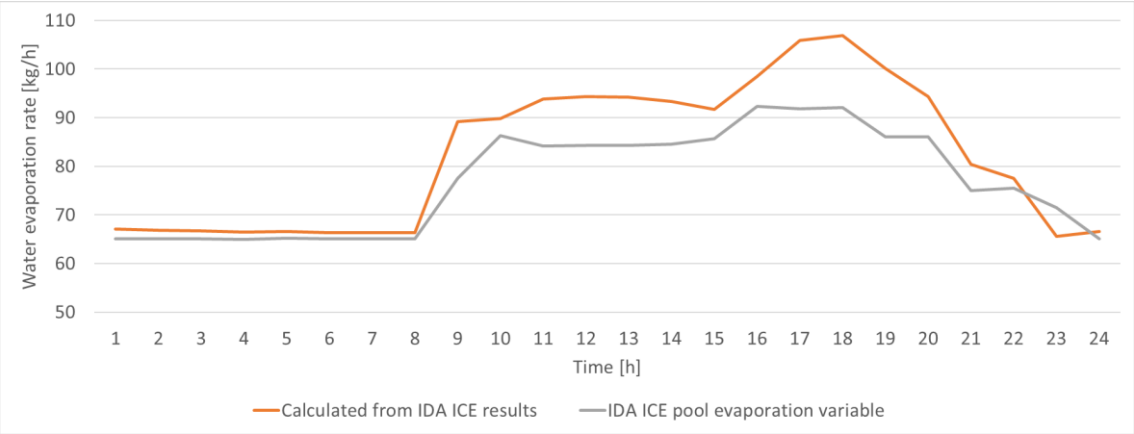

Figure 4-9: Hourly values for water evaporation in the IDA ICE model

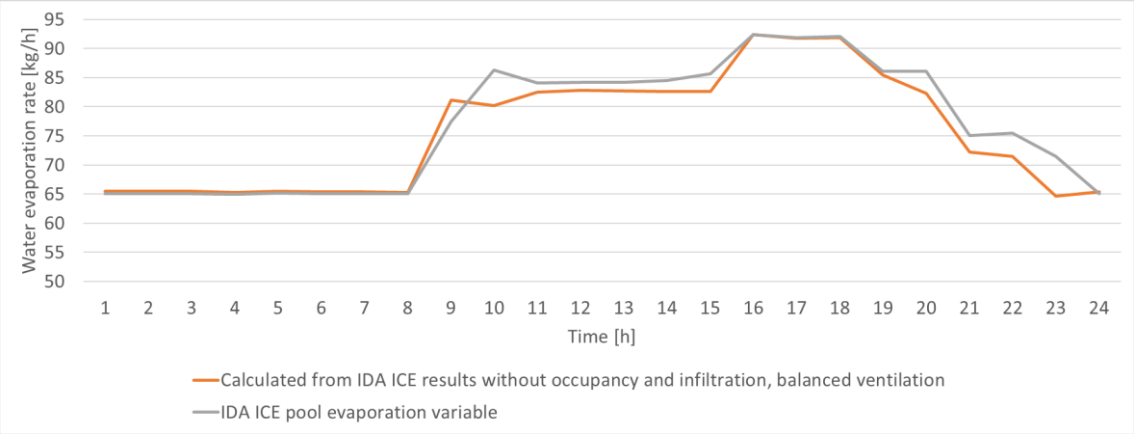

Figure 4-10: Hourly values for water evaporation in the IDA ICE model without occupancy, with minimal infiltration and balanced ventilation

4.2 Comparisons of measured data and simulation results

4.2.1 Thermal properties of return and supply air

The results are shown in Figure 4-11 to Figure 4-14. The minute values for both temperature and RH shows that the measured properties in Pirbadet changes more frequent than the simulated results.

Looking at the hourly temperature values in Figure 4-12, one can see that the difference between the measured temperature and simulated temperature is quite small for the return air. The error band for the measured temperatures occasionally overlap the IDA ICE temperatures. For the supply air, the measured temperature is up to 2 °C higher than the simulated temperature this day. This can be a cause of the higher heat demand as described in section 4.2.2.

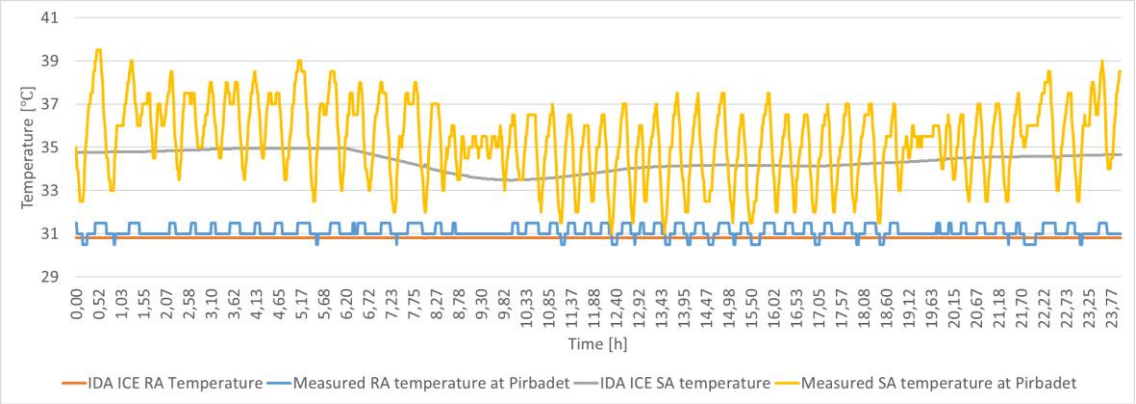

Figure 4-11: Minute values for temperature in RA and SA

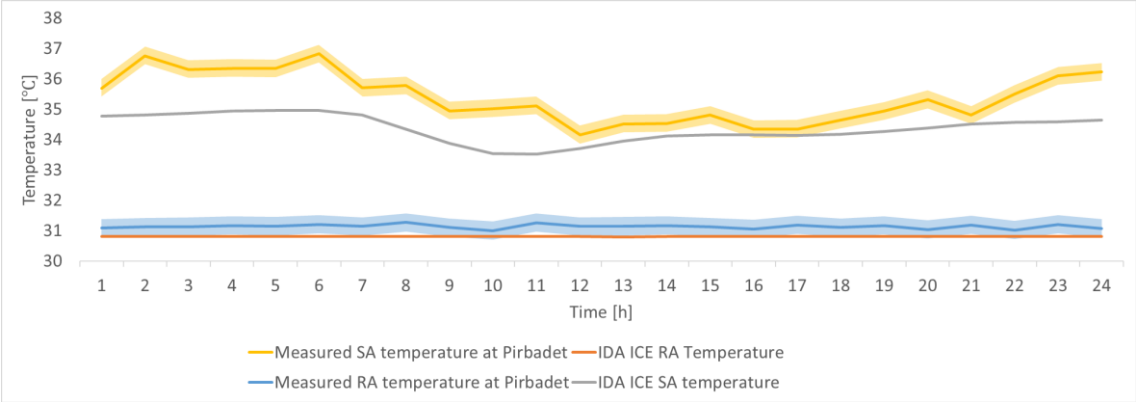

Figure 4-12: Hourly values for temperature in RA and SA (with error bands of 0.3 °C)

Figure 4-13 shows the minute values for RH. The hourly values for RH showed in Figure 4-14 are corresponding quite well during daytime. There are however some differences due to different control strategies. During night-time, the RH in RA is a couple percent lower in the measured dataset than the simulated results. For the SA, the RH is about 5 % lower in the measured dataset than the simulated results at night. This lower RH in SA is probably to make the RH in the return air lower to compensate that the air rates is less in Pirbadet than in the simulated model during night as explained in section 3.3.3.1.

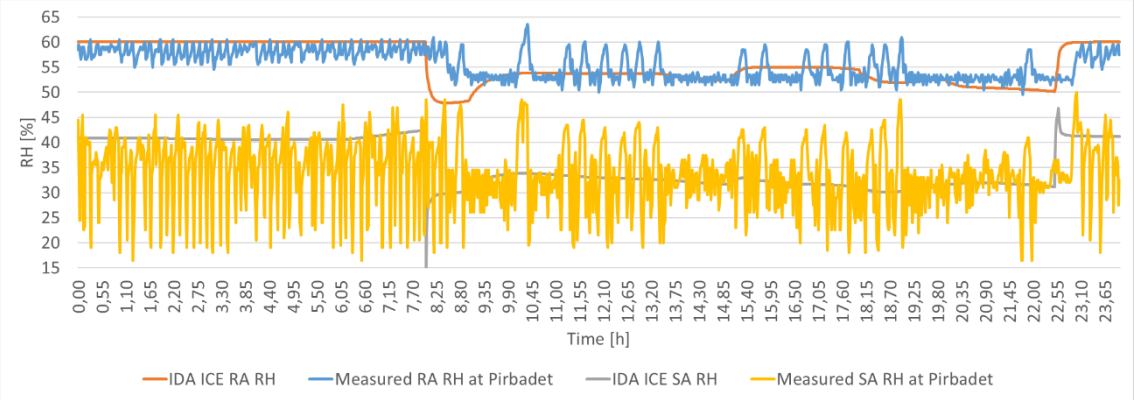

Figure 4-13: Minute values for RH in RA and SA

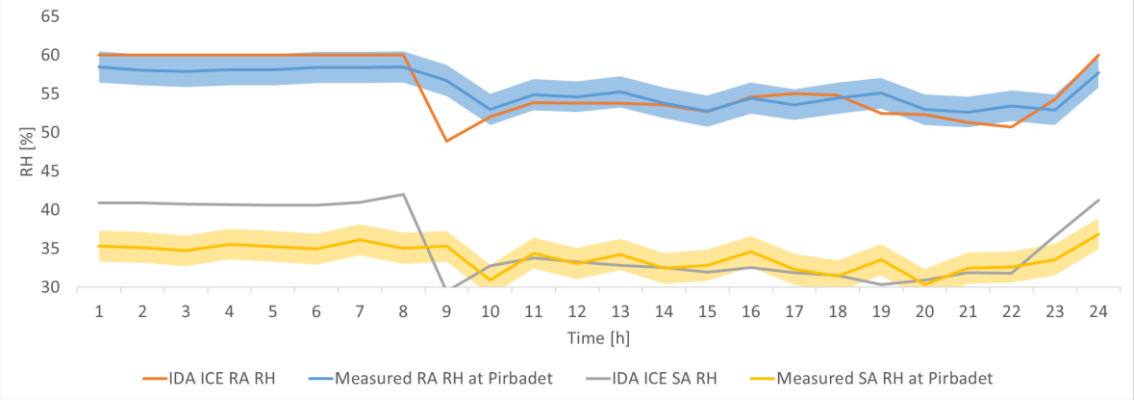

Figure 4-14: Hourly values for RH in RA and SA (with error bands of 2 %RH)

4.2.2 Delivered heating power to the swimming hall through ventilation

Due to a more variable supply air temperature in Pirbadet than in the IDA ICE model, the heating through ventilation also fluctuates more as one can see in Figure 4-15. Looking at the average hourly values in Figure 4-16, the heating power for the two ventilation systems are more similar. During night-time, the heating power for both is about 22 kW. During daytime, the heating need through ventilation is somewhat lower, probably due to heat gain from the

visitors and higher heat gain from the pool surface. At daytime the IDA ICE model needs less heating than measured in Pirbadet.

Since the heat power is directly connected to the supply air mass flow, which is higher at daytime in Pirbadet than in the IDA ICE model, it is reasonable that the heating through ventilation also gets higher at daytime in Pirbadet than in the IDA ICE model. The blue line in Figure 4-16 is the heating through ventilation with the same airflow rate as in Pirbadet at daytime. This means that the IDA ICE model anyway needs less heat supply. There are more heat losses in reality than in the model.

The average accuracy is ± 2.3 kW.

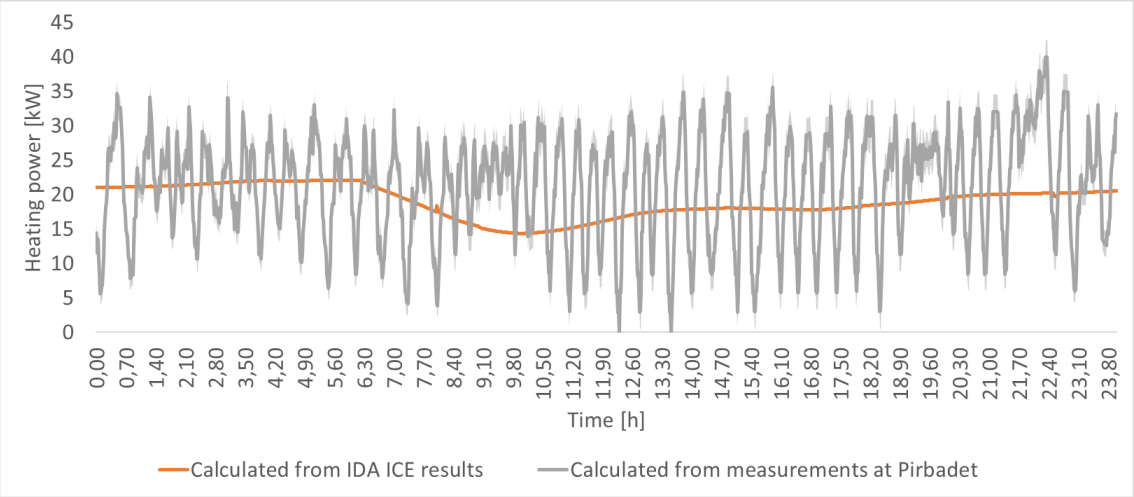

Figure 4-15: Minute-values for heating through ventilation

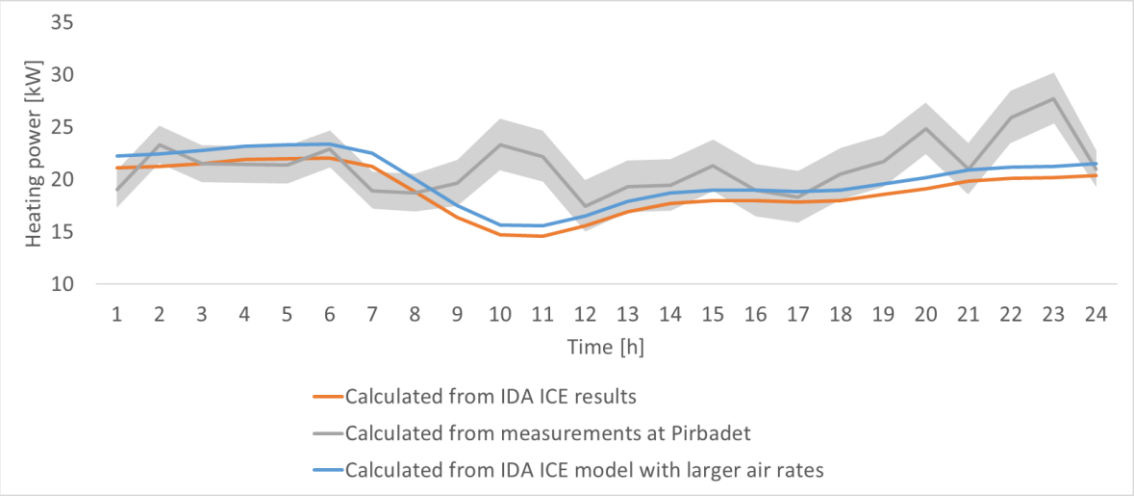

Figure 4-16: Hourly values for heating through ventilation

4.2.3 Dumped heating power to the outdoor

Figure 4-17 shows the amount of dumped heat power to outdoor from the AHU in Pirbadet and the modelled AHU in IDA ICE. The IDA ICE model seems to be better (in terms of dumping less heat) than Pirbadet during night-time, but much worse during daytime. The main reason for the huge difference at daytime is use of the heat pump in Pirbadet. Due to heating need, the heat pump is turned on and the evaporator (dehumidifier) is therefore cooling the exhaust air. This results in less dumped heat power to outdoor.

During night-time, the IDA ICE model is not supplying any fresh air, so the only exhaust air is the return air ensuring underpressure. In Pirbadet on the other hand, fresh air is supplied also during night-time. This results in a higher exhaust air volume flow rate and therefore more dumped heat power to outdoor. Due to an average error of ± 7.8 kW, the error band overlaps the IDA ICE line during night-time. It is though, most likely some difference due to the different control strategies. Figure 4-17 also shows a wider error band at night than at daytime. The calculation for the error is found in Attachment 2 and shows that the error depends on the temperature difference between exhaust and fresh air. Since this temperature difference is larger at night-time, also the error increases.

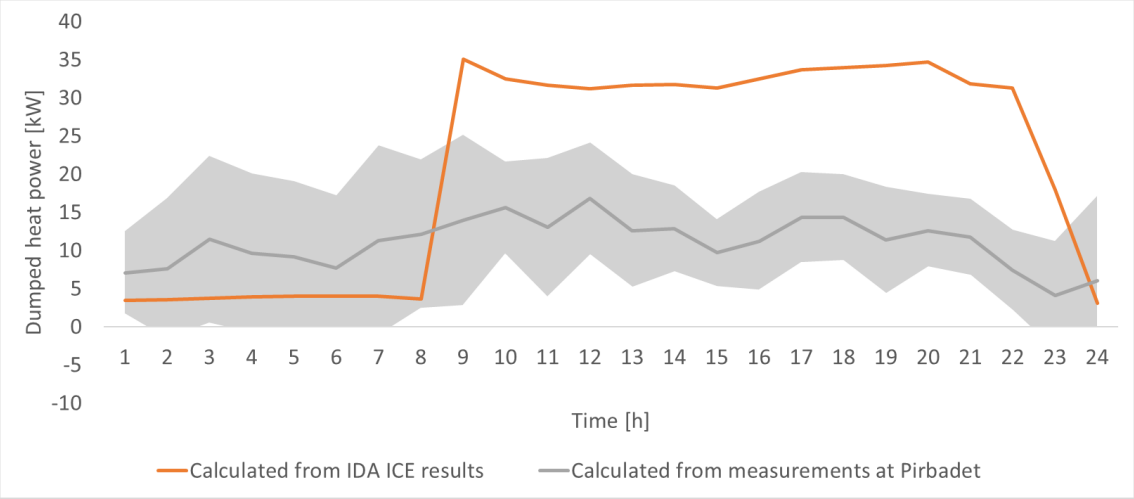

Figure 4-17: Hourly values for dumped heat power to outdoor

4.2.4 Volume flow rates

Figure 4-18 shows the volume flow rates in and out of the IDA ICE AHU and the AHU in Pirbadet. The volume flow rates at the pool side (RA and SA) are as described in 3.3.3.1. The resulting airflow rates at the outdoor side are more stable for the AHU in Pirbadet than the IDA ICE AHU since there are supply of fresh air even during night in Pirbadet. The fresh air rate and the resulting exhaust air rate is higher during daytime for the IDA ICE model than in Pirbadet due to different control strategy.

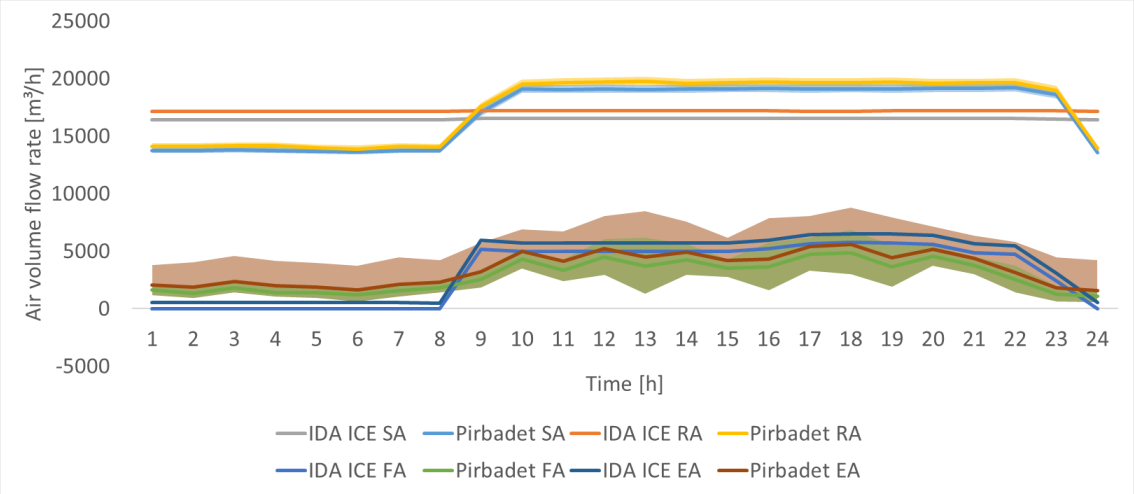

Figure 4-18: Air volume flow rates

4.2.5 Evaporation rate

As the thermal properties of the supply air changes very frequently, the water evaporation rate calculated based on the return and supply air behaves the same way as illustrated in Figure 4-19. The resulting hourly values in Figure 4-20 gives a better representation of the water evaporation rates.

According to the graph in Figure 4-20, the resulting evaporation rates for the IDA ICE model and Pirbadet, both based on water content in return and supply airflow, are corresponding quite well. Overall, the evaporation rate from IDA ICE is somewhat higher than measured in Pirbadet during night-time, but opposite at daytime. This might be because of the less volume flow rate, so less infiltration, during night-time and opposite at daytime. The error band of the measured data is overlapping the IDA ICE results all the time. The average accuracy is about ± 18 kg/h. Since the total swimming pool area is 341 m^2, the evaporation rates based on the experienced numbers should be between $0.35 * 341 = 119$ kg/h and $0.5 * 341 = 170$ kg/h during daytime for heated pools. At night-time it should be $0.1 * 341 = 34$ kg/h. This means both the measured and simulated values are about twice as large as the experienced values during night-time, but actually smaller than the experienced values at daytime.

The calculated evaporation rate from the method of Basin & Krumm is about 92 kg/h daytime and about 57 kg/h night-time. This fits very good to the measured and simulated results.

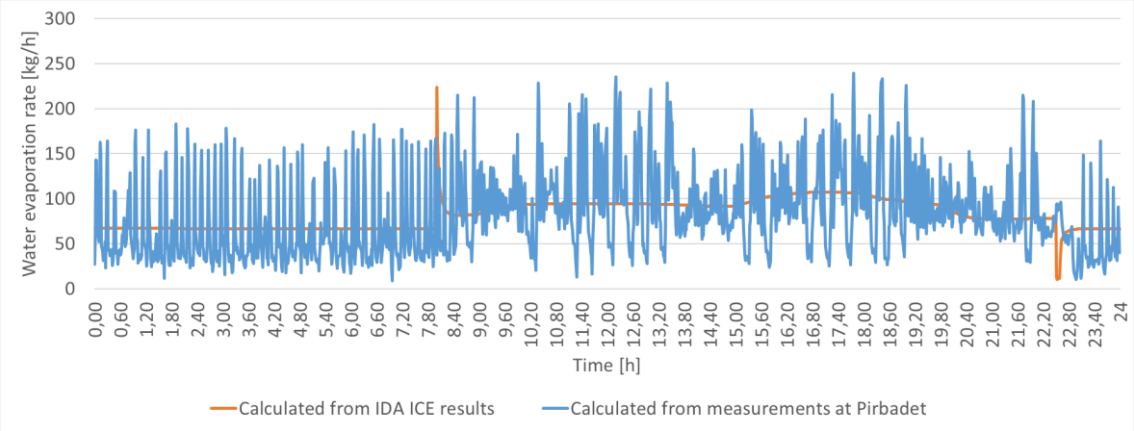

Figure 4-19: Calculated minute values for water evaporation in the IDA ICE model and in Pirbadet

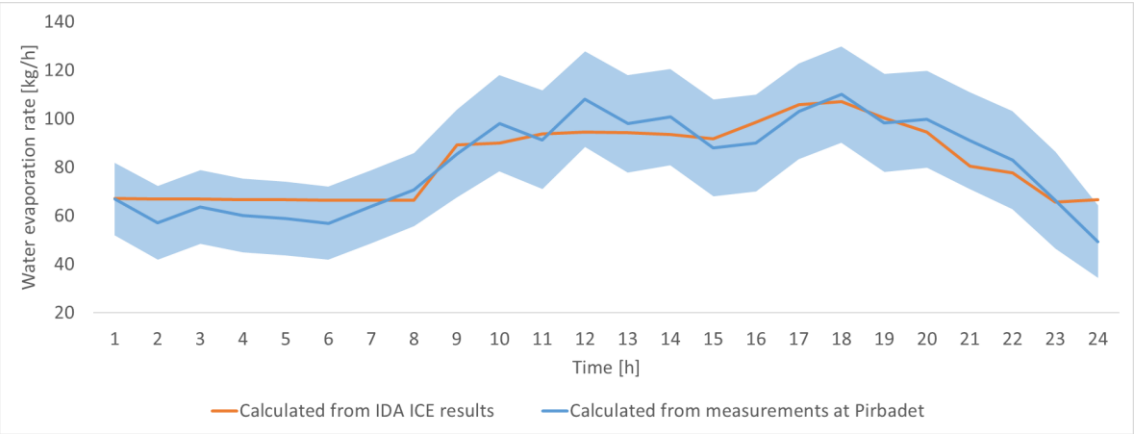

Figure 4-20: Calculated hourly values for water evaporation in the IDA ICE model and in Pirbadet

4.2.6 AHU heating need

The heating power measured in the AHU in Pirbadet is larger than in the simulated model throughout the day as the graph in Figure 4-21 shows. The difference between those two is less during night-time than during daytime. It is also clear that the condenser accounts for most of the heating need, while the heating coil supports the condenser if necessary, mostly at daytime. Another observation is that the AHU heating need is restricted to between about 23 kW and 33 kW for the real AHU in Pirbadet, and between about 14 kW and 24 kW for the simulated model. So, the heating need varies with about 10 kW this day.

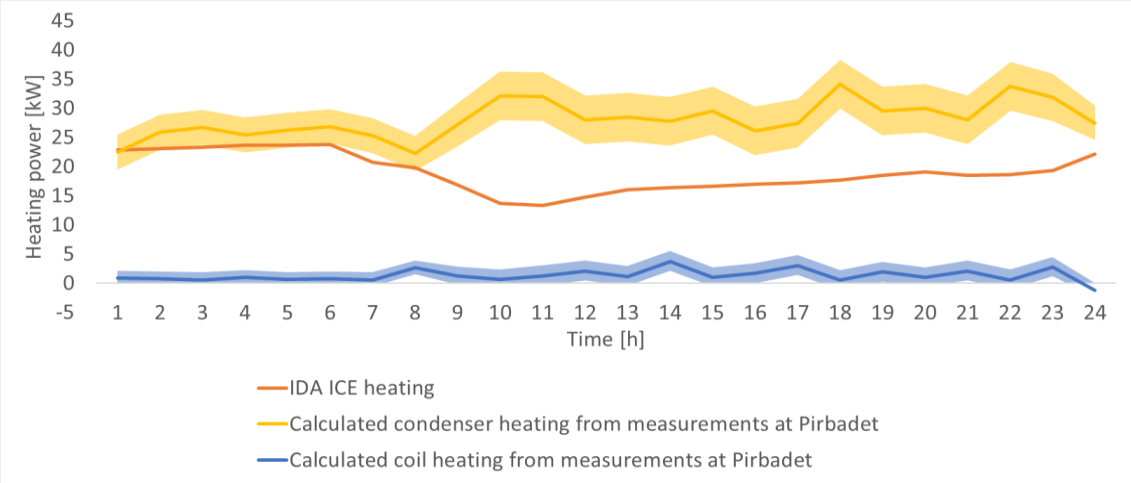

Figure 4-21: Calculated hourly values for AHU heating power

4.2.7 AHU dehumidification

The dehumidification or cooling results are shown in Figure 4-22. There is a big difference between the results from the simulated model and the results from the measurements in Pirbadet regarding dehumidification or cooling. For the IDA ICE model, the fresh air supply during daytime is enough for dehumidification. Since there is no fresh air supply during night-time, the dehumidifier works almost constant at about 54 kW.

The AHU dehumidification result in Pirbadet is not very accurate as seen in Figure 4-22. There is a simulation error in the 7th hour, but otherwise the error is around 30-50 kW, several times more than the measured data. This huge error band originates from the error of the temperature between the heat recovery unit and the dehumidifier which has a lot of propagation error due to the many calculations.

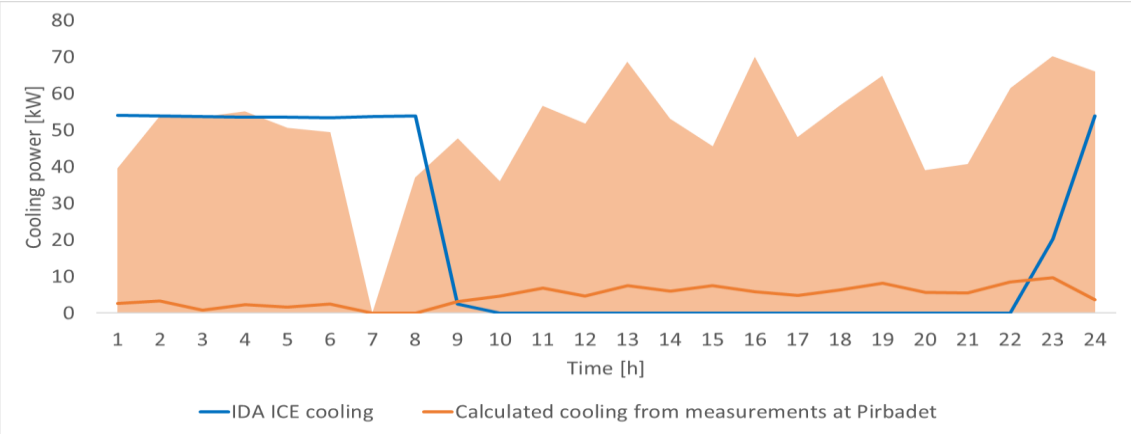

Figure 4-22: Calculated hourly values for AHU cooling (dehumidification) power

4.3 Temperature after heat recovery unit in supply air

The temperature logged with sensor EL6 and EL7 is presented in Figure 4-23. The overall result is that the lower sensor (EL7) measures a lower temperature than the upper one (EL6). Occasionally, the temperatures do a jump and at the same time they are getting closer to each other, the temperature gets higher and more equal in the heat recovery unit.

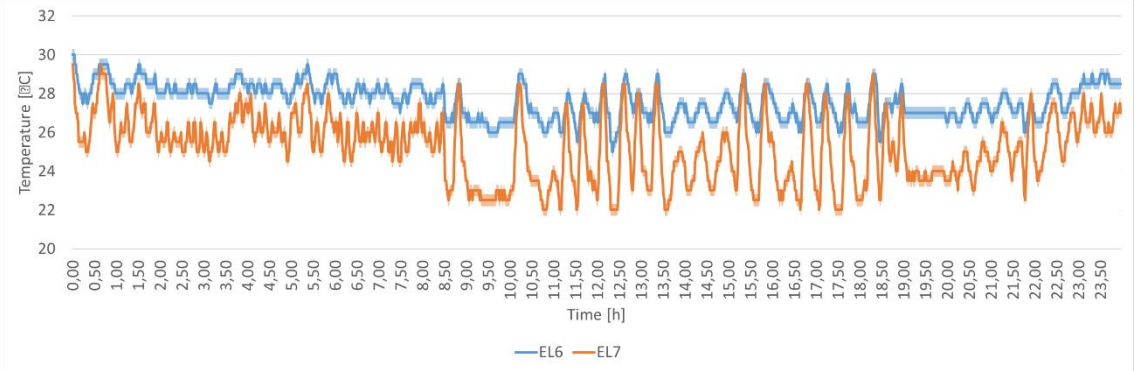

Figure 4-23: Temperature measured with EL6 and EL7 after heat recovery unit in supply air

5. Discussion

All measurements will involve some measuring fault. In this case, the placing of the sensors does probably not represent a huge source of error. This since the sensors are placed in the middle of the channels and since there are used more sensors where there might be differences over the cross-section. The measuring equipment used in this experiment is not of the best quality regarding accuracy, but it should at least be able to give some reasonable results. The probably biggest source of error in this experiment is the propagation of error in the calculations. When using many parameters with an uncertainty in an equation, the resulting uncertainty will be larger than if using a few parameters.
There are in general higher errors on the outdoor side of the AHU than on the indoor side. So, use of more sensors, for example for volume flow rate would be helpful to reduce this propagation of error, and a conclusion would have been more accurate. Due to propagation of error, the temperature between the heat recovery unit and the dehumidifier has a large uncertainty. This makes the uncertainty of the cooling need large as well. Perhaps another calculation method for the temperature should be used or perhaps do the experiment on an AHU with separated heat recovery unit and dehumidifier.

The IDA ICE building model is made to be a representative model of the swimming facility in Pirbadet with the specifications available. The validation of the model showed that it reacts as supposed to changes of different important parameters, but that is no guarantee for a correct model. It is important to have in mind that the purpose of this project was not to model a true copy of the AHU in Pirbadet, but to make a model that ensured the same indoor climate and recycled thermal energy from the return air. And since the correct control of the components was not handed over from Menerga before the end of the project period, the control in the model is not precise enough. Beneath, the results from the comparisons of the simulated model and the measured data are discussed in order to decide if the IDA ICE model is usable for design of swimming pools.

The comparison between the integrated variable for evaporation rate and the calculated evaporation rate based on water content in return and supply air shows that the calculation method is functioning. Therefore, this calculation method can be used for comparison between the simulated model and the measured datasets from Pirbadet. This calculation method can also be used for control of the AHU model.

Since the supply air temperature in Pirbadet is higher than in the simulated model throughout the day, and the air volume flow is higher during daytime in Pirbadet than in the simulated model, the heating through ventilation is bigger in Pirbadet. This is the case even when the measurement uncertainty is accounted for. Night-time, there is almost no difference though. So, the model of the swimming hall is not a perfect model and the resulting energy needs will be affected by this.

The fact that the AHU model in IDA ICE is made without a heat pump makes the results for the energy use in the AHU quite different to the measured results in Pirbadet. This has to do with the control of the heat pump. Since the heat pump is controlled to work both if there is a dehumidification need and if there is a heating need, the dehumidifier works more often than in the simulated model. This influences the results for dehumidification power so that the simulated model uses less power for dehumidification during daytime. This also makes the dumped heating power at daytime for the simulated model much larger than the reality in Pirbadet. During night-time the situation is the opposite due to the fact that there is a fresh air supply in Pirbadet, but nothing in the simulated model. This makes the dehumidifier in the simulated model work at night-time and cool down the exhaust air. In Pirbadet, fresh air supply and less use of the dehumidifier makes the dumped heat to outdoor bigger night-time.
If a correct AHU model was made in IDA ICE, an interesting test would have been to use the heat pump to utilize more of the exhaust heat during night-time to preheat water in a tank for use whenever needed. This might probably make the AHU more energy efficient, but perhaps the investment of a tank system not would be financially reasonable.

The impact of the different air volume flow rates is present and makes the model imperfect. Also, the fact that the outer bypass controls the fresh air volume flow rate as a volume ratio instead of a mass ratio (that would be correct) makes the model worse.

The comparing of evaporation rate between the simulated model and the measurements in Pirbadet is very positive as Figure 4-20 shows. If having in mind the measuring uncertainty in Pirbadet that overlaps the IDA ICE result, the IDA ICE model can actually have correct evaporation rate. They are not completely similar to each other, but they are definitely following each other's reactions. If the IDA ICE model had been more similar to the real

swimming facility, the results could have been even better. This on the other hand, requires quite good specifications of the building body, use and ventilation system.

When it comes to the heating and cooling (dehumidification) need in the AHU, the results are not sufficiently good enough. The procedure to find the heating need in the AHU in Pirbadet is not completely accurate, but with a correct building model, the results should be more equal. It is hard to compare the cooling power in the dehumidifier in the AHU for the two datasets due to the different control strategies. The results however show that the fresh air supply in the simulated model ensures sufficient dehumidification during daytime, while there is a huge dehumidification need (54 kW) at night-time without fresh air supply. Since there is a heating need at daytime, but no dehumidification need (beyond the fresh air supply), the warm exhaust air could advantageously be utilized in a heat pump system as in reality.

The way the dehumidifier power is calculated in this thesis is not very accurate. The power calculation assume that the cooling and heating is equal in the heat recovery unit. And the heating power in the heat recovery unit is based on a calculated temperature of airflow 6 where the assumption that the product of mass and temperature is in balance (Equation (3-10)). This calculation would have been better if it was possible to directly measure the temperature change over the dehumidifier.

The temperature difference of the upper and lower temperature sensor after the heat recovery unit in the supply air is interesting. Even when considering sensor accuracy, the difference is quite big. One reason for this might be that the dehumidifier is connected too close to the heat recovery unit that it cools the air in the lower part. Another possible reason is that the upper air in the heat recovery unit is heated more than the lower part since the intake of warm return air is at the top. The third possible reason discussed here has to do with fresh air supply. Perhaps the fresh air creates a layer at the bottom of the heat recovery unit while the recirculated warmer air creates a layer on the upper half. This can also explain the occasionally higher and more equal temperatures after the heat recovery unit which might be the case when no fresh air is supplied.

6. Conclusion

IDA ICE is used to make a model of part of the swimming facility in Pirbadet in Trondheim. The pool extension is used to model the pools. The software is user friendly and it mostly has the desired opportunities when building such a model, but there are some negative aspects. For example, the lack of possibility (at least as known) of setting the airflow rates different at night-time compared to daytime is crucial for the simulation results.
After setting up the model of the specific swimming hall and its AHU, a sensitivity analysis was done in order to validate the model. The validation showed that the model worked just as expected.

One of the issues for this thesis was to evaluate the evaporation rate from the IDA ICE pool. The evaporation rate calculated based on difference in water content in return and supply air was compared to an integrated variable for evaporation rate in IDA ICE. The result was that the calculated value is usable for further analysis. By comparing the IDA ICE model to the measured data from Pirbadet, using the calculation method, the two evaporation rates seem to correspond quite good. Also, the calculation method of Basin & Krumm gave corresponding results. Having in mind the resulting error band that overlapped the IDA ICE result, the evaporation rate in IDA ICE works quite well, given that the correct input values are used.
Though, comparing the evaporation rate with the experienced values in Byggforsk is less positive. The experienced evaporation rate is lower at night-time and higher at daytime, so perhaps these are not accurate enough to be used for pool design?

The goal for this project was not necessarily to make a completely correct AHU, but to make an AHU that ensures the correct indoor climate and that recycles the thermal energy from the return air. This was done by using bypasses and a heat recovery unit. A consequence of using different control strategy from the real AHU is that the fresh air supply and therefore also the dehumidifier (cooling) need becomes different in the two cases. The heating need on the other hand, should in theory be the same as long as the correct setpoint temperature is used. The results showed that the IDA ICE model had lower AHU heating need than the AHU in Pirbadet, which is also seen at the averagely lower supply temperature. This has though, probably more to do with the properties of the building body than the AHU control itself.

Due to the large differences in heating need for the simulated model and the measured swimming hall, the basis for this experiment is weak. A more correct building model with correct heat losses should therefore be made by adjusting the heat loss. To be able to measure the temperature over the dehumidifier would be a huge advantage in order to validate the cooling power of the IDA ICE model.

All in all, one can conclude that the IDA ICE pool extension works quite similar to the real pool in terms of evaporation rate. The resulting heating power for the IDA ICE AHU did not correspond to the measured value, but a better model of the building should be made in order to decide if a simple model like this can be used for swimming pool design. Regarding cooling power in the AHU, it is hard to compare the IDA ICE model to the cooling power in the AHU in Pirbadet due to the control of the dehumidifier as part of a heat pump. A completely equal AHU model should be used for this purpose.

7. Further work

For further work, there are two main tasks to fix. The water evaporation rate from the pool model seems to work as supposed, but the heating need of both the air space and the pool water is still not fully validated. Since there were no sensor on the heat supply to the pool water in Pirbadet, this was not considered in this thesis. So, modelling a swimming facility even more in detail with possibility for also measuring the pool water heating would be a huge step in the right direction in order to be able to predict heating need. Then, detailed information about the building envelope and some information about the infiltration/exfiltration should be accessible. Use of a new swimming hall built as a passive house would be a solution, else adjustment of the heat loss of the building model can be done to match the real heating need. If possible, in IDA ICE, the correct volume airflow should be modelled both daytime and night-time.

The second main task is to model an exact copy of the real AHU to be able to predict the use of and to size the heat exchangers in the heat pump system. Without this it is possible to simulate the model and get the resulting cooling power for dehumidification. But, since the dehumidifier is used whenever there is a heating need, the total use of it is still unknown without making this AHU copy. Also, a solution for a smaller uncertainty of the temperature between the heat recovery unit and the dehumidifier should be investigated. A correct copy of the AHU demands correct control of the components and use of a heat pump system. The control strategy of the MENEREGA ThermoCond was not handed over before the end of the period for this master thesis, but it should be used to make a better model for further work.

An interesting experiment would be to investigate the impact of mounting the dehumidifier in contact with the heat recovery unit. This can e.g. be done by measuring the temperature over the heat recovery unit and check for different reactions with the dehumidifier on and off.

If IDA ICE manages to model a swimming facility correct, the model can be used for design of swimming facility. A sensitivity analysis by using the parametric run method can be used in order to fine-tune the model to be as energy efficient as possible and at the same time ensure a good indoor environment.

References

1. *Lov om klimamål (klimaloven)*. 2017 [cited 2018 22.09.18]; Available from: https://lovdata.no/dokument/NL/lov/2017-06-16-60.
2. *Bygningsenergi*. Available from: https://www.standard.no/fagomrader/bygg-anlegg-og-eiendom/bygningsenergi/.
3. Kampel, W., B. Aas, and A. Bruland, *Energy-use in Norwegian swimming halls.* Energy and Buildings, 2013. **59**: p. 181-186.
4. Limane, A., H. Fellouah, and N. Galanis, *Simulation of airflow with heat and mass transfer in an indoor swimming pool by OpenFOAM.* International Journal of Heat and Mass Transfer, 2017. **109**: p. 862-878.
5. ASHRAE, *2009 ASHRAE Handbook Fundamentals.* 2009.
6. Smedegård, O.Ø., *Building performance simulation for natatoriums*. 2017.
7. *Byggteknisk forskrift (TEK17)*. 2017; Available from: https://dibk.no/byggereglene/byggteknisk-forskrift-tek17/.
8. Bøhlerengen, T., et al., *Bade- og svømmeanlegg*. Håndbok (Norges byggforskningsinstitutt : trykt utg.). Vol. 52. 2004, Oslo: Norges byggforskningsinstitutt.
9. *Byggteknisk forskrift (TEK97)*. 1999 [cited 2019 15.05]; Available from: https://dibk.no/globalassets/byggeregler/tidligere_regelverk/tekniske_forskrifter_1999.pdf.
10. *Kriterier for passivhus og lavenergibygninger - Yrkesbygninger* 2012 [cited 2019 15.05]; 1 (2012-09-01) [Available from: https://www.standard.no/no/Nettbutikk/produktkatalogen/Produktpresentasjon/?ProductID=587802.
11. Byggforsk, *Ventilasjon og avfukting i svømmehaller og rom med svømmebasseng.* 2003.
12. Byggforsk, *Garderober for ansatte og publikum.* 2006.
13. Mancic, M., et al., *Mathematical modelling and simulation of the thermal performance of a solar heated indoor swimming pool*. 2014. p. 999-1010.
14. *Retningslinjer for vannbehandling i offentlige bassengbad*. Versjon 5. ed. 2000, Skien: Norsk bassengbad teknisk forening.
15. Lochner, G. and L. Wasner, *Ventilation Requirements For Indoor Pools.* ASHRAE J., 2017. **59**(7): p. 16-24.
16. Smith, C.C., G.O.G. Lof, and R.W. Jones. *Rates of evaporation from swimming pools in active use*. in *ASHRAE Transactions*. 1998.
17. Lebon, M., et al., *Numerical analysis and field measurements of the airflow patterns and thermal comfort in an indoor swimming pool: a case study.* Energy Efficiency, 2017. **10**(3): p. 527-548.
18. *Klima og luftkvalitet på arbeidsplassen*. 2016, Arbeidstilsynet: Arbeids- og sosialdepartementet.
19. Byggforsk, *Byggskader. Oversikt.* 2010.
20. Wikipedia, *Graph of Dewpoint vs. Air Temperature at Varying Relative Humidities. Based on the Magnus-Tetens approximation*. 2008, Wikipedia: Wikipedia.
21. Lochner, G. *Ventilation and air distribution in indoor aquatic facilities*. 2016; Available from: http://www.innoventair.com/Portals/3/Breathe%20Content/Ventilation-and-air-distribution-in-indoor-aquatic-facilities.pdf.

22. Johansson, L. and L. Westerlund, *Energy savings in indoor swimming-pools: comparison between different heat-recovery systems.* Applied Energy, 2001. **70**(4): p. 281-303.
23. Pearson, A., *King of the Charts: Richard Mollier.(COLUMN: REFRIGERATION APPLICATIONS).* ASHRAE Journal, 2017. **59**(12): p. 131.
24. Cambridge. *Ideal Gas Properties of Air*. Table E-1]. Available from: https://www.cambridge.org/us/files/9513/6697/5546/Appendix_E.pdf.
25. Abu Bakar, N.N., et al., *Energy efficiency index as an indicator for measuring building energy performance: A review.* Renewable and Sustainable Energy Reviews, 2015. **44**: p. 1-11.
26. Kampel, W., *Energy Efficiency in Swimming Facilities*. 2015, NTNU.
27. Åas, B. *Energibruk i norske svømmehaller*. 2016 30.05.2018; Available from: https://www.godeidrettsanlegg.no/aktuelt/energibruk-i-norske-svømmehaller.
28. *Climate statistics for Værnes observation site*. [cited 2019 28.03.2019]; Available from: https://www.yr.no/sted/Norge/Trøndelag/Stjørdal/Trondheim_lufthavn,_Værnes/klima.html#måned.
29. *Google Maps*. [cited 2019; Available from: https://www.google.no/maps.
30. Pirbadet. *All about us - Facts*. Available from: https://www.pirbadet.no/en/2609-2/.
31. Hjertenes, T., *Effectiveness of heat recovery unit*, H. Alvestad, Editor. 2019: E-mail.
32. *Water - Saturation Pressure* Available from: https://www.engineeringtoolbox.com/water-vapor-saturation-pressure-d_599.html.

Attachment 1: Blueprint of Pirbadet

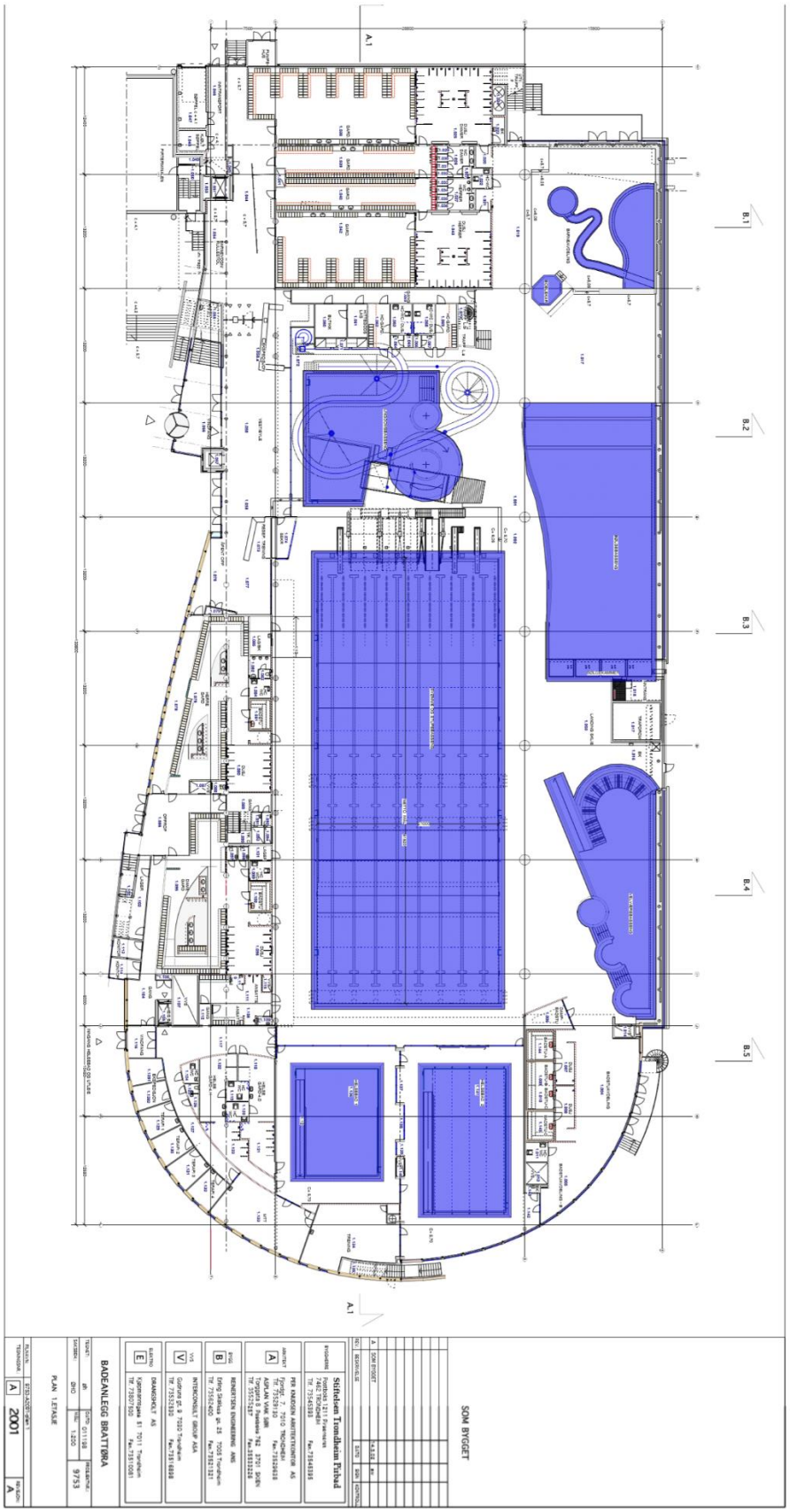

Attachment 2: Fault analysis calculations

The accuracy of the temperature, RH and volume flow measurements are already known from the sensor specifications. The accuracy of the calculated properties must be calculated. These calculations are explained here.

The accuracy of the output from the Excel extension hxLib is estimated.

Deriving the Δx:

$$RH = \frac{x}{x_{saturated}} \quad \rightarrow \quad x = RH * x_{saturated}$$

$x_{saturated}$ is calculated for the temperatures 1 to 30 °C using hxLib with 100 %RH. Then, regression in Excel is done to find a function $x_{saturated}(T)$:

$$x_{saturated} = 2 * 10^{-7} * T^2 + 9 * 10^{-7} * T + 4 * 10^{-5}$$

And then

$$x = RH * (2 * 10^{-7} * T^2 + 9 * 10^{-7} * T + 4 * 10^{-5})$$

The fault analysis described in section 3.2.6.9 is used for finding Δx.

The already known and constant $\Delta u's$ are the following:

$\Delta T_{EL} = 0.3\ °C$[8]

$\Delta T_T = 0.5\ °C$[9]

$\Delta RH = 2\ \%RH$

$$\frac{dx}{dRH} = 2 * 10^{-7} * T^2 + 9 * 10^{-7} * T + 4 * 10^{-5}$$

$$\frac{dx}{dT} = RH * (4 * 10^{-7} * T + 9 * 10^{-7})$$

$$\Delta x = \pm \sqrt{\begin{matrix}\left((2 * 10^{-7} * T^2 + 9 * 10^{-7} * T + 4 * 10^{-5}) * \Delta RH\right)^2 \\ +(RH * (4 * 10^{-7} * T + 9 * 10^{-7}) * \Delta T)^2\end{matrix}}$$

[8] For the EasyLog sensors
[9] For the thermocouples

Deriving the Δv:

The specific volume (v) is calculated for the temperatures 1 to 30 °C using hxLib with 100 %RH. Then, regression in Excel is done to find a function v(T), neglecting the small change of changing RH:

$$v = 3 * 10^{-5} * T^2 + 0.003 * T + 0.808$$

The fault analysis described in section 3.2.6.9 is used for finding Δv.

$$\frac{dv}{dT} = 6 * 10^{-5} * T + 0{,}003$$

$$\Delta v = \sqrt{((6 * 10^{-5} * T + 0{,}003) * \Delta T)^2}$$

Beneath, the calculations for the accuracy of the calculated properties are shown for the different airflows. The method described in section 3.2.6.9 is used.

Airflow 1

$$\Delta \dot{V}_1 = \pm \dot{V}_1 * 0{,}02$$

$$\dot{m}_1 = \frac{\dot{V}_1}{v_1 * 3600} \rightarrow \frac{d\dot{m}_1}{d\dot{V}_1} = \frac{1}{v_1 * 3600} \quad , \quad \frac{d\dot{m}_1}{dv_1} = \frac{-\dot{V}_1}{v_1^2 * 3600}$$

$$\Delta \dot{m}_1 = \pm \sqrt{\left(\frac{1}{v_1 * 3600} * \Delta \dot{V}_1\right)^2 + \left(\frac{-\dot{V}_1}{v_1^2 * 3600} * \Delta v_1\right)^2}$$

Airflow 2

$$\Delta \dot{V}_2 = \Delta \dot{V}_1$$

$$\dot{m}_2 = \frac{\dot{V}_2}{v_2 * 3600} \rightarrow \frac{d\dot{m}_2}{d\dot{V}_2} = \frac{1}{v_2 * 3600} \quad , \quad \frac{d\dot{m}_2}{dv_2} = \frac{-\dot{V}_2}{v_2^2 * 3600}$$

$$\Delta \dot{m}_2 = \pm \sqrt{\left(\frac{1}{v_2 * 3600} * \Delta \dot{V}_2\right)^2 + \left(\frac{-\dot{V}_2}{v_2^2 * 3600} * \Delta v_2\right)^2}$$

Airflow 3

$$\dot{m}_3 = \dot{m}_2 - (\dot{m}_8 - \dot{m}_7) = \dot{m}_2 - \dot{m}_8 + \dot{m}_7 \quad \rightarrow \quad \frac{d\dot{m}_3}{d\dot{m}_2} = 1 \quad , \quad \frac{d\dot{m}_3}{d\dot{m}_8} = -1 \quad , \quad \frac{d\dot{m}_3}{d\dot{m}_7} = 1$$

$$\Delta\dot{m}_3 = \pm\sqrt{\Delta\dot{m}_2{}^2 + (-\Delta\dot{m}_8)^2 + \Delta\dot{m}_7^2}$$

Airflow 4

$$\dot{m}_4 = \frac{\dot{m}_3 * x_3 - (\dot{m}_6 - \dot{m}_5) * x_3}{x_4} \rightarrow \frac{d\dot{m}_4}{d\dot{m}_3} = \frac{x_3}{x_4} \ , \ \frac{d\dot{m}_4}{dx_3} = \frac{\dot{m}_3 - \dot{m}_6 + \dot{m}_5}{x_4} \ ,$$

$$\frac{d\dot{m}_4}{d\dot{m}_6} = -\frac{x_3}{x_4} \ , \ \frac{d\dot{m}_4}{d\dot{m}_5} = \frac{x_3}{x_4} \ , \ \frac{d\dot{m}_4}{dx_4} = \frac{(\dot{m}_6 - \dot{m}_5) * x_3 - \dot{m}_3 * x_3}{x_4^2}$$

$$\Delta\dot{m}_4 = \pm\sqrt{\left(\frac{x_3}{x_4} * \Delta\dot{m}_3\right)^2 + \left(\frac{\dot{m}_3 - \dot{m}_6 + \dot{m}_5}{x_4} * \Delta x_3\right)^2 + \left(-\frac{x_3}{x_4} * \Delta\dot{m}_6\right)^2 + \left(\frac{x_3}{x_4} * \Delta\dot{m}_5\right)^2 + \left(\frac{(\dot{m}_6 - \dot{m}_5) * x_3 - \dot{m}_3 * x_3}{x_4^2} * \Delta x_4\right)^2}$$

$$\dot{V}_4 = \dot{m}_4 * v_4 * 3600 \rightarrow \frac{d\dot{V}_4}{d\dot{m}_4} = v_4 * 3600 \ , \quad \frac{d\dot{V}_4}{dv_4} = \dot{m}_4 * 3600$$

$$\Delta\dot{V}_4 = \pm\sqrt{(v_4 * 3600 * \Delta\dot{m}_4)^2 + (\dot{m}_4 * 3600 * \Delta v_4)^2}$$

Airflow 5

$$\dot{m}_5 = \frac{\dot{m}_6 * (x_6 - x_3)}{x_5 - x_3} \rightarrow \frac{d\dot{m}_5}{d\dot{m}_6} = \frac{x_6 - x_3}{x_5 - x_3} \ , \quad \frac{d\dot{m}_5}{dx_6} = \frac{\dot{m}_6}{x_5 - x_3} \ ,$$

$$\frac{d\dot{m}_5}{dx_3} = \frac{\dot{m}_6 * x_5}{(x_5 - x_3)^2} \ , \ \frac{d\dot{m}_5}{dx_5} = -\frac{\dot{m}_6 * (x_6 - x_3)}{(x_5 - x_3)^2}$$

$$\Delta\dot{m}_5 = \pm\sqrt{\left(\frac{x_6 - x_3}{x_5 - x_3} * \Delta\dot{m}_6\right)^2 + \left(\frac{\dot{m}_6}{x_5 - x_3} * \Delta x_6\right)^2 + \left(\frac{\dot{m}_6 * x_5}{(x_5 - x_3)^2} * \Delta x_3\right)^2 + \left(-\frac{\dot{m}_6 * (x_6 - x_3)}{(x_5 - x_3)^2} * \Delta x_5\right)^2}$$

$$\dot{V}_5 = \dot{m}_5 * v_5 * 3600 \rightarrow \frac{d\dot{V}_5}{d\dot{m}_5} = v_5 * 3600 \ , \quad \frac{d\dot{V}_5}{dv_5} = \dot{m}_5 * 3600$$

$$\Delta\dot{V}_5 = \pm\sqrt{(v_5 * 3600 * \Delta\dot{m}_5)^2 + (\dot{m}_5 * 3600 * \Delta v_5)^2}$$

Airflow 6

$$T_6 = \frac{T_5 * \dot{m}_5 + T_4 * (\dot{m}_3 - \dot{m}_4)}{\dot{m}_6} \rightarrow \frac{dT_6}{dT_5} = \frac{\dot{m}_5}{\dot{m}_6} \ , \ \frac{dT_6}{d\dot{m}_5} = \frac{T_5}{\dot{m}_6} \ ,$$

$$\frac{dT_6}{dT_4} = \frac{\dot{m}_3 - \dot{m}_4}{\dot{m}_6} \ , \ \frac{dT_6}{d\dot{m}_3} = \frac{T_4}{\dot{m}_6} , \ \frac{dT_6}{d\dot{m}_4} = -\frac{T_4}{\dot{m}_6} \ , \ \frac{dT_6}{d\dot{m}_6} = -\frac{T_5 * \dot{m}_5 + T_4 * (\dot{m}_3 - \dot{m}_4)}{\dot{m}_6^2}$$

$$\Delta T_6 = \pm \sqrt{\begin{matrix} \left(\frac{\dot{m}_5}{\dot{m}_6} * \Delta T_5\right)^2 + \left(\frac{T_5}{\dot{m}_6} * \Delta\dot{m}_5\right)^2 + \left(\frac{\dot{m}_3 - \dot{m}_4}{\dot{m}_6} * \Delta T_4\right)^2 + \left(\frac{T_4}{\dot{m}_6} * \Delta\dot{m}_3\right)^2 \\ + \left(-\frac{T_4}{\dot{m}_6} * \Delta\dot{m}_4\right)^2 + \left(-\frac{T_5 * \dot{m}_5 + T_4 * (\dot{m}_3 - \dot{m}_4)}{\dot{m}_6^2} * \Delta\dot{m}_6\right)^2 \end{matrix}}$$

Airflow 7

$$\dot{m}_7 = \frac{\dot{m}_8 * (x_8 - x_1)}{x_7 - x_1} \rightarrow \frac{d\dot{m}_7}{d\dot{m}_8} = \frac{x_8 - x_1}{x_7 - x_1} \ , \ \frac{d\dot{m}_7}{dx_8} = \frac{\dot{m}_8}{x_7 - x_1} \ ,$$

$$\frac{d\dot{m}_7}{dx_1} = \frac{\dot{m}_8 * (x_8 - x_7)}{(x_7 - x_1)^2} \ , \ \frac{d\dot{m}_7}{dx_7} = \frac{\dot{m}_8 * (x_1 - x_8)}{(x_7 - x_1)^2}$$

$$\Delta\dot{m}_7 = \pm \sqrt{\begin{matrix} \left(\frac{x_8 - x_1}{x_7 - x_1} * \Delta\dot{m}_8\right)^2 + \left(\frac{\dot{m}_8}{x_7 - x_1} * \Delta x_8\right)^2 + \left(\frac{\dot{m}_8 * (x_8 - x_7)}{(x_7 - x_1)^2} * \Delta x_1\right)^2 \\ + \left(\frac{\dot{m}_8 * (x_1 - x_8)}{(x_7 - x_1)^2} * \Delta x_7\right)^2 \end{matrix}}$$

Airflow 11

$$\Delta\dot{V}_{11} = \pm\dot{V}_{11} * 0{,}02$$

$$\dot{m}_{11} = \frac{\dot{V}_{11}}{v_{11} * 3600} \rightarrow \frac{d\dot{m}_{11}}{d\dot{V}_{11}} = \frac{1}{v_{11} * 3600} \ , \ \frac{d\dot{m}_{11}}{dv_{11}} = \frac{-\dot{V}_{11}}{v_{11}^2 * 3600}$$

$$\Delta\dot{m}_{11} = \pm \sqrt{\left(\frac{1}{v_{11} * 3600} * \Delta\dot{V}_{11}\right)^2 + \left(\frac{-\dot{V}_{11}}{v_{11}^2 * 3600} * \Delta v_{11}\right)^2}$$

Heating power from condenser

$$Q = \dot{m}_8 * 1.005 * (T_9 - T_8) \rightarrow \frac{dQ}{d\dot{m}_8} = 1.005 * (T_9 - T_8) \ , \quad \frac{dQ}{dT_9} = \dot{m}_8 * 1.005 \ ,$$

$$\frac{dQ}{dT_8} = -\dot{m}_8 * 1.005$$

$$\Delta Q = \pm\sqrt{(1.005 * (T_9 - T_8) * \Delta\dot{m}_8)^2 + (\dot{m}_8 * 1.005 * \Delta T_9)^2 + (-\dot{m}_8 * 1.005 * \Delta T_8)^2}$$

Heating power from heating coil

$$Q = \dot{m}_{10} * 1.005 * (T_{11} - T_{10}) \rightarrow \frac{dQ}{d\dot{m}_{10}} = 1.005 * (T_{11} - T_{10}) \ , \ \frac{dQ}{dT_{11}} = \dot{m}_{10} * 1.005 \ ,$$

$$\frac{dQ}{dT_{10}} = -\dot{m}_{10} * 1.005$$

$$\Delta Q = \pm\sqrt{\begin{matrix}(1.005 * (T_{11} - T_{10}) * \Delta\dot{m}_{10})^2 + (\dot{m}_{10} * 1.005 * \Delta T_{11})^2 \\ +(-\dot{m}_{10} * 1.005 * \Delta T_{10})^2\end{matrix}}$$

Temperature between heat recovery unit and dehumidifier

$$\mathrm{T_b} = \frac{\dot{m}_2 * T_2 - \dot{m}_6 * (T_7 - T_6)}{\dot{m}_3} \rightarrow \frac{dT_b}{d\dot{m}_2} = \frac{T_2}{\dot{m}_3} \ , \quad \frac{dT_b}{dT_2} = \frac{\dot{m}_2}{\dot{m}_3} \ , \quad \frac{dT_b}{d\dot{m}_6} = \frac{T_6 - T_7}{\dot{m}_3} \ ,$$

$$\frac{dT_b}{dT_7} = -\frac{\dot{m}_6}{\dot{m}_3} \ , \quad \frac{dT_b}{dT_6} = \frac{\dot{m}_6}{\dot{m}_3} \ , \quad \frac{dT_b}{d\dot{m}_3} = \frac{\dot{m}_6(T_7 - T_6) - \dot{m}_2 * T_2}{\dot{m}_3^2}$$

$$\Delta T_b = \pm\sqrt{\begin{matrix}\left(\frac{T_2}{\dot{m}_3} * \Delta\dot{m}_2\right)^2 + \left(\frac{\dot{m}_2}{\dot{m}_3} * \Delta T_2\right)^2 + \left(\frac{T_6 - T_7}{\dot{m}_3} * \Delta\dot{m}_6\right)^2 + \left(-\frac{\dot{m}_6}{\dot{m}_3} * \Delta T_7\right)^2 \\ + \left(\frac{\dot{m}_6}{\dot{m}_3} * \Delta T_6\right)^2 + \left(\frac{\dot{m}_6(T_7 - T_6) - \dot{m}_2 * T_2}{\dot{m}_3^2} * \Delta\dot{m}_3\right)^2\end{matrix}}$$

Cooling power

$$Q = \dot{m}_3 * 1.005 * (T_b - T_3) \rightarrow \frac{dQ}{d\dot{m}_3} = 1.005 * (T_b - T_3) \ , \quad \frac{dQ}{dT_b} = \dot{m}_3 * 1.005 \ ,$$

$$\frac{dQ}{dT_3} = -\dot{m}_3 * 1.005$$

$$\Delta Q = \pm\sqrt{(1.005 * (T_b - T_3) * \Delta\dot{m}_3)^2 + (\dot{m}_3 * 1.005 * \Delta T_b)^2 + (-\dot{m}_3 * 1.005 * \Delta T_3)^2}$$

Delivered heating power to the hall

$$Q = \dot{m}_{11} * 1.005 * (T_{11} - T_1) \rightarrow \frac{dQ}{d\dot{m}_{11}} = 1.005 * (T_{11} - T_1) \ , \ \frac{dQ}{dT_{11}} = \dot{m}_{11} * 1.005 \ ,$$

$$\frac{dQ}{dT_1} = -\dot{m}_{11} * 1.005$$

$$\Delta Q = \pm\sqrt{(1.005 * (T_{11} - T_1) * \Delta\dot{m}_{11})^2 + (\dot{m}_{11} * 1.005 * \Delta T_{11})^2 + (-\dot{m}_{11} * 1.005 * \Delta T_1)^2}$$

Dumped heating to outdoor

$$Q = \dot{m}_4 * 1.005 * (T_4 - T_5) \rightarrow \frac{dQ}{d\dot{m}_4} = 1.005 * (T_4 - T_5) \ , \quad \frac{dQ}{dT_4} = \dot{m}_4 * 1.005 \ ,$$

$$\frac{dQ}{dT_5} = -\dot{m}_4 * 1.005$$

$$\Delta Q = \pm\sqrt{(1.005 * (T_4 - T_5) * \Delta\dot{m}_4)^2 + (\dot{m}_4 * 1.005 * \Delta T_4)^2 + (-\dot{m}_4 * 1.005 * \Delta T_5)^2}$$

Evaporation rate

$$\dot{m} = (\dot{m}_1 * x_1 - \dot{m}_{11} * x_{11}) * 3600 \rightarrow \frac{d\dot{m}}{d\dot{m}_1} = x_1 * 3600 \ , \quad \frac{d\dot{m}}{dx_1} = \dot{m}_1 * 3600 \ ,$$

$$\frac{d\dot{m}}{d\dot{m}_{11}} = -x_{11} * 3600 \ , \quad \frac{d\dot{m}}{dx_{11}} = -\dot{m}_{11} * 3600$$

$$\Delta\dot{m} = \pm\sqrt{\begin{matrix}(x_1 * 3600 * \Delta\dot{m}_1)^2 + (\dot{m}_1 * 3600 * \Delta x_1)^2 + (-x_{11} * 3600 * \Delta\dot{m}_{11})^2 \\ +(-\dot{m}_{11} * 3600 * \Delta x_{11})^2\end{matrix}}$$

Attachment 3: Evaporation rate calculation methods

Symbols used

$\dot{m}_w$ – mass flow rate (kg·h^{-1})
F – evaporation area (m^2).

$p_w^{"}$ – water vapor partial pressure at water temperature in boundary layer at saturation state (Pa),
p_w – water vapor partial pressure at the air temperature (Pa),
x" – humidity content in boundary layer at water temperature (kg·kg^{-1}),
x – humidity content for saturated air at pool temperature (kg·kg^{-1}).

Shah's method for unoccupied swimming pools

$$\dot{m}_w = K \cdot \rho_w \cdot (\rho_p - \rho_w)^{0,333} \cdot (x" - x) \cdot F$$

$(\rho_p - \rho_w) < 0 \rightarrow \rho_w - \rho_p$
$(\rho_p - \rho_w) > 0{,}02 \rightarrow K = 35$
$(\rho_p - \rho_w) < 0{,}02 \rightarrow K = 40$

Shah's method for occupied swimming pools

$$\dot{m}_w = \left(5{,}95 \cdot \frac{N}{F} + 1{,}2\right) \cdot K \cdot \rho_w \cdot (\rho_p - \rho_w)^{0,333} \cdot (x" - x) \cdot F \quad (19)$$

For $\frac{F}{N} > 45$

$$\dot{m}_w = \left(14{,}85 \cdot \frac{N}{F} + 1\right) \cdot K \cdot \rho_w \cdot (\rho_p - \rho_w)^{0,333} \cdot (x" - x) \cdot F \quad (20)$$

For $\frac{F}{N} > 4{,}5 \div 4$

$$\dot{m}_w = 2{,}5 \cdot K \cdot \rho_w \cdot (\rho_p - \rho_w)^{0,333} \cdot (x" - x) \cdot F$$

Dla $\frac{F}{N} < 4{,}5$

$(\rho_p - \rho_w) < 0 \rightarrow \rho_w - \rho_p$
$(\rho_p - \rho_w) > 0{,}02 \rightarrow K = 35$
$(\rho_p - \rho_w) < 0{,}02 \rightarrow K = 40$
N – number of users

Basin & Krumm's method for unoccupied swimming pools

$$\dot{m}_w = \left[-0{,}059 + \left(0{,}0105 \cdot \frac{p_w^{"} - p_w}{1{,}333}\right)\right] \cdot F$$

$p_w^{"}$, p_w (hPa)

Basin & Krumm's method for occupied swimming pools

$$\dot{m}_w = \left[0{,}119 + \left(0{,}01995 \cdot 6 \cdot \frac{N}{F}\right) \cdot \frac{p_w^{"} - p_w}{1{,}333}\right] \cdot F$$

$p_w^{"}$, p_w (hPa)
N – number of users

NTNU

Kunnskap for en bedre verden